ZINC AND COPPER TOXICITY THRESHOLDS ON *CELLULOMONAS FLAVIGENA*

by

Alison M. Ruhs

ProQuest LLC.
789 East Eisenhower Parkway
P.O. Box 1346
Ann Arbor, MI 48106 – 1346

A thesis submitted to the Faculty and Board of Trustees of the Colorado School of Mines in partial fulfillment of the requirements for the degree of Master of Science (Environmental Science and Engineering).

Golden, Colorado
Date 11-02-06

Signed: Alison Ruhs
Alison M. Ruhs

Approved: Linda Figueroa
Dr. Linda Figueroa
Thesis Advisor

Golden, Colorado
Date 11-09-06

Signed:
Dr. Robert L. Siegrist
Professor and Director
Division of Environmental
Science and Engineering

ABSTRACT

The effective use of anaerobic passive treatment systems (APTS), such as sulfate-reducing bioreactors, to treat acid rock drainage will help to mitigate water contamination caused from mining as well as reduce current treatment costs. One drawback to APTS has been an observed decline in long-term performance. APTS contain a complex microbial ecosystem, and metal toxicity may be indirectly affecting sulfate-reduction by inhibiting other important microbes. Cellulose degraders (cellulolytic-fermenters) are dominant within a sulfate reducing bioreactor (Pruden et al., 2005), and their ability to produce viable substrates for the sulfate-reducing bacteria (SRB) is the rate-limiting step in sulfate reduction (Logan, 2003). This investigation examines the individual effect of zinc and copper on a pure culture of *Cellulomonas flavigena* (ATCC 482), a cellulolytic-fermenter.

Batch growth experiments were run for 10 days (240 hours) under anaerobic conditions. Copper and zinc concentrations at or above 4 μM (0.26 mg/L) and 6.1 μM (0.4 mg/L), respectively, completely inhibited growth, and greatly reduced glucose consumption and organic acid production. Reduced growth rates, relative to the control bottles, were observed in bottles containing less than or equal to Cu = 3.2 μM (0.2 mg/L) and Zn = 4.3 μM (0.28 mg/L), with total cell protein reaching concentrations comparable to the control bottles by the end of the experiment. Therefore, *C. flavigena* was able to overcome toxicity at or below these copper and zinc concentrations during the 10 day experiment. The chemical speciation calculated using MINTEQ suggests that at least 50% of the copper and 10% of the zinc was complexing with the organic acids produced by *C. flavigena*, even at very low concentrations of organic acid. The percentage of complexed metal increased as the organic acid concentration increased during the experiment, and this suggests that *C. flavigena* may have been able to recover from the

toxicity threshold experienced at or above 4 μM (0.26 mg/L) of copper and 6.1 μM (0.4 mg/L) of zinc if the experiments were run for a longer period of time. Also, the metabolic pathway for glucose utilization appears to change in the presence of copper and zinc, based on observed shifts in the amount of each organic acid produced relative to the control bottles. When comparing *C. flavigena*'s toxicity experiments with previous toxicity research studies conducted on SRB, *C. flavigena* is much more sensitive to copper and zinc toxicity than SRB.

TABLE OF CONTENTS

LIST OF FIGURES

LIST OF TABLES

LIST OF EQUATIONS

ACKNOWLEDGEMENTS

I want to begin by thanking my advisor and committee members. I am grateful to my advisor Dr. Linda Figueroa for her ideas and support, she made this project possible, and it would not have been accomplished without her efforts. Her positive feedback and genuine desire to develop my ideas has been invaluable. Thank you Linda for believing in me. Dr. Tom Wildeman, thank you for taking such an active role in my research by providing numerous articles on current microbial toxicity work, and finding the value in my research. You were the stable force that kept me heading in the right direction. Thank you for sharing your knowledge and your commitment to my research. To Dr. John Spear, thank you for sharing your expertise in microbiology. Your insights improved my experimental approach as well as my understanding of microbial research. Thank you John for always being open minded and easy to approach. Dr. Ron Cohen, you always brought a fresh perspective to my work, and most of all fostered a comfortable and friendly environment. Thank you so much Ron for your positive and humorous nature, it made the research fun. I also want to give a special thanks to Judy Bolis for always offering a helpful hand and providing mentorship. Although Judy was not officially on my committee, she was a personal committee member. Thank you Judy for your patience and consistent participation in my research efforts.

Secondly, I would like to thank several of my peers for providing insight and support. Thank you to my fellow researchers and office mates Ruth Tinnacher, Emma Buccambuso, Andy Miller, Angelique Diaz, Daphne Place, Patsy Buckley, Shiloh Hernandez, Barbara Butler, and many others. They always offered to listen, and they helped me see the light at the end of the tunnel with respect to my course work and research. The best way to describe their impact on me would be in a quote taken from Oliver Wendell Holmes. "What lies behind us and what lies ahead of us are tiny matters

compared to what lies within us." Thank you all so much for always reminding me that it is the journey that is important, not the destination.

And last but not least, a special thank you to my family and friends. All of you have made me who I am today, and without your continual support and love, my efforts would seem meaningless. Ethel Percy Andrus once said "It is only in the giving of oneself to others that we truly live", and each and every one of you do this everyday. Thank you all for inspiring me to do better.

CHAPTER 1 INTRODUCTION

1.1 Brief Overview of Acid Mine Drainage

Surface mining and deep mining activities have been found to enhance a phenomenon known as acid mine drainage (AMD), which is caused by the oxidation of sulfide minerals, and typically leads to acidic conditions with high levels of dissolved metals and sulfate. AMD is detrimental to aquatic life and expensive to treat. There are currently thousands of abandoned mines throughout the Western United States, 51,700 of these abandoned mine sites are within EPA Region 8, and many of these mines are in remote locations (Western Governor's Association 1998). Benner et al. (1997) estimated that 5,000 to 10,000 miles of streams in the western United States are impacted by AMD. Typical treatment for AMD would include the addition of alkaline chemicals, such as lime, in an attempt to neutralize the acidic water and precipitate out dissolved metals. Such traditional treatment techniques can be very expensive and are not feasible for remote and abandoned mining-related sites (USEPA 1995). Due to a need for a cost effective, long-term, and low maintenance treatment technology, passive treatment systems, such as permeable reactive barriers (PRB's) and man-made wetlands, have become increasingly important for the treatment of AMD at remote mining locations.

1.2 Passive Treatment Systems and Metal Toxicity Research

Anaerobic passive treatment systems (APTS) rely on sulfate-reducing bacteria (SRB) for the treatment of AMD. The SRB reduce the sulfate ion to sulfide, which leads to an increase in pH and precipitates the dissolved metals as insoluble sulfide metals

(Barton and Tomei, 1995; Utgikar et al., 2000). Two generic equations for this process are shown below ("CH_2O" represents an organic carbon source):

$$SO_4^{2-} + 2CH_2O \rightarrow H_2S + 2HCO_3^{2-}$$
$$Me^{2+} + H_2S \rightarrow MeS_{(s)} + 2H^+$$

Equation (1.1)

Unfortunately the presence of heavy metals can be harmful to the biological process of the SRB by deactivating enzymes, denaturing proteins, and competing with essential cations (Mazidji et al., 1992; Mosey and Hughes, 1975). One approach used to determine metal toxicity is to observe cell growth patterns, and in some cases establish an LC_{50}, or the solution concentration of a toxic substance that will render a loss of activity or death for 50% of the population. A second approach would be to determine a threshold, where at a particular metal concentration the activity (substrate utilization, byproduct production, or growth) of concern is completely stopped. And finally, a third approach examines inhibition of activity, which would result in a decrease in growth rate, substrate utilization rate, or by-product production rate.

Several research studies have been conducted in an attempt to quantify the toxic impact of metal ions on SRB. Heavy metals have been reported to reach toxic concentrations (when sulfate reduction no longer occurs) for SRB over a wide range, spanning from a few mg/L to as much as 100 mg/L (Booth and Mercer, 1963; Saleh et al., 1964; Temple and Le Roux, 1964; Loka Bharathi et al., 1990; Hao et al., 1994; Poulsen et al., 1997; Sani et al., 2001; Utgikar et al., 2001 and 2002). Utgikar et al. (2001) looked at the effects of zinc and copper ions on sulfate utilizations for a mixed-culture of SRB, and found the toxic concentrations (when sulfate reduction no longer occurred) of zinc and copper to be 20 mg/L and 12 mg/L, respectively. Sani et al. (2001) took a different approach by preventing sulfate production all together, and established toxicity based on changes in total cell protein production. This approach mimics that of

LC_{50} determination, and Sani et al. (2001) found that 16μM (1.0 mg/L) of Cu(II) caused 50% inhibition in final cell protein for *Desulfovibrio desulfuricans*, a SRB. At 16 μM of Zn(II), Sani et al. found inhibition in growth based on the slight increase in the lag phase, but very little inhibition in growth rate was observed, and no toxic effects were apparent based on complete recovery in total cell protein relative to the control.

1.2.1 Microbial Sorption and Internalization of Metals

In order to maintain normal cell function, organisms require a specific concentration of essential metals. Zinc and copper are both essential for normal cell function (Hopkin 1989). When the concentration of the essential metal exceeds the nutritional requirement toxic effects to the organism occur.

LC_{50} can be difficult to quantify. Unlike macroorganisms, bacteria multiply and grow rapidly, and often exhibit inhibitory patterns, and/or threshold growth patterns, which make quantification of LC_{50} impractical or impossible. In addition, bacteria are able to absorb and/or internalize many metals, and this can occur concurrently with other reactions in the system, such as precipitation. Several research studies have looked at the cell wall of microorganisms and the binding of metal ions (Beveridge T.J. and Murray R.G.E. 1976, 1980; Marquis et al., 1976; Beveridge et al., 1978; Hoyle B.D. and Beveridge T.J., 1983). With respect to Gram-positive bacteria, the carboxyl groups of the peptidoglycan cell wall and the phosphodiester groups from the teichoic acid polymer act as binding sites for metals. The Gram-negative bacteria cell wall results in a more complex interaction with metals, due to the outer membrane above the peptidoglycan layer. The outer membrane tends to have a chelating effect on metals, similar to the teichoic acid polymer (which is present in Gram-positive bacteria). Some metals get transported through the outer membrane and bind with the underlying peptidoglycan layer. It is also interesting to note that dead cells can adsorb metals, and in the case of

Cd, dead cells will adsorb more than living cells (Beveridge T.J. and Doyle R.J. (eds) 1989).

Three transport mechanisms are recognized for the internalization of metals within a bacterial cell. One way is through "carriers", another possibility is through "specific transport" of metals complexed with ligands, and finally "nonspecific transport" where metals are complexed with substrates that carry the metal through unintentionally via the transport system specific to that substrate (Beveridge T.J. and Doyle R.J. (eds) 1989). The rate and extent of metal sorption to cell surfaces, or internalization, are not well understood, and few studies have been done to determine the rate of these reactions relative to the rate and extent of metal precipitation. Determining the rate of internalization relative to precipitation could be useful in our understanding of metals removal in microbial based AMD treatment systems. A study conducted by Hu et al. (2003) looked at the impact of sorption and internalization for Cu, Zn, Ni, and Cd on nitrification inhibition. They found that inhibition by these metals was directly related to the intracellular fraction of metal, and the slow kinetics for internalization indicated that metal inhibition can easily be under predicted if you only conduct short-term toxicity tests using an LC_{50} approach (Hu.et al. 2003). The fact that LC_{50} could under predict metal inhibition, and little is known about the kinetics of sorption and internalization relative to metal precipitation, we may find that microorganisms within an APTS are actually being greatly inhibited even when a large percentage of the solution phase metals appear to be removed through precipitation based on effluent measurements taken. This suggests that the problems with reliability and longevity for APTS may be related to the delayed observable effects of metal toxicity on the microbial population.

1.2.2 Microbial Adaptation and Increase in Tolerance to Heavy Metals

Several studies have been conducted on mixed cultures, specifically soil microorganisms, to determine metal resistance and increased tolerance capabilities within microbial population. Three factors are usually suggested as the main reason for increased metal tolerance within a microbial community. One suggestion is that the sensitive species are killed, leaving only the metal tolerant species behind to grow. The second hypothesis is that there is a competitive selection for metal tolerance capabilities within the surviving bacteria population. And the third possibility is that bacterial adaptation occurs due to genetic and/or physiological changes (Duxbury T. and Bicknell B., 1983; Díaz-Raviña M. and Bååth E., 1996; Lakzian et al., 2002). It is very likely that all of these possibilities play a role, to one degree or another, in increased metal tolerances observed in mixed culture studies. Duxbury and Bicknell (1983) make the suggestion that phenotypic selection may account for the majority of metal tolerant bacteria present at low metal levels in soil, whereas genetic diversity and metal tolerance could be more important in heavily polluted soils.

1.2.3 Complexation of Metals can Decrease Toxicity

The chemical speciation, or form, of a heavy metal can greatly reduce or enhance a metals toxic effect on a microorganism. When a metal's mobility is decreased via precipitation, for example, or its chemical state won't allow binding to occur on a cells surface, the metal can no longer have a toxic effect. Some examples include hydroxylation of metal species due to changes in pH, a reduced oxidation-reduction potential of the environment could promote the combining of a metal with sulfide ions that immobilize the metal, or the metal could complex with inorganic anions. Naturally occurring organic matter can provide ligand sites that also influence the mobility of a

metal, and this would include compounds such as dicarboxylic acid, amino acid, and humic acid (Beveridge T.J. and Doyle R.J. (eds) 1989). SRB produce HCO_3^- and CO_3^{2-} which can combat toxicity by complexing the metal ions in solution. Fermenting bacteria produce organic acids such as acetate, butyrate, and lactate which can also complex metals, and this will be described further in the discussion section of this report.

There are other ways a metal's toxicity can be affected without changing the chemical speciation or availability of the metal. Water hardness, which is associated with the presence of dissolved alkaline earth ions such as calcium and magnesium can create competition with the metal for cell binding sites (Beveridge T.J. and Doyle R.J. (eds) 1989). Temperature can effect the physiological state of the bacteria, and it has been found that toxicity usually increases when temperature are above optimum growth conditions (Babich H. and Stotszky G., 1983; Szeto C. and Nyberg D., 1979; Huisman et al., 1980).

1.3 The Importance of a Healthy Microbial Community on APTS Performance

Anaerobic Passive treatment systems however are comprised of a complex microbial consortium, the SRB being only one of many different types of bacteria present in a sulfate reducing biozone. The survival of SRB is closely related to the health of the microbial community in which they live. Master's thesis research done by Miranda Virginia Logan, from Colorado School of Mines, looked at the possibility "that sulfate reduction in anaerobic passive treatment systems was limited by one or more upstream microbial activities that function as rate-limiting steps in generating substrate for sulfate-reducing bacteria". Column experiments conducted by Logan showed that nickel inhibited overall sulfate reduction, but when lactate (a known substrate for many sulfate reducers) was added to bioassays of the column material the observed extent of sulfate reduction from inhibited and uninhibited columns were the same. This suggests that the

"upstream" microbial populations were affected by the nickel and were unable to produce the substrates needed by the sulfate reducing population. (Logan 2003).

Logan's results indicated that the hydrolysis of cellulose was the rate-limiting step for the support of sulfate reduction. Because SRB are unable to breakdown cellulose directly for their energy needs they must rely on cellulolytic - fermenting bacteria to provide the necessary substrates, such as lactate and butyrate. Considering the fact that PRB's, constructed wetlands (CW), and APTS are comprised mainly of organic material in the form of cellulose, one can see the need to look at the environmental constraints necessary to maintain a healthy community of cellulolytic - fermenting bacteria, who are responsible for the hydrolysis of cellulose into cellobiose and glucose and subsequent fermentation to lactate and butyrate. A simplified APTS microbial nutrient pathway is shown in Figure 1.1 below, from Hemsi et al (2005).

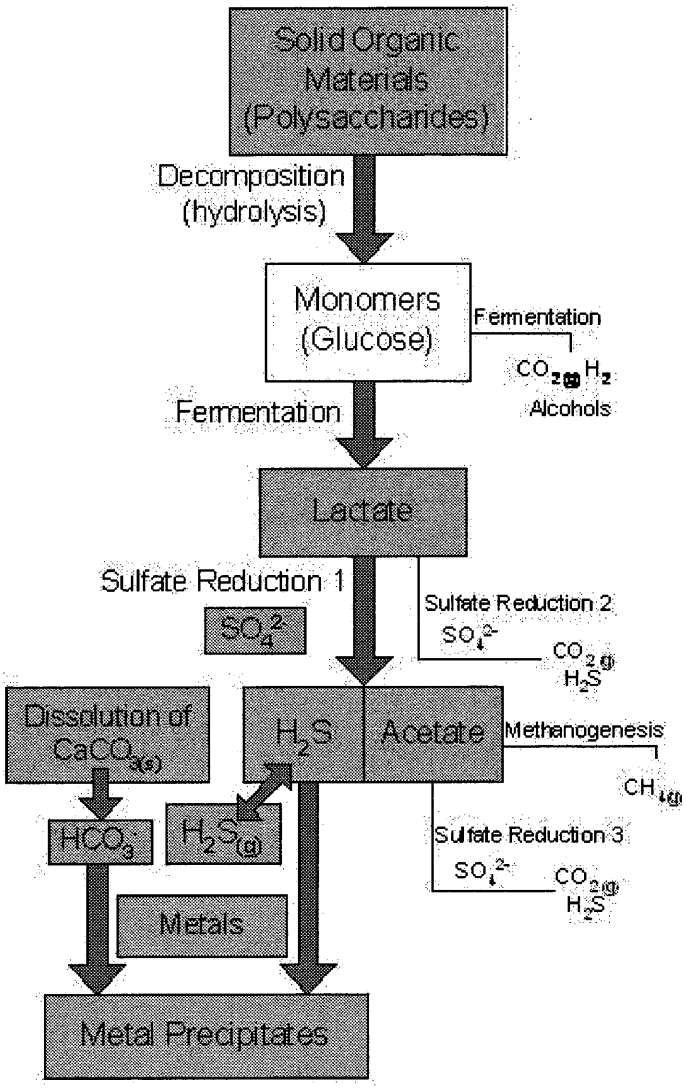

Figure 1.1 Microbial nutrient pathway within an APTS

1.3.1 Cellulolytic-Fermenting Bacteria

Photosynthesis is responsible for the production of plant biomass, which is comprised primarily of cellulose, and life is dependent on the action of cellulose-utilizing

microorganisms present in soil and the guts of animals to break this cellulose down into useable forms for other organisms. Thus, microbial cellulose utilization is responsible for one of the largest material flows on earth. With regard to APTS, cellulose utilization is also an integral component of anaerobic digestion and composting. (Lynd et al. 2002) Although none of the Archaea microorganisms have been found to hydrolyze cellulose, many of the bacteria within the eubacteria are cellulolytic capable. The order *Actinomycetales* (phylum *Actinobacteria*), which are predominantly aerobic, and order *Clostridiales* (phylum *Firmicutes*), predominantly anaerobic, contain many of the known cellulose degraders (Lynd et al. 2002). Table 1.1 below shows the species capable of cellulose degradation, and was compiled and created by Lynd et al. (2002). It is interesting to note, from reviewing Table 1, that cellulose utilization generally proceeds via organisms that are either aerobic or anaerobic. Genus *Cellulomonas* are the only reported facultatively anaerobic cellulose degraders. In addition, a study looking at the physiological properties of *Cellulomonas fermentans* found that cell yield was similar under both aerobic and anaerobic conditions, which suggests that fermentative metabolism is the dominant pathway even in the presence of O_2 for *Cellulomonas* bacteria (Bagnara et al. 1987).

Microorganisms that are capable of degrading cellulose (woody material) and subsequently degrade the glucose byproduct into organic acids, such as lactate and butyrate, are known as cellulolytic-fermenting bacteria. A ubiquitous soil microbe called *Cellulomonas flavigena*, of the order *Actinomycetales,* was examined in the following experiments. *C. flavigena* is a rod shaped, non-spore forming, Gram-positive, facultative anaerobe. This bacteria hydrolyzes cellulose extracellularly to produce glucose which is then up-taken for its energy needs.

Table 1.1 Major morphological features of cellulolytic bacteria

TABLE 1. Major morphological features of cellulolytic bacteria

Oxygen relationship	Genus	Representative species[a]	Gram reaction	Morphology	Growth temp.[b]	Resting state	Motility	Features of cellulase system	References
Aerobic	*Acidothermus*	*A. cellulolyticus*	+	Rod	Thermo			Noncomplexed, cell free	48
	Bacillus	*B. pumilis*	+	Rod	Meso	Endospore	Flagellar	Noncomplexed, cell free	220
	Caldibacillus	*C. cellovorans*	+	Rod	Thermo	Endospore		Noncomplexed, cell free	48
	Cellulomonas[c]	*C. flavigena, C. uda*	+	Rod	Thermo	None	Flagellar	Noncomplexed, cell free	25, 26, 493
	Cellvibrio	*C. fulvus, C. gilvus*	−	Curved rod	Meso	None	Flagellar	Noncomplexed, cell free	612
	Cytophaga	*C. hutchinsonii*	−	Rod	Meso	None	Gliding	Noncomplexed?, cell free?	322, 384
	Erwinia	*C. carotovora*	−	Rod	Meso	None	Flagellar	Noncomplexed, cell free	29
	Micromonospora	*M. chalcae*	+	Filamentous rod	Meso	Spore[d]	Nonmotile	Noncomplexed, cell free	200, 215
	Pseudomonas	*P. fluorescens* var. *cellulosa*	−	Rod	Meso	None	Flagellar	Noncomplexed, cell free	331
	Sporocytophaga	*S. myxococcoides*	−	Rod	Meso	Spore[d]	Gliding	Noncomplexed, cell free	697
	Rhodothermus	*R. marinus*		Rod	Thermo				11, 48
	Streptomyces	*S. reticuli*	+	Filamentous rod	Meso	Spore[d]	Nonmotile	Noncomplexed, cell free	715
	Thermobifida	*T. fusca*	+	Filamentous rod	Thermo	Spore[d]	Nonmotile	Noncomplexed, cell free	777
Anaerobic	*Acetivibrio*	*D. cellulolyticus*	−	Curved rod	Meso	None	Nonmotile	Complexed	327, 387, 589
	Anaerocellum	*D. thermophilum*	+	Rod	Thermo	None	Flagellar	Noncomplexed, cell free	659
	Butyrivibrio	*B. fibrisolvens*	+	Curved rod	Meso	None	Flagellar	Noncomplexed	294
	Caldicellulosiruptor	*C. saccharolyticum*	−	Rod	Thermo	None	Flagellar	Noncomplexed, cell free	549
	Clostridium	*C. thermocellum, C. cellulolyticum*	+	Rod	Thermo, meso	Endospore	Flagellar	Complexed, mostly cell bound[e]	392, 415, 485, 532, 613
	Eubacterium	*E. cellulosolvens*	+	Rod	Meso	None	Nonmotile		699
	Fervidobacterium	*F. islandicum*	−	Rod	Thermo	None	Flagellar		292
	Fibrobacter	*F. succinogenes*	−	Rod	Meso	None	Nonmotile	Complexed, cell bound	88, 294, 463, 645
	Halocella	*H. cellulolytica*	−	Rod	Meso	None	Flagellar	Noncomplexed, cell free	622
	Ruminococcus	*R. albus, R. flavefaciens*	+	Coccus	Meso	None	Nonmotile	Complexed, cell bound	88, 294
	Spirochaeta	*S. thermophila*	+	Spiral	Thermo	None		Noncomplexed, cell free	8, 48
	Thermotoga	*T. neapolitana*	−	Rod	Thermo				48

[a] Not all strains of the indicated species are cellulolytic, and some less active or less studied cellulolytic species within these genera are not listed.
[b] Meso, mesophilic; Thermo, thermophilic.
[c] Most strains can also grow anaerobically.
[d] Unlike true endospores, these spores have only moderate resistance to environmental stress.
[e] Except for *C. stercorarium* (81, 83, 606).

1.3.2 Cellulose Structure

Cellulose is a polysaccharide, comprised of unbranched polymer of glucose residues joined by β-1,4 linkages.(Berg et al. 2002). Cellulose fibers are commonly embedded in a matrix of other structural biopolymers, such as hemicelluloses and lignin, and it is one of the most abundant organic compounds on the planet. Cellulose is a crystalline structure, which is unusual for a polysaccharide. Approximately 30 individual cellulose molecules are assembled into larger units known as elementary fibrils (protofibrils), which are packed into larger units called microfibrils, and these are in turn assembled into the familiar cellulose fibers. (Lynd et al. 2002). The degradation of cellulose is slow, and could be considered the rate limiting step. As cellulose is degraded, cellobiose and glucose are produced, and this is a form that can be directly ultilized by microorganisms for energy.

1.4 Metabolic Kinetics Modeling – Monod Equation

The Monod equation is used to represent bacterial growth kinetics. It is a good equation to represent a smooth transition from a first-order relationship (when substrate concentration is low) to a zero-order relationship (when substrate concentration is high) observed between maximum specific growth rate and substrate concentration (Rittmann B.E. and McCarty P.L. 2001). The basic equations, which represent net specific growth rate of active biomass (μ), and decay of that biomass are represented by equation (1.2), (1.3), and (1.4). Equation (1.5) shows how the rate of change in biomass concentration over time can be calculated when measurements are taken during an experiment.

$$\mu_{syn} = \left(\frac{1}{X_a} * \frac{dX_a}{dt} \right) = \mu_{\max} * \frac{S}{K+S}$$

Equation (1.2)

$$\mu_{decay} = \left(\frac{1}{X_a} * \frac{dX_a}{dt} \right)_{decay} = -b$$

Equation (1.3)

$$\mu = \mu_{syn} + \mu_{decay} = \mu_{\max} * \frac{S}{K+S} - b$$

Equation (1.4)

$$\frac{dX_a}{dt} = \frac{X_{n+1} - X_n}{t_{n+1} - t_n} \;\; ; \;\; X_a = X_n$$

Equation (1.5)

where

$X = biomass\ concentration = \dfrac{mg\_cell\_protein}{L}$

$S = substrate\ concentrations = \dfrac{mg\_glucose}{L}$

$\mu_{syn} = specific\ growth\ rate\ due\ to\ synthesis = \dfrac{1}{hours}$

$\mu_{dec} = specific\ growth\ rate\ due\ to\ decay = \dfrac{1}{hours}$

$\mu_{max} = maximum\ specific\ growth\ rate = \dfrac{1}{hours}$

$K = concentration\ resulting\ at\ half\ the\ maximum\ growth\ rate$

$= \dfrac{mg\_glucose}{L}$

$t = time = hours$

$b = decay\ coefficient = \dfrac{1}{hours}$

$Y = cell\ yield = \dfrac{mg\_cell\_protein}{mg\_glucose}$

By manipulating equation (1.2) above, growth data for a particular microorganism can be modeled, and inhibited growth patterns can be compared back to an optimum growth state. Based on the changes made to the kinetic values in the monod equation the type of inhibition that the microorganism is experiencing can be inferred.

1.4.0 Types of Inhibition

The rate of growth and substrate utilization by microbes can be slowed by inhibitory compounds such as heavy metals, antibiotics, and solvents. Inhibition of an organism's metabolism can occur several ways. Perhaps indirectly the inhibitor causes reduced biomass concentration by affecting a key component of cell function, or perhaps it is more direct, such as inhibiting a specific enzyme necessary for substrate utilization. (Rittmann B.E. and McCarty P.L. 2001). These are just two of the possible pathways by which inhibitors can affect cells.

There are three classic ways a particular enzyme can be affected by an inhibitor: competitive, noncompetitive, and non-specific. An inhibitor may compete with the substrate for the active site of an enzyme, and this would result in an increase in K, because more available substrate is required to overcome the competition of the inhibitor in order to maintain the same net specific growth rate (μ). This is called "competitive inhibition". As for noncompetitive inhibition, both the inhibitor and the substrate can bind simultaneously to the enzyme, which means that the substrate can still bind to the active site of the enzyme. However, the enzyme with the inhibitor and substrate attached will not proceed to form useable product for the microbe. With noncompetitive inhibition K is unaffected, because increasing the amount of substrate will not increase the enzyme activity, and ultimately μ_{max} will decrease. The third type of inhibition is called nonspecific, or mixed, which is produced when a single inhibitor both hinders the binding

of substrate and decreases the enzymes activity (effectively decreasing μ_{max} and increasing K) (Berg et al. 2002).

1.5 Research Objective

To date, very little work has been done to determine the toxicity affects of metal ions on the bacteria that hydrolyze cellulose. Without resolving the inhibitory effects of metals on bacteria such as the cellulolytic - fermenters, we could fail to completely understand the applicability of APTS. By determining the toxicity thresholds of common AMD heavy metals, such as copper and zinc, we may be able to predict in advance where anaerobic wetlands or sulfate reducing bioreactors will be successful, and mitigate some unnecessary costs associated with installing APTS in locations where long-term benefits cannot be achieved. By recognizing realistic limitations of APTS we can begin to focus on ways to supplement or compliment APTS and improve AMD passive treatment technologies.

In an effort towards improving our understanding of APTS, the toxic effects of copper and zinc ions were examined for a cellulolytic - fermenting bacteria, specifically *Cellulomonas flavigena*. The following two hypotheses were established: 1) *C. flavigena* will experience greater inhibition by copper and zinc then found for SRB's and 2) copper will be more toxic than zinc. The first hypothesis seemed likely because SRB produce H_2S gas which can complex metals and protect them from metals toxic effects. The second hypothesis is based on prior research conducted on other microorganisms, where copper was found to be more toxic than zinc (Utgikar et al. 2003).

CHAPTER 2 MATERIALS AND METHODS

2.1 Experimental Approach

A ubiquitous soil microbe called *Cellulomonas flavigena*, was examined in the following experiments. This bacterium hydrolyzes cellulose extracellularly to produce glucose which is then up taken for its energy needs. We chose to use glucose for kinetic experiments, rather than cellulose, because glucose is the substrate directly utilized by the microbes for energy and growth. The fermentation of glucose occurs much more rapidly than the hydrolysis of cellulose, which also allowed the experiments to run for a shorter time frame. Toxicity effects were determined based on inhibition of final cell protein concentration and decreased growth rates. This approach was also used by several other toxicity studies conducted on SRB (Poulson et al., 1997; Sani et al., 2001; Utigikar et al., 2001; Utigikar et al., 2003).

2.1.1 Experimental Method Based on Substrate Utilization

The original approach for determining metal inhibition on *C. flavigena* was to assess the metal's effects on metabolic activity. Activity was directly correlated with rate of substrate utilization over a 9 hour period keeping biomass constant. Glucose is the energy source for *C. flavigena*, and the rate of substrate utilization could be inferred for each serum bottle from the amount of glucose consumed during the experiment. Glucose concentration was measured every one to two hours, along with the pH, cellular biomass, and solution phase metals concentration. *C. flavigena* was concentrated down by centrifuging in order to obtain the appropriate final protein concentrations of 250 mg/L

and 500 mg/L within each serum bottle. High cell concentrations were used to simulate a healthy population. By having two different cell protein concentrations one could determine if cell biomass could have an effect on metal inhibition. All experiments were done in quadruplicate, and 2 different concentrations of zinc were examined for toxicity effects. Unfortunately, no significant difference could be found between control bottles containing no zinc, and the zinc containing bottles, with respect to rate of glucose consumption. This was due to slower consumption rates than anticipated, which was likely caused by the change in substrate from beef broth to strictly glucose, and moving the bacteria from an aerobic to an anaerobic environment. Based on these findings, metal inhibition needed to be measured by other means

2.1.2 Experimental Method Based on Growth

The second approach examined the inhibition of growth caused by the presence of zinc or copper, rather than inhibition in rate of substrate utilization. This approach has been performed by many other researchers who looked at metal toxicity on sulfate reducing bacteria (SRB) (Poulson et al., 1997; Sani et al., 2001; Utigikar et al., 2001; Utigikar et al., 2003), and would allow for better comparisons to be made with previous research findings. The experiments were performed in capped, sterile, 125 mL serum bottles which contained a lab created nutrient broth emulating media used to grow and isolate *C. flavigena* (Starr et al. 1981). Table 2.1 below gives the exact content and concentration of ingredients of the lab created nutrient broth.

Table 2.1 Nutrient broth used for toxicity experiments

Compound	Concentration
NH_4Cl	500 mg/L
K_2HPO_4	250 mg/L
$MgSO_4$	250 mg/L
KCl	250 mg/L
Yeast Extract	125 mg/L
PIPES Buffer $C_8H_{16}N_2O_6S_2K_2$	11.36 g/L
Glucose	1000 mg/L

Metals added	Concentration (as Cu or Zn)
$CuCl_2*2H_2O$	0, 0.13, 0.16, 0.2, 0.26, 0.38, 0.51, 0.57 mg/L
$ZnCl_2$	0, 0.28, 0.4, 0.5, 0.8, 1, 1.5 mg/L

Step #1 of the experiment required that the contents of a 2 mL freezer vial, containing *C. flavigena*, be placed in a serum bottle using a disposable sterile needle and syringe, and the bacteria was allowed to grow for 5 days, slowly depleting the oxygen inside the bottle and allowing for maximum cell density. After 5 days of acclimating the bacteria to new media and anaerobic conditions, 2 mL of liquid from the step #1 bottles was removed and placed into new serum bottles that had been purged with argon, to create anaerobic conditions, and contained fresh media (Step #2). The biomass was tracked over a five day period, and the maximum cell density was established within 4 to 5 days. Once the maximum cell density had been achieved 2 mL of liquid from the step #2 bottles was inoculated into (Step #3) anaerobic serum bottles, containing nutrient broth and various concentrations of zinc or copper. Experiments (Step #3) were conducted over a 10 day period, because this was when total cell mass began to decline in the control bottles. All experimental bottles were performed in quadruplicate. Samples were taken throughout

the experiment to measure glucose consumption, biomass concentration, solution phase metals concentration, organic acid production, and pH changes.

2.2 Preparation of *C. flavigena* for Experiments

A pure culture was used, specifically *Cellulomonas flavigena* (ATCC 482), purchased from the American Type Culture Collection (Rockville, MD). The microbes were grown in 250 mL autoclaved Erlenmeyer flasks containing beef nutrient broth, base for nonfastidious microorganisms (ISO 9000 registered, 8 g/l; Difco, Sparks, Md.) (Sani et al. 2002). Inoculation of the bacteria was completed under a sterile hood and the flasks were plugged with styrofoam in order to avoid any microbial contamination while still allowing for the diffusion of oxygen. *C. flavigena* was grown at ambient temperature on a shaker table under aerobic conditions to speed up the growth process. *C. flavigena* was allowed to grow aerobically for 36 hours before being concentrated down by centrifuging at 10,000 g (the acceleration of gravity, $1g = 9.8\ m.s^{-2}$) for 10 minutes, and then being re-suspended in sterile broth and glycerol (for freezing preparation) and aliquated into 2 mL freezer vials and placed into a -80°C freezer until required for experiment.

2.2.1 Agar Plating to Insure Purity

Using beef nutrient broth, base for nonfastidious microorganisms (ISO 9000 registered, 8 g/l; Difco, Sparks, Md.) agar plates were created to grow colonies of *C. flavigena*. Under sterile conditions *C. flavigena* from the freezer vials were inoculated onto the plates and allowed to colonize for 24-48 hours. Fuzzy, pale yellow colonies were the characteristic for *C flavigena*, and this was primarily the basis for insuring a

pure culture. If other types of colonies formed it could be determined that contamination had occurred. Contamination was never observed during experiments.

2.2.2 Growth Conditions During Experiment

Step #1: A 2 mL freezer vial, containing *C. flavigena*, was placed in a sterile serum bottle containing lab prepared nutrient broth using a disposable sterile needle and syringe. *C. flavigena* was allowed to grow for 5 days at ambient room temperature on a shaker table at a slow agitation (175 rpm). Over the 5 day period the oxygen inside the bottle was slowly depleted and allowed *C. flavigena* to acclimate to the new environment and reach maximum cell density. Step #1 was conducted in duplicate to insure no contamination when inoculating into the next step. 2 mL from step #1 was placed in Step #2 serum bottles which contained the same nutrient broth (final volume equal to 100 mL), and were purged with argon prior to inoculation to maintain anaerobic conditions. Step #3 was inoculated from Step #2 once maximum cell density was achieved (4 to 5 days, at a cell concentration of 25 mg/L). Step #3 contained varying concentrations of metals, and effects were observed over a 10 day period. All experiments were conducted at ambient room temperature and serum bottles were continually agitated at a moderate level (175 rpm).

2.2.3 Creating an Anaerobic Environment

One crucial aspect of APTS, in which microbial treatment occurs, is the absence of oxygen. Therefore, it was necessary to perform all of the experiments as anaerobic batch studies. The 125 mL serum bottles were closed with a rubber septum and a metal crimp. They were then purged with argon for 30 minutes at 40 psi, and a redox dye

indicator (Resazurin) was used at a concentration of 0.5 mg/L, in non-experimental bottles containing a high concentration of cells for reducing potential, to insure anoxic conditions were established, as well as maintained throughout experiments. Before samples were taken from the serum bottles both needle and syringe were purged 3 times with argon. Argon gas was also put into serum bottles to replace the volume of liquid and gas removed for sampling to maintain a slightly positive pressure gradient with the outside atmosphere. Argon was used because it is an inert gas. CO_2 could not be used because the formation of carbonic acid and related species would occur as the CO_2 dissolved in water, which would cause fluctuations in pH as well as interact with the zinc in solution.

2.2.4 Buffers and pH requirements

Microbial activity is affected by pH, thus a buffer called PIPES ($C_8H_{16}N_2O_6S_2K_2$; 378.54 g/L) was used to minimize pH changes during the experiments. This buffer was chosen for a couple of reasons, one being that it is known for successfully autoclaving (no variation of pH is noted after autoclaving, pK_a of 6.8), and secondly, this buffer is very unlikely to complex and/or form a solid with zinc or copper. A concentration of 30 mM of PIPES was used for all serum bottle, and the pH was adjusted to 7.

2.3 Conditions Monitored Throughout Experiment

Several conditions were monitored throughout the experiments. Growth was monitored to establish inhibition relative to growth in control bottles. Glucose consumption was measured 3 to 4 times during the 10 day experiments to determine rate of substrate utilization at varying metal concentrations. Metals concentration was

analyzed at the beginning and the end of each experiment to verify that concentrations were maintained throughout. Analysis of organic acid production was also conducted at the beginning, middle, and end of experiments to establish amounts, types, and possible changes in fermentation products (duplicates were run for each sample). And finally, to assure that environmental conditions, such as optimal growth pH and anaerobic conditions, were maintained throughout, pH was monitored and resazurin containing bottles were used along side experimental bottles. Every bottle was performed in quadruplicate to insure accuracy of sample measurements and all data values used for interpretation were the average of the 4 replicates.

2.3.1 Monitoring Growth: Optical Density versus Coomassie Protein Assay

The log growth phase for *Cellulomonas* was determined in aerobic conditions at ambient temperature, by taking multiple Optical Density readings throughout a 40 hour period, which showed that the culture was well into a log growth phase within 24 hours. Optical Density was measured on a spectrophotometer at a wavelength of 600 nm. Dry weight analysis using a Mettler Toledo MT5 scale with an accuracy of +/- $1x10^{-4}$ grams, was compared back to Optical Density and Coomassie Protein Assay readings that were taken on a Beckman Coulter DU800 spectrophotometer. Coomassie Protein Reagent Kit contains a dye that works by binding with amino acids such as arginine and lysine, which absorb light at 595 nm. Known concentrations of bovine albumin protein were used to create a standard curve, and cellular protein concentration for *C. flavigena* could be established and compared to optical density readings. Cellular protein concentration was determined to be roughly 25% of the dry weight. The Coomassie procedure proved to be quite accurate and time efficient. The Coomassie protocol used during these experiments was established by Sani et al. (2001).

2.3.2 Monitoring Glucose Concentration

Each serum bottle initially contained 1000 mg/L of glucose. A colorimetric method was used for determining the concentration of glucose throughout the experiment (Dubois et al., 1956.). The phenol – sulfuric acid assay is a broad spectrum method for carbohydrates, which measures both mono- and polysaccharides. A calibration curve using known concentrations of glucose was created for determining glucose concentrations in the experimental bottles at any given time. Samples taken from experimental bottles were centrifuged, to remove liquid from cell mass, and the decant was then frozen and analyzed within 24 hours of when sample was taken to insure no further consumption of glucose would occur beyond sampling time. Samples were taken at time zero, 24 hours, 72 hours, and 240 hours. All absorbance readings were performed at a wavelength of 490 nm.

2.3.3 Solution Phase Metals Analysis

The desired concentration of either copper or zinc was calculated and added to the designated bottles, and samples were taken at the beginning and end of the experiment for Inductive Coupled Plasma Atomic Emissions Spectrometer (ICP-AES) analysis (Perkin Elmer, Optima 3000). This was done in order to quantify the amount of copper or zinc that remained in solution relative to the initial metal concentration. Quality control standards (CCV), for both metals and non-metals were run at the beginning, after every 15 samples, and at the end to insure instrument accuracy and precision.

2.3.4 Analysis of Organic Acid Production

As *C. flavigena* consumes glucose organic acids are produced, and the type and extend of organic acid production can be measured using a High Performance Liquid Chromatography (HPLC) machine. HPLC uses a refractory index detection to determine which organic acids are produced and at what concentration relative to known standard solutions. A ChemStation Agilent 1100 Series HPLC was used to analyze samples, and the organic acids such as acetate, lactate, butyrate, formate, succinate, and propionate were examined for their possible presence and concetration within each experimental sample. Samples were taken at the beginning, middle and end of experiments. Samples taken from experimental bottles were centrifuged, to remove liquid from cell mass, and the decant was then frozen to insure no further consumption of glucose would occur beyond sampling time.

2.4 Modeling Data: Monod Equation

Growth and substrate consumption patterns for experimental data were modeled using the Monod Equation. The Monod equation is used to represent bacterial growth kinetics. It is a good equation to represent a smooth transition from a first-order relationship (when substrate concentration is low) to a zero-order relationship (when substrate concentration is high) observed between maximum specific growth rate and substrate concentration. (Rittmann B.E. and McCarty P.L., 2001). Constant kinetic values in the model can be determined for control bottles containing no zinc or copper, and these values can be adjusted to better fit growth and glucose consumption patterns observed in zinc or copper containing bottles. Based on the changes made to kinetic values (K and μ_{max}) within the Monod equation, one can then determine the possible type of inhibition experienced by *C. flavigena* at that particular copper or zinc concentration.

It is likely that competitive inhibition of the substrate enzyme is occurring when K is increased to get the model to fit the data, and noncompetitive inhibition when μ_{max} is decreased to fit the model to the data (the rationale for this was discussed previously in the background section of this paper). Table 2.2 below is a list of symbol definitions and units for Monod variables, and equations (2.1), (2.2), and (2.3) show the kinetic equations used for modeling the data collected from this research.

Table 2.2 Typical monod constant units used during this experiment:

$$X = Biomass\_Concentration = \frac{mg\_cell\_protein}{L}$$

$$S = Substrate\_Concentration = \frac{mg\_glu\cos e}{L}$$

$$\mu_{max} = Maximum\_Specific\_Growth\_Rate = \frac{1}{hours}$$

$$K = \frac{mg\_glu\cos e}{L}$$

$$t = Time = hours$$

$$b = Decay\_Cons\tan t = \frac{1}{hours}$$

$$Y = Cell\_Yield = \frac{mg\_cell\_protein}{mg\_glu\cos e}$$

To solve for biomass concentration at a given point in time, the equation for overall net specific growth rate (Eq 1.4), and substituting in Equation (1.5) where applicable, the following Equation (2.1) is achieved.

$$X_{n+1} = X_n + \left[\left(\frac{\mu_{max} * S_n * X_n}{K_s + S_n} * (t_{n+1} - t_n)\right) - b * X_n * (t_{n+1} - t_n)\right]$$

Equation (2.1)

Rate of substrate utilization:

$$\left(\frac{1}{X_a} * \frac{dS}{dt}\right) = \mu_{\max} * \frac{S}{K+S} * \frac{1}{Y} \quad ; \quad \frac{dS}{dt} = \frac{S_{n+1} - S_n}{t_{n+1} - t_n}$$

Equation (2.2)

To solve for substrate concentration at a given point in time, the above equation must be rearranged to Equation (2.3).

$$S_{n+1} = \left(S_n + \left[\frac{\mu_{\max} * S_n * X_n}{K + S_n} * \frac{1}{Y}\right]\right) * \left(t_{n+1} - t_n\right)$$

Equation (2.3)

CHAPTER 3 EXPERIMENTAL RESULTS AND DISCUSSION

3.1 Growth Kinetics for *C. flavigena*: Dry Weight

To determine microbial doubling time and when *C. flavigena* would be in exponential growth phase, dry weight was measured at several points in time during a 48 hour period. Figure 3.1 below shows that *C. flavigena* is well into an exponential growth phase within 24 hours under aerobic conditions. When determining *C. flavigena*'s growth curve pattern, a 500 mL flask, containing 250 mL of inoculated broth, was kept growing for up to two weeks as a "stock" inoculum for growth tests. All flasks were inoculated with 10 mL from "stock" flask, which had been growing *C. flavigena* for 48 hours. At 48 hours the cell concentration (dry weight) in this flask was roughly 300 mg/L. When 10 mL of this broth was transferred to 90 mL of fresh broth, the new cell concentration was roughly 25 mg/L. Figure 3.1 below shows the average growth curve for *C. flavigena* under aerobic conditions, and based off of this graph, the doubling time seems to be around 12-14 hours.

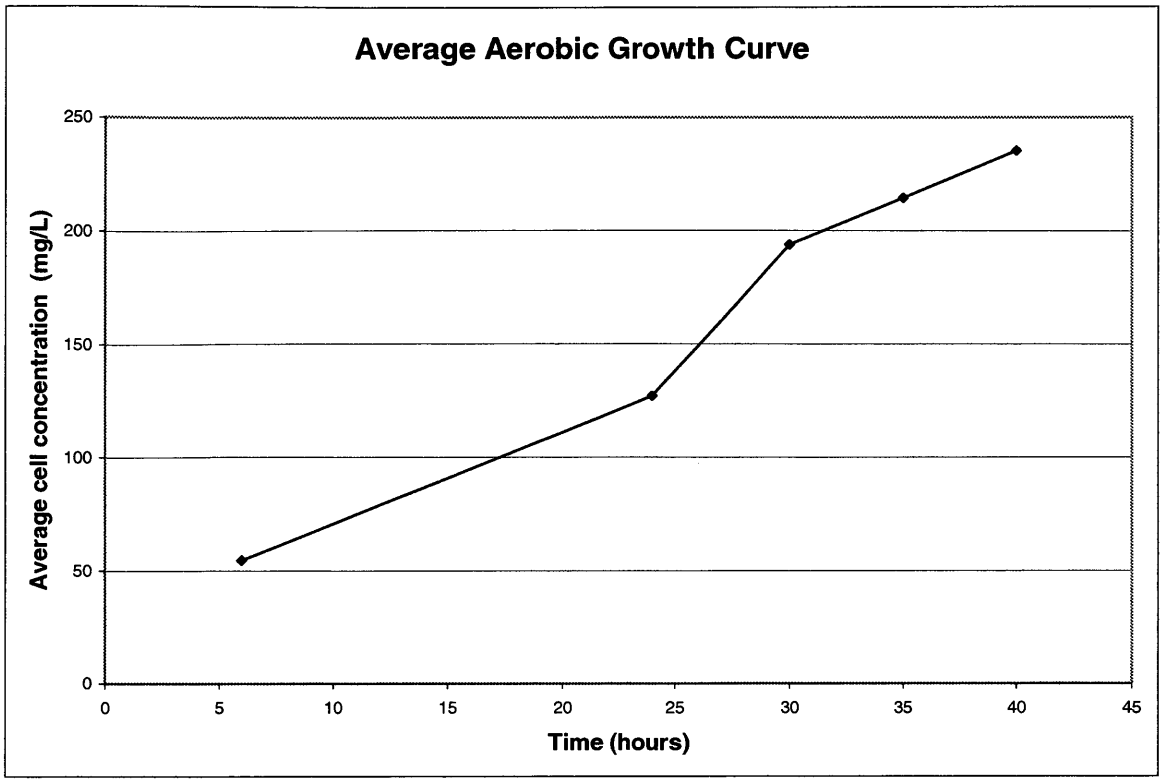

Figure 3.1 Growth curve for *C. flavigena*

3.2 Spectrophotometer Calibration Curves

Sample measurements for cell protein and glucose were conducted on the spectrophotometer. These measurements were put into equations that were generated through standard calibration curves in order to determine actual concentrations. The calibration curves were created by taking spectrophotometer readings of known cell protein and glucose concentrations. Using the spectrophotometer for cell concentration measurements was more efficient than counting cells via the microscope.

3.2.1 Optical Density Calibration Curve

Optical Density is a very quick way to determine a correlation between cell concentration and absorbance readings on the spectrophotometer. The cell concentration was determined through dry weight analysis, and a linear equation represents the relationship between dry weight and absorbance values quite well. Figure 3.2 below demonstrates the relationship between dry weight measurements and the corresponding absorbance reading for *C. flavigena*.

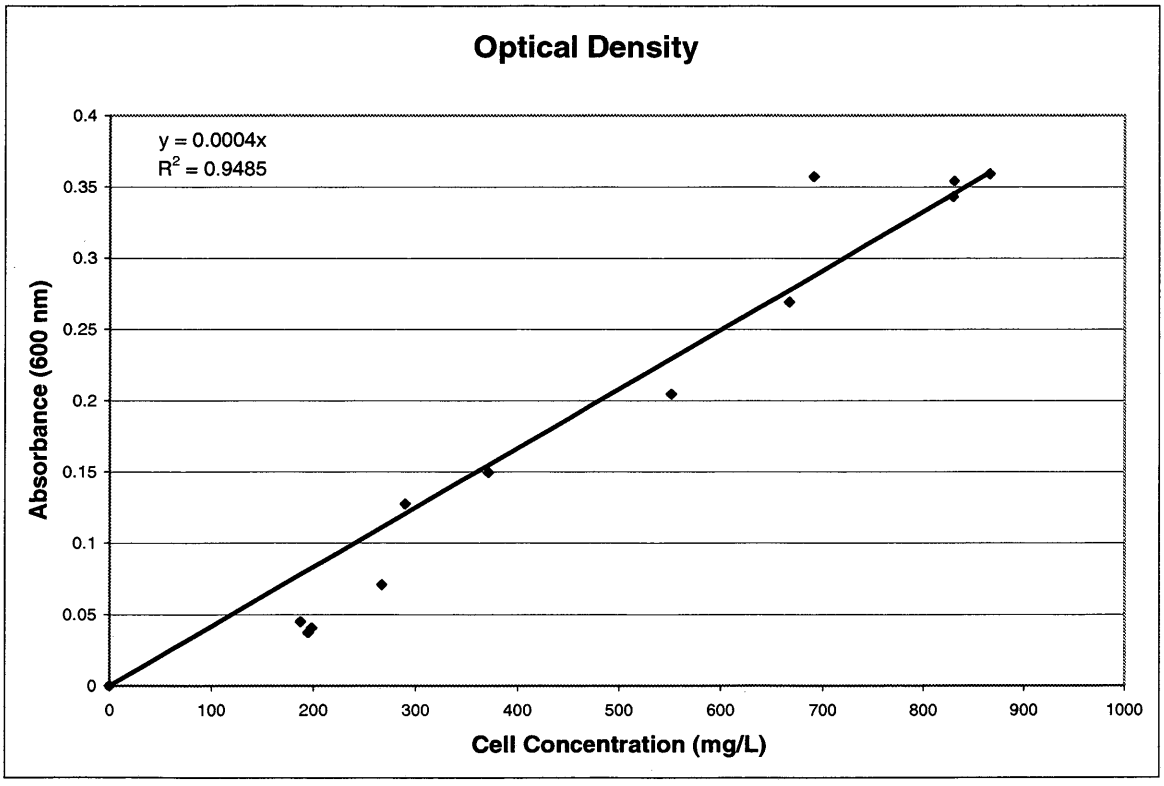

Figure 3.2 Optical density curve

3.2.2 Coomassie Protein Assay Calibration Curve

Although optical density is a quick way to determine cell concentration, it is not as accurate as cell protein assessment using a Coomassie Protein Assay. Known concentrations of bovine albumin protein were used to create the standard calibration curve, and cellular protein concentration for *C. flavigena* could be established and compared to optical density readings. Figure 3.3 and Figure 3.4 represent two of the calibration curves used to establish an equation for calculating changes in cell protein during experiments.

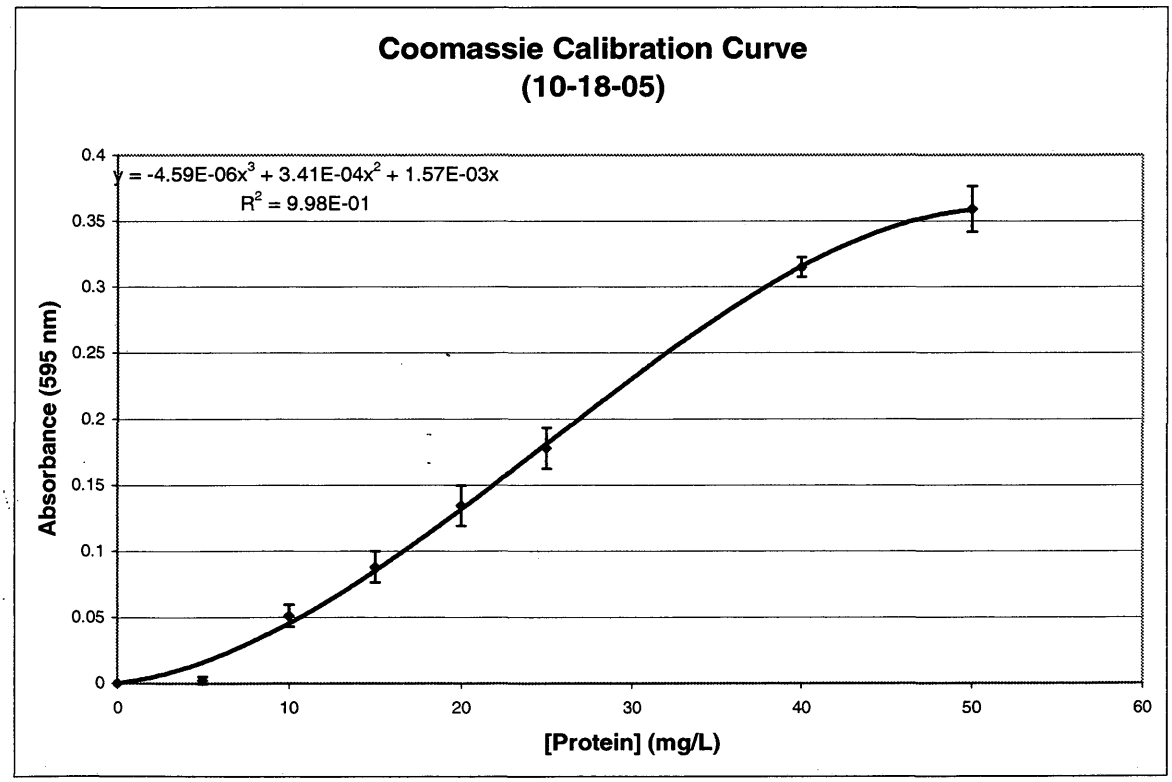

Figure 3.3 Coomassie protein assay calibration curve (10-18-05)

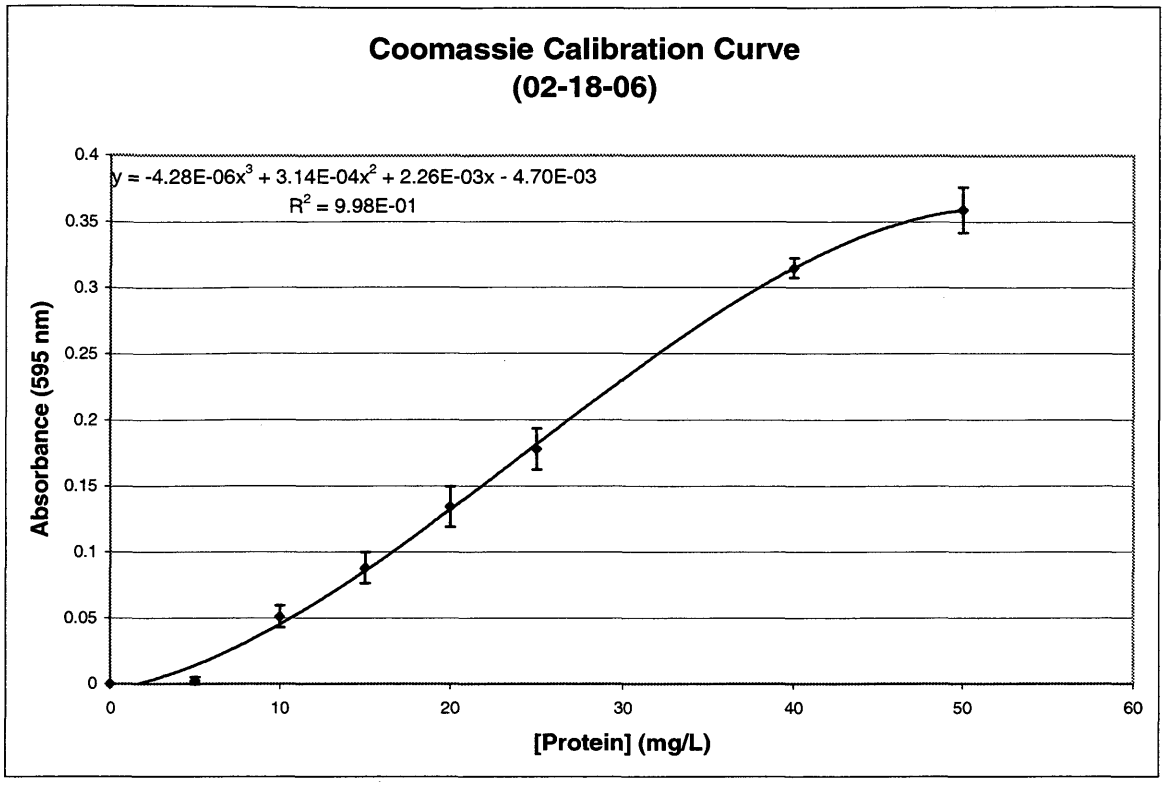

Figure 3.4 Coomassie protein assay calibration curve (02-18-06)

These curves were created before each set of experiments and standards were run with every 15 samples to insure that the equation accurately represented the spectrophotometer readings. As can be seen for the equations listed on the top left corners of Figure 3.3 and 3.4, very little change was observed over a four month period. The best fitting equation was a third power polynomial, and the cell protein concentration was calculated using the solver function in Microsoft Excel. Figure 3.5 below compares coomassie absorbance readings for standards in DI water versus the nutrient broth, and because very little variation is observed, the equations generated from the DI calibration curves were used to make all cell protein calculations.

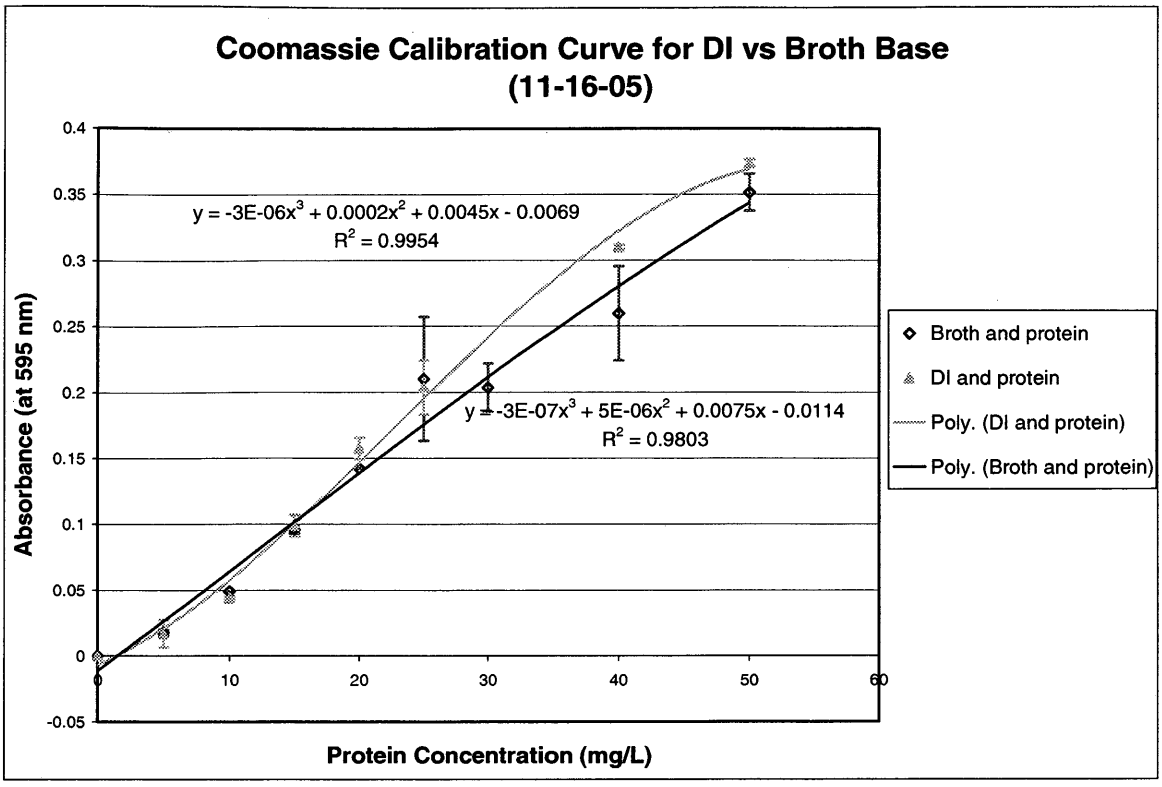

Figure 3.5 Comparison of coomassie absorbance with DI versus nutrient broth

3.2.3 Comparison of Optical Density and Coomassie Cell Protein Values

To allow for comparison of cell protein values of *C. flavigena* with actual cell mass, absorbance readings for both coomassie and optical density (correlated back to dry weight) were conducted on the same set of samples. Table 3.1 below shows the correlation between cell protein and dry weight of cell. For *C. flavigena*, approximately ¼ of the total dry weight is due to cell protein.

Table 3.1 Correlation between cell protein and dry weight of cell

Dry weight cell conc. (mg/L)	Cell Protein (mg/L)	Factor diff. for [Protein] vs [Cell]
289.86	90	3.22
266.64	86	3.10
371.7	127	2.93
690.78	165	4.19
666.64	150	4.44
551.43	140	3.94
829.4	187	4.44
830.6	199	4.17
866.27	160	5.41
Avg. Factor of Diff.		**3.98**

3.2.4 Glucose Calibration Curve

A Colorimetric method was used for determining the concentration of glucose throughout the experiment (Dubois et al., 1956.). Calibration curves using known concentrations of glucose were created before each set of experiments and standards were run with every 15 samples to insure that the equation accurately represented the spectrophotometer readings. All absorbance readings were performed at a wavelength of 490 nm. A linear equation fit the data very well, as can be seen from the R^2 value in Figure 3.6 below.

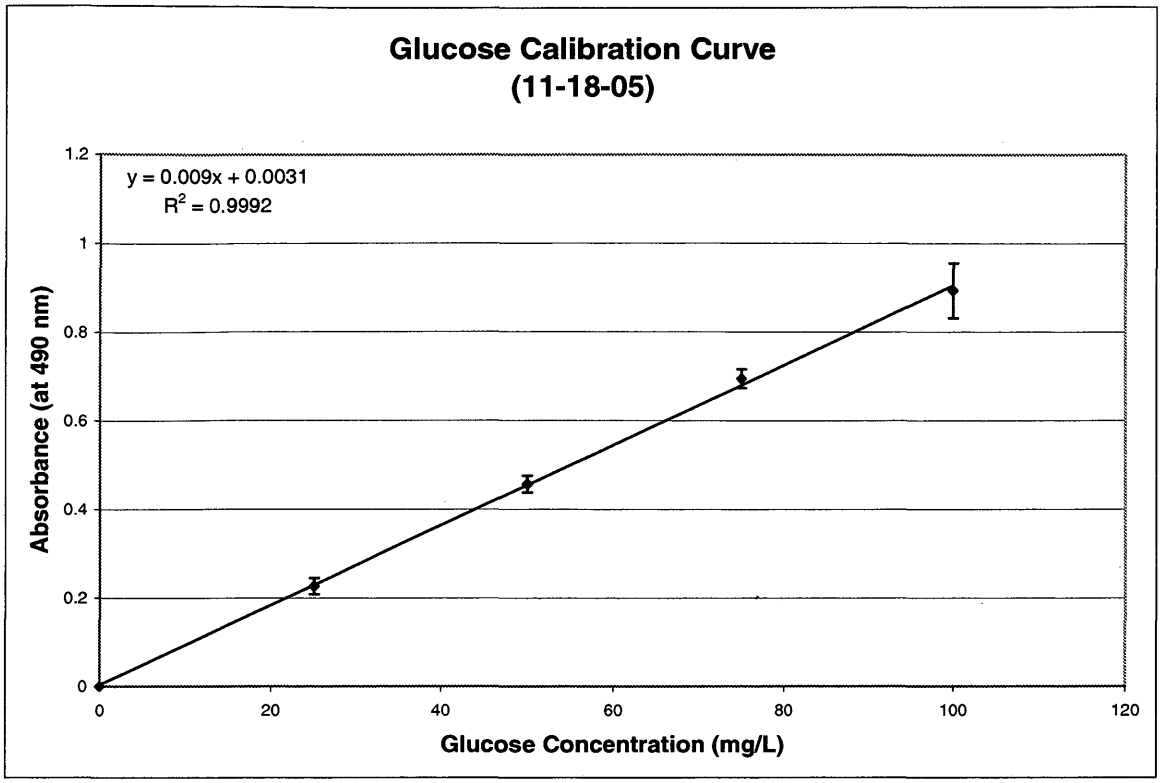

Figure 3.6 Glucose Calibration Curve

3.3 Copper Results

Concentrations of copper ranging from 0 μM to 50 μM (3.2 mg/L) were used for the experiments. The determination of a threshold concentration at which cell growth would not occur, and/or the establishment of an LC_{50}, was the goal of these experiments. Since experiments were conducted in batch, using serum bottles, the experiments were run until cell concentration declined in the control bottles, which was 10 days (240 hours) for *C. flavigena*. As noted in the materials and method section, samples were taken periodically throughout experiments to determine changes in cell, glucose, and solution phase metal concentrations, organic acid production, and pH. Every bottle was

performed in quadruplicate to insure precision of sample measurements and all data values used for interpretation were the average of the 4 replicates.

3.3.1 Growth Curves

The first experiment only examined the effects of two concentrations of copper on cell growth. Sani et al. (2001) found copper at a concentration of 16 μM caused 50% inhibition in final cell protein for *Desulfovibrio desulfuricans*, and based on these findings, 15 μM seemed like a good starting place for *C. flavigena*. Since initially there was no way to know what copper concentration would cause significant inhibition, a higher concentration of 50 μM was also examined. Figure 3.7 shows the results from the first growth experiment.

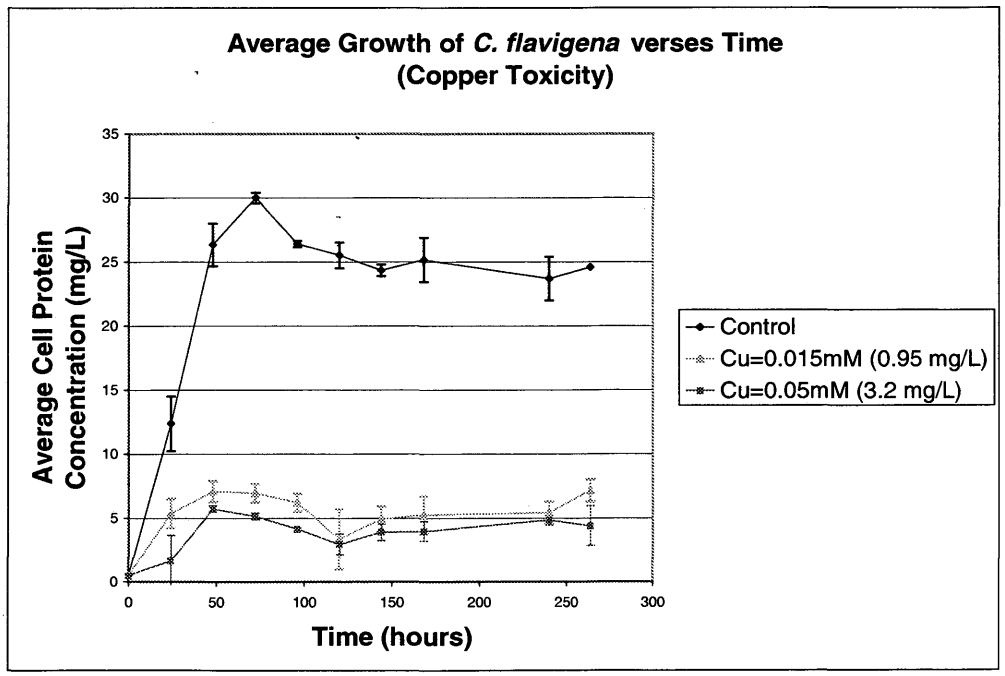

Figure 3.7 Growth curves at copper concentrations of 0 μM, 15 μM, and 50 μM

Lower concentrations of copper needed to be examined to determine a threshold concentration and/or to establish an LC_{50} for cell growth. Figure 3.8 represents the growth curves for copper concentrations ranging from 0 μM to 9 μM.

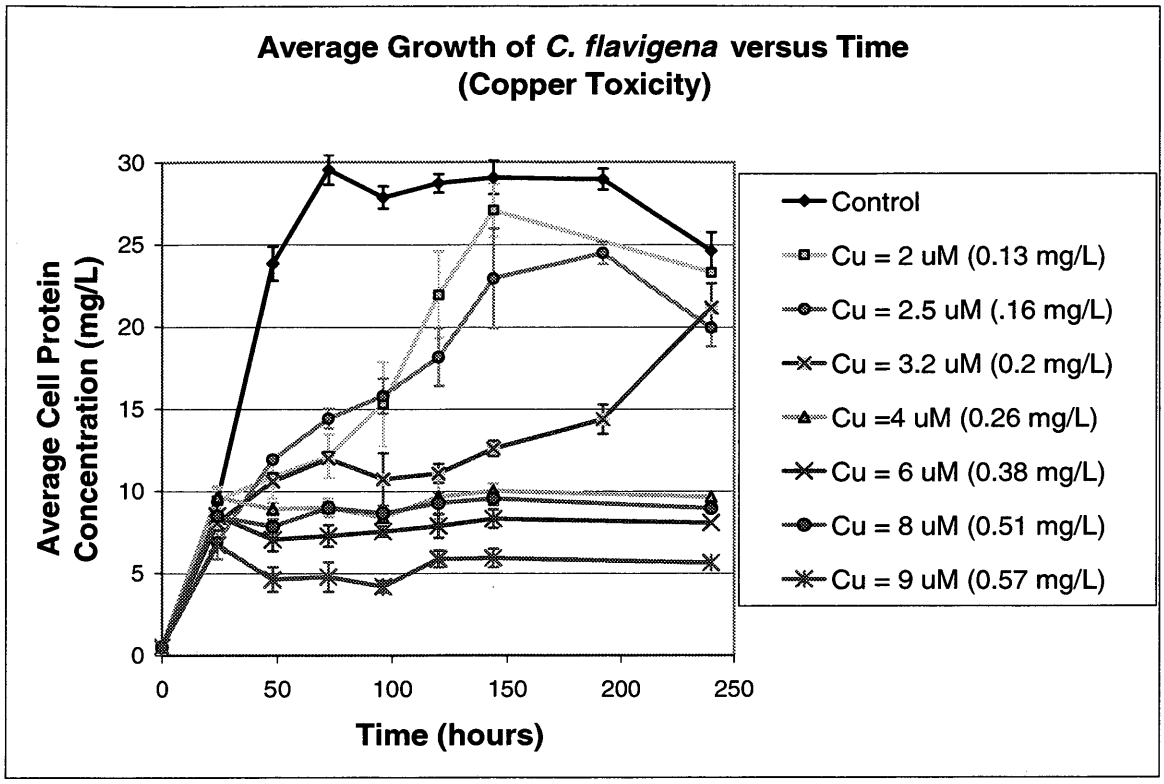

Figure 3.8 Growth curves at copper concentrations of 0 μM to 9 μM

There are 4 things to notice on Figure 3.8. First thing to note is that the copper containing bottles for the initial 24 hours of the experiment showed very little inhibition in growth relative to the control bottles. Secondly, it appears that a copper toxicity threshold is achieved between 0.2 mg/L and 0.26 mg/L. Thirdly, at a copper concentration of 0.2 mg/L (3.2 μM), both a lag in growth and a decrease in growth rate is observed. For copper concentrations at or below 0.16 mg/L (2.5 μM) only a decrease in growth rate is observed. This phenomenon would best be described as growth inhibition.

The fourth thing to note is if the length of time of the experiment was shortened by 4 days then a different conclusion would have been drawn. Rather than establish a toxicity threshold, a LC_{50} approach could have been used to explain toxicity after 6 days, because the final total cell protein seemed to decrease with increasing copper concentrations. Had the experiments been stopped after 6 days it would have been appropriate to establish the percent inhibition of the total cell protein relative to the control bottles (or establish a LC_{50}), but since the experiments were run for 10 days, it is clear that *C. flavigena* is able to recover from the inhibitory effects of copper concentrations at or below 0.2 mg/L (3.2 μM), then establishing a LC_{50} would not accurately represent the data. The best way to describe the toxic effects experienced by *C. flavigena* would be to separate the findings into two categories, as either inhibition in growth rate or toxicity threshold.

3.3.2 Glucose Consumption Curves

Each serum bottle initially contained 1000 mg/L of glucose. Samples taken from experimental bottles were centrifuged, to remove liquid from cell mass, and the decant was then frozen and analyzed within 24 hours of when sample was taken to insure no further consumption of glucose would occur beyond sampling time. All absorbance readings were performed at a wavelength of 490 nm. Figure 3.9 represents glucose consumption at copper concentrations ranging from 0 μM to 9 μM.

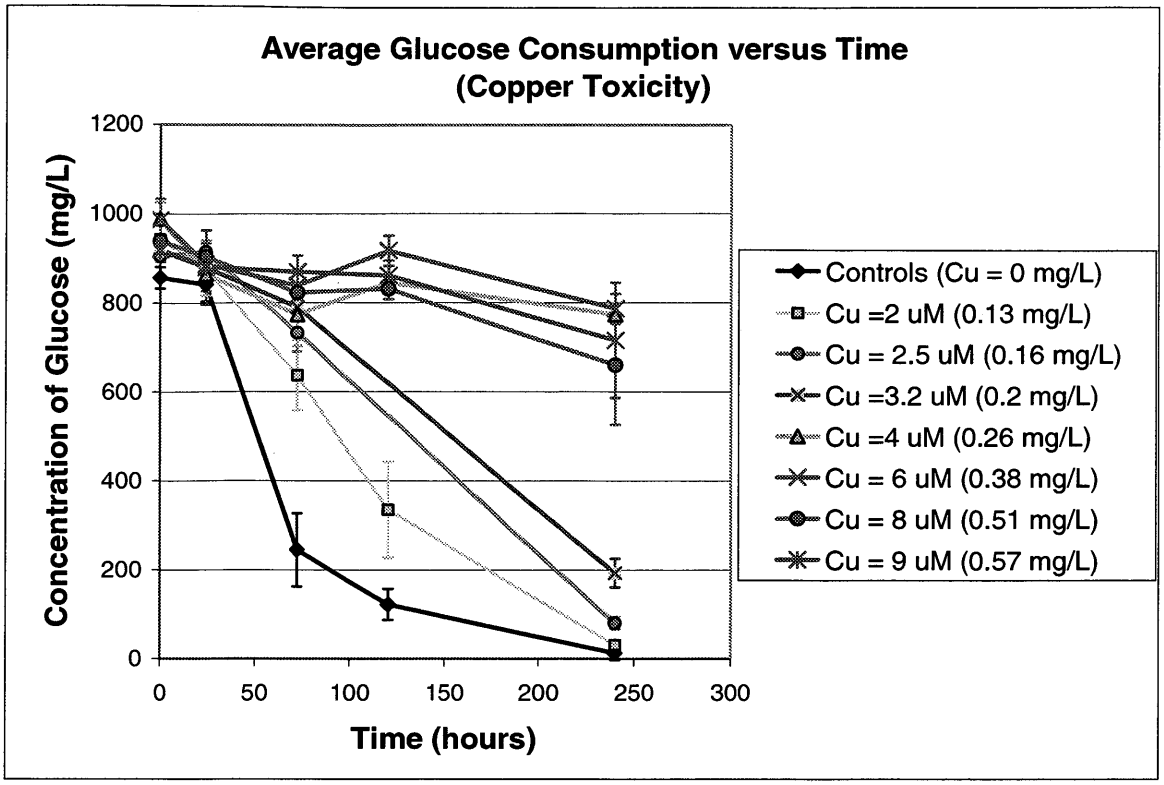

Figure 3.9 Glucose consumption for copper concentrations of 0 μM to 9 μM

There are three patterns that stand out on Figure 3.9. First, there appears to be very little consumption of glucose during the initial 24 hours of the experiment. That means that *C. flavigena* did not use the glucose provided initially for growth needs when placed in the experimental bottles, and that perhaps food stored within the cell was available for energy and synthesis needs during the first 24 hours. This is plausible because the bacteria originally came from an optimal growth environment. Secondly, the toxicity threshold observed for growth at copper concentrations at or greater than 0.26 mg/L (4 μM) is reflected in the glucose consumption data. A very slow rate of glucose consumption is observed in these bottles, which is likely due to the low biomass concentrations present during the experiment. Thirdly, a reduced glucose consumption

rate is seen in bottles containing copper concentrations between 0.13 mg/L and 0.2 mg/L, which compliments the reduced growth rates observed in these bottles.

3.3.3 Solution Phase Metals Analysis

Copper concentration for the beginning and the end of the 10 day experiments was verified through ICP (AES) analysis. This was done to insure that the proper concentration of copper was added and maintained throughout the experiment. The results from ICP analysis are summarized in Figure 3.10 below.

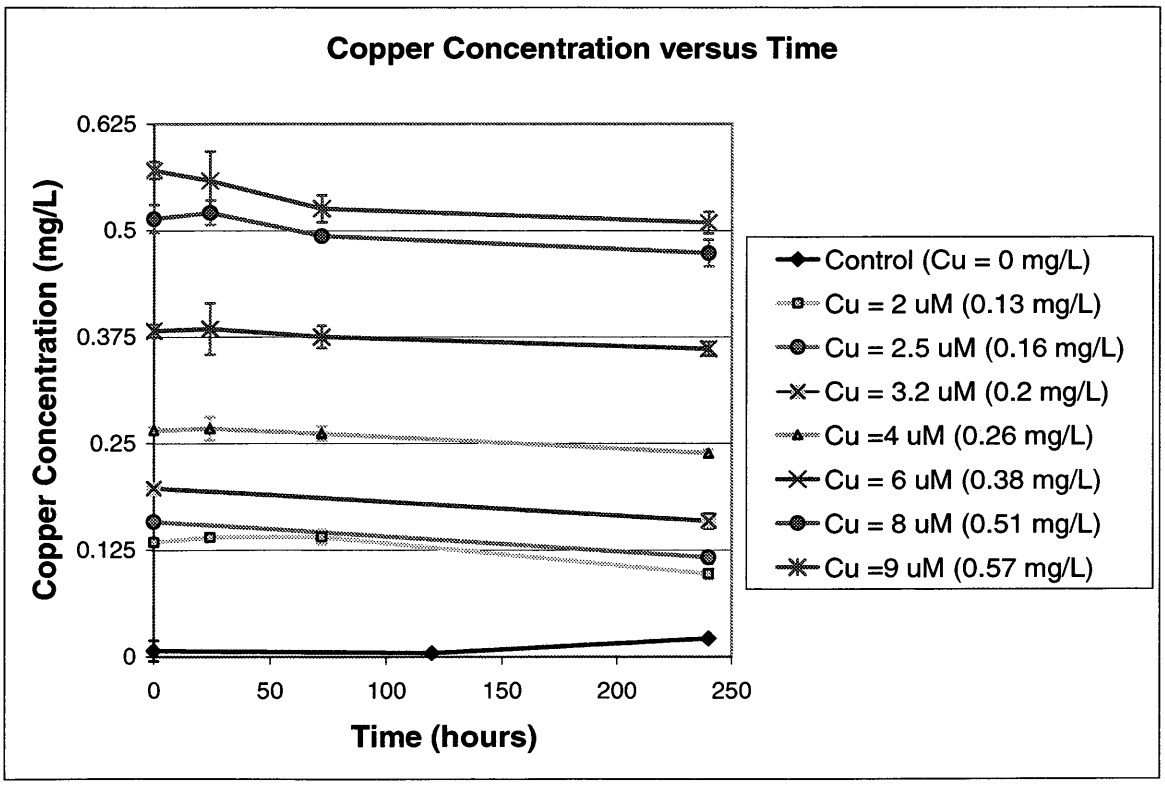

Figure 3.10 Solution Phase Metals Analysis

Figure 3.10 shows that little change was observed in copper concentrations during the course of the experiment. It should be noted that the detection limit of the instrument was around 0.00419 mg/L of copper, and the control bottles are very close to this value. The average percent difference from beginning to end for a given metal concentration was about 15%. Although a slight decrease in concentration from beginning to end was observed for all the bottles, none dropped below that of the next lower copper concentrations. Thus, the changes in concentration were not noted when determining toxicity.

3.3.4 Organic Acid Analysis

The type and extend of organic acid production can be measured using a High Performance Liquid Chromatography (HPLC) machine. Organic acids such as acetate, lactate, butyrate, formate, succinate, and propionate were examined for their possible presence and concentration within each experimental sample. Figure's 3.11, 3.12, 3.13, and 3.14 show the quantity of succinate, lactate, formate, and acetate produced.

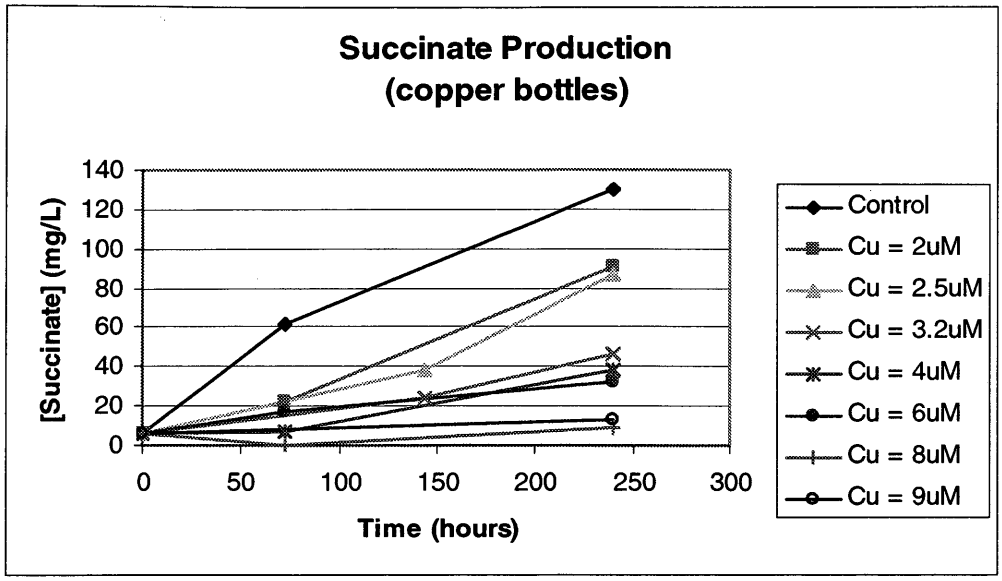

Figure 3.11 Succinate production in copper containing bottles

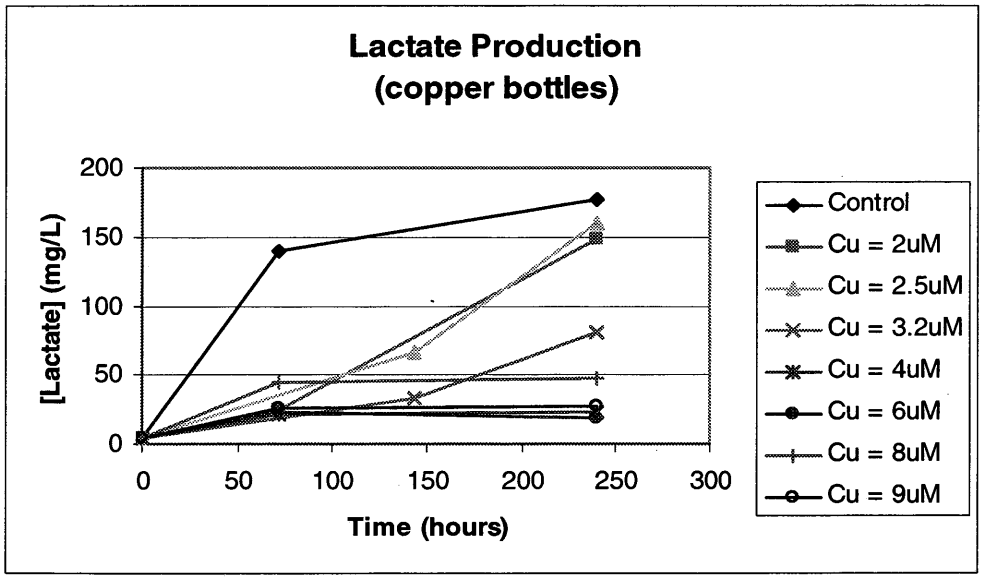

Figure 3.12 Lactate production in copper containing bottles

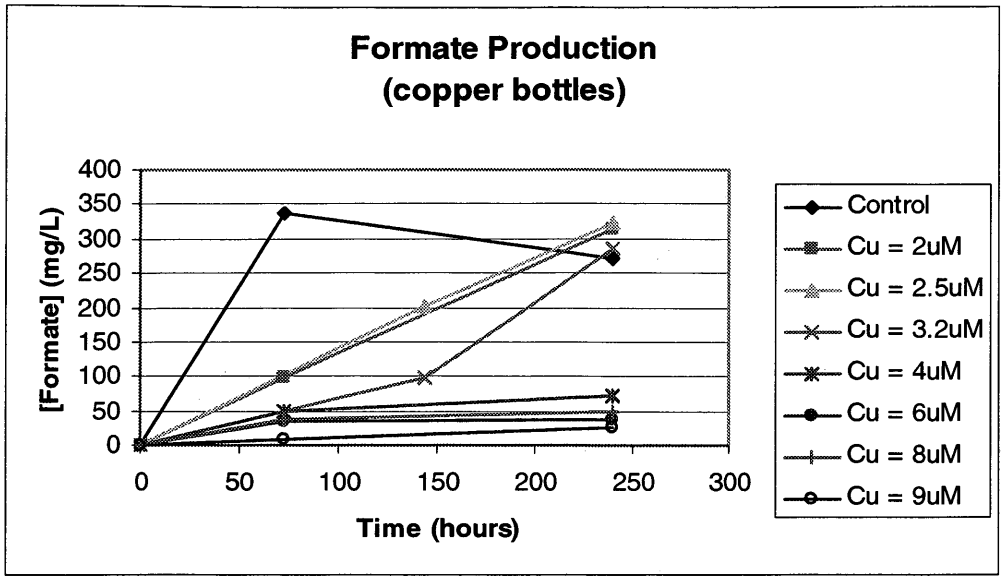

Figure 3.13 Formate production in copper containing bottles

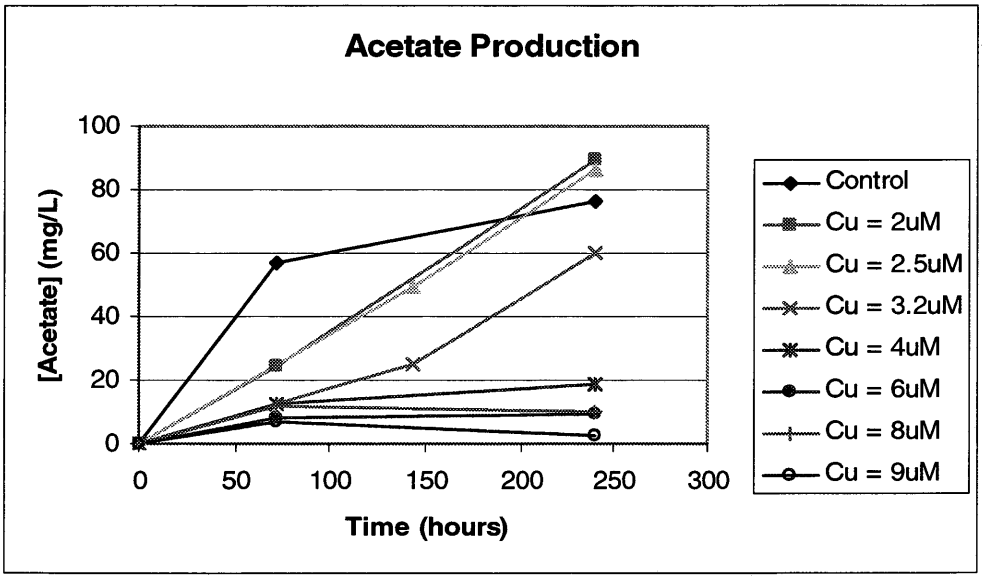

Figure 3.14 Acetate production in copper containing bottles

When looking at figure 3.11 for succinate production, it appears that the rate of succinate produced is decreasing as the copper concentration increases. This makes sense

because the growth rates are suppressed in the copper containing bottles. Fewer cells mean less organic acid production. This phenomenon is also observed in Figures 3.12, 3.13, and 3.14 for copper concentrations at or below 3.2 μM (0.2 mg/L), but a threshold in organic acid production is also apparent at copper concentrations at 4 μM (0.26 mg/L) and greater for lactate, formate, and acetate, where production rate is strongly decreased. With respect to formate production, bottles containing 3.2 M (0.2 mg/L) of copper or less actually exceed formate concentrations produced in the control bottles, and this is also true for acetate production in bottles containing 2.5 M (0.16 mg/L) of copper or less. This suggests that substrate utilization pathways within the cell could be affected by the presence of copper and cause a shift in the type of organic acid produced. When looking at Appendix G, there appears to be no correlation between the shift in quantity of organic acid production and the ability of the organic acid to complex metals.

3.3.5 Complexation of Copper with Organic Acids – MINTEQ Modeling

To determine if the organic acids being produced throughout the experiments were binding up free Cu^{2+}, which is the metal species assumed to be harming the bacteria, a free equilibrium chemical speciation model called MINTEQ was used to calculate the changes in free metal ion concentrations as organic acid concentrations increased. Organic acid production was measured at the beginning, once in the middle of the experiment, and at the end, so these three points in time were used to establish the effective copper ion concentration in solution. The pH in the system was assumed to remain constant at 7, based on the relatively small pH fluxuation observed during the experiments. Figure 3.15 shows the graphical interpretation of the concentration of free copper ion available at a particular time within the bottles containing an initial copper ion concentration ranging between 0.16 mg/L (2.5 μM) to 0.51 mg/L (8 μM).

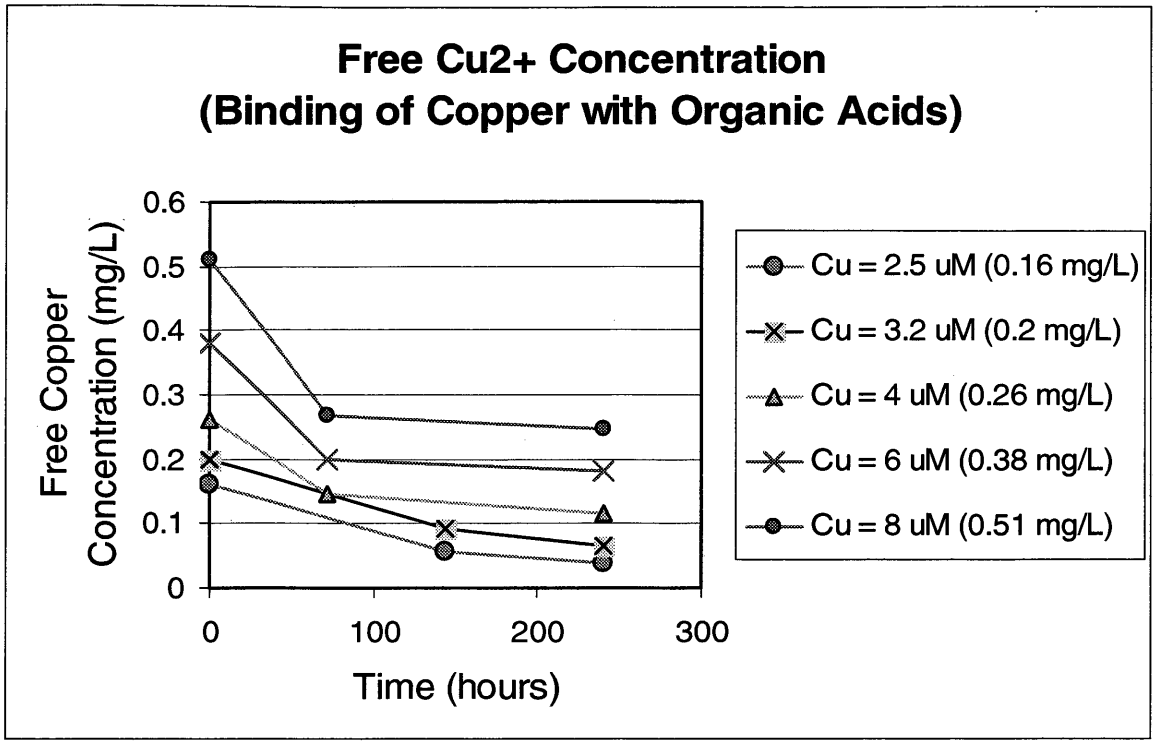

Figure 3.15 Free Cu^{2+} solution concentration: binding with organic acids

It is interesting to note, that even at low organic acid concentrations roughly 50% of the Cu^{2+} ion is bound-up, mostly with organic acids, with about 15% speciated as $Cu(OH)^{+}$. As the organic acid concentration increased, the percentage of bound copper also increased, but this is hard to detect on the graph. Appendix G shows the raw output from MINTEQ.

3.3.6 Monitoring of pH

Solution pH was monitored throughout the experiments to insure that optimal growth conditions were maintained. Figure 3.16 below shows that the pH in any given bottle did not drop below pH 6.2 (rate of growth is the same between pH 5 to 8).

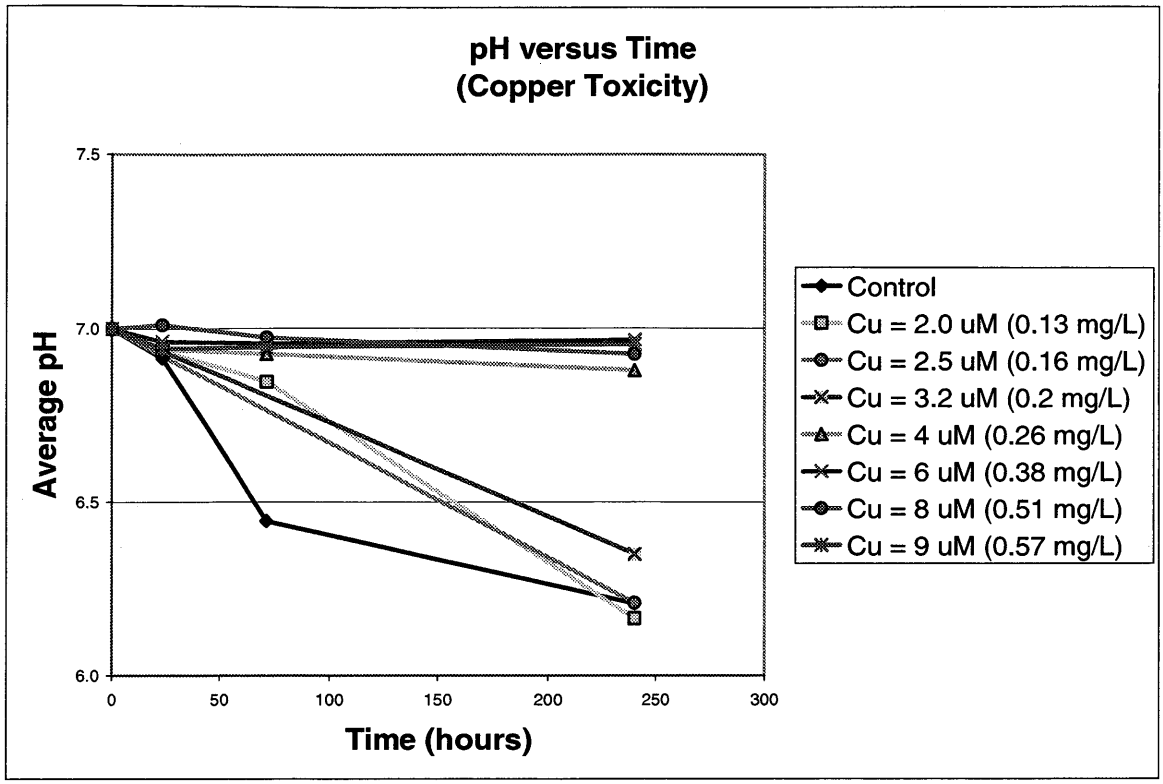

Figure 3.16 pH in copper containing bottles

3.3.7 Monod Modeling of Growth – Inhibition Determination

Growth and substrate consumption patterns for experimental data were modeled using the Monod equation. The Monod equation is used to represent bacterial growth kinetics. Constant kinetic values in the model can be determined for control bottles containing no zinc or copper, and these values can be adjusted to better fit growth and glucose consumption patterns observed in zinc or copper containing bottles. Based on the changes made to kinetic values (K and μ_{max}) within the Monod equation, one can then determine the possible type of inhibition experienced by *C. flavigena* at that particular copper or zinc concentration. It is likely that competitive inhibition of the substrate

enzyme is occurring when K is increased to get the model to fit the data, and noncompetitive inhibition when μ_{max} is decreased to fit the model to the data. Equations (2.1) and (2.3) were used for modeling the data collected from this research. Table 3.2 shows the best fit values for Monod constants that were used for modeling the control bottle data. Figure 3.17 is a graphical representation of the Monod model compared with the control bottles growth and glucose consumption data. The R^2 obtained for the control bottles when comparing the sample data with the model generated data, for cell protein concentration, there was a strong correlation (0.972). A 2-tailed paired t-test had a probability (P) value of 0.5487, and this is greater than the maximum P value of 0.05, which signifies that the difference in mean values for the model and the sample data are not statistically significantly different from one another.

Table 3.2 Monod constants values for control bottles (copper experiments)

Control	
μ_{max}, 1/hr	0.09
Y, mg Protein/mg glu	0.025
K_s, mg glucose/L	700
b, 1/hr	0.0006

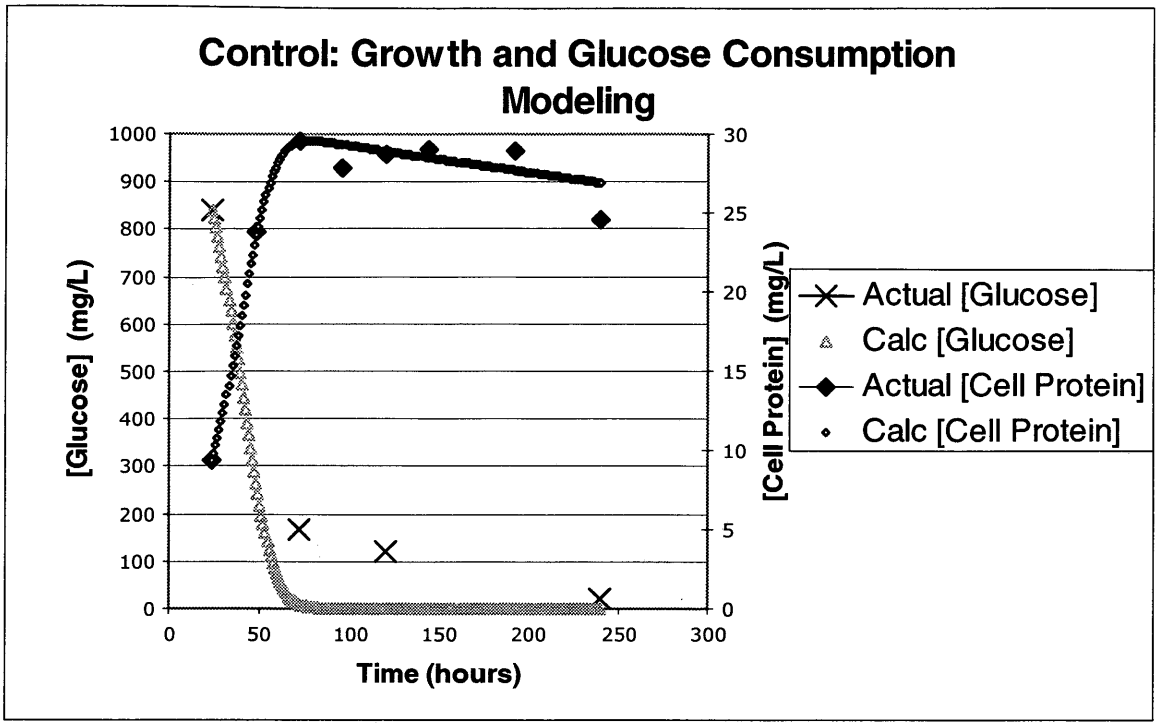

Figure 3.17 Monod modeling of control bottles data

Table 3.3 below shows the Monod values changed to make the Monod equation effectively model the growth in bottles containing copper at a concentration of 2 μM. Only the K constant had to be altered, and this would suggest that competitive inhibition between the substrate and the copper is occurring. Figure 3.18 gives a graphical representation of the Monod model values compared with the experimental values obtained for growth and glucose consumption at a copper concentration of 2 μM. The R^2 obtained for the bottles with 2 μM of copper showed a strong correlation between the measured and modeled values for cell protein concentration (0.805), and the high P value from the t-test (0.775) reconfirms the good fit of the model to the data.

Table 3.3 Monod constants values for bottles containing Cu = 2 μM

Cu = 2 uM	
μ_{max}, 1/hr	0.09
Y, mg Protein/mg glu	0.025
K_{eff}, mg glucose/L	7000
b, 1/hr	0.0006

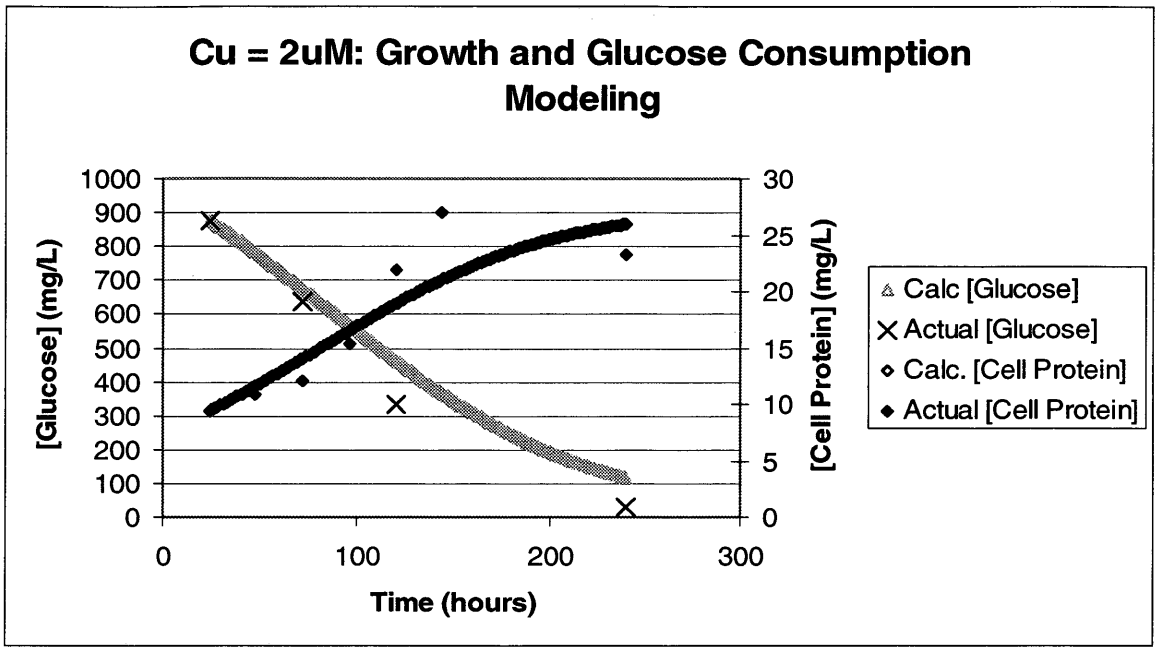

Figure 3.18 Monod data modeling of bottles containing Cu = 2 μM

Since competitive inhibition could explain the changes in growth and glucose consumption patterns thus far, it seemed appropriate to continue to change only the K constant within the model for the remaining modeling of copper containing bottles. Table 3.4 and figure 3.19 show the modeling changes and graphical results for bottles containing 2.5 μM of copper.

Table 3.4 Monod constants values for bottles containing Cu = 2.5 μM

Cu = 2.5 uM	
μ_{max}, 1/hr	0.09
Y, mg Protein/mg glu	0.025
K_{eff}, mg glucose/L	5000
b, 1/hr	0.0006

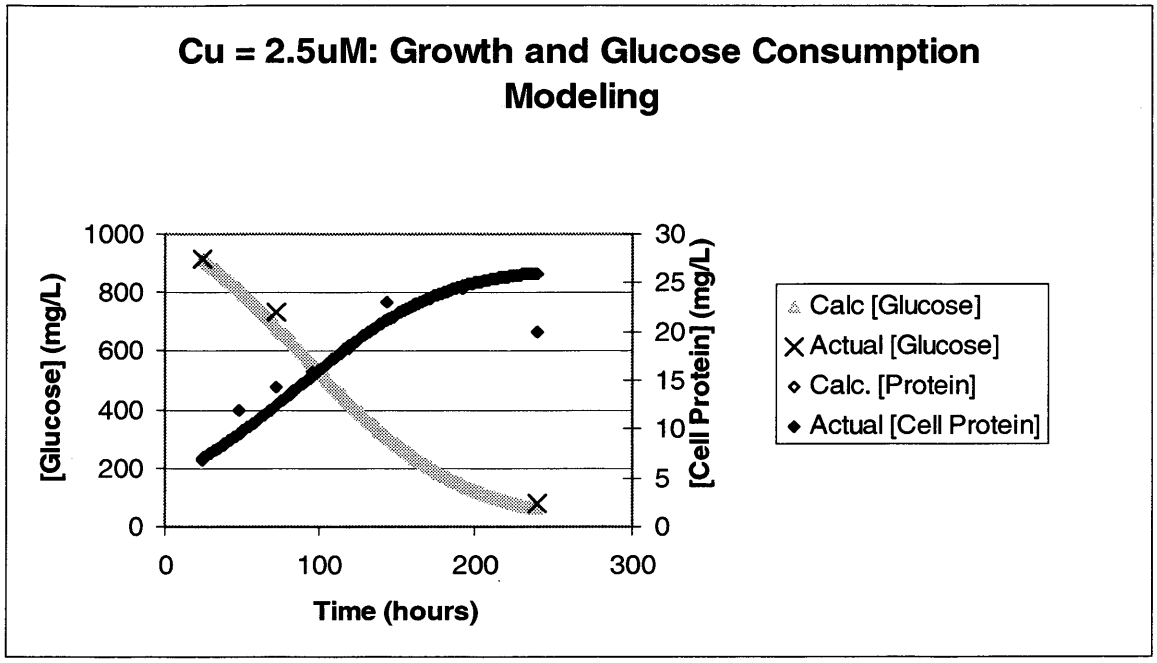

Figure 3.19 Monod data modeling of bottles containing Cu = 2.5 μM

Again, the model seems to fit the data rather well, with an R^2 value of 0.862, and a P value of 0.988.

Table 3.5 and Figure 3.20 below show the modeling results for bottles with a copper concentration of 3.2 μM.

Table 3.5 Monod constants values for bottles containing Cu = 3.2 μM

Cu = 3.2 uM	
μ_{max}, 1/hr	0.09
Y, mg Protein/mg glu	0.025
K_{eff}, mg glucose/L	12000
b, 1/hr	0.0006

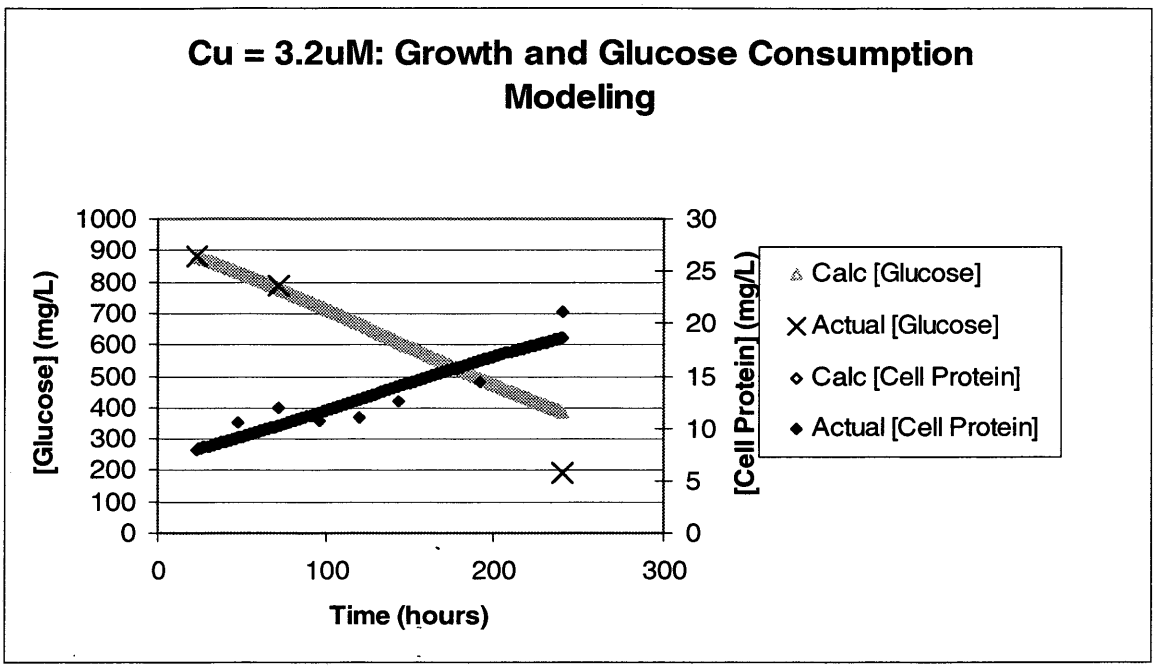

Figure 3.20 Monod data modeling of bottles containing Cu = 3.2 μM

The model fits the sample data quite well, having and R^2 value of 0.8, and a P value of 0.959.

Table 3.6 and figure 3.21 show the modeling of bottles containing 4 μM of copper.

Table 3.6 Monod constants values for bottles containing Cu = 4 μM

Cu = 4 uM	
μ_{max}, 1/hr	0.09
Y, mg Protein/mg glu	0.025
K_{eff}, mg glucose/L	68000
b, 1/hr	0.0006

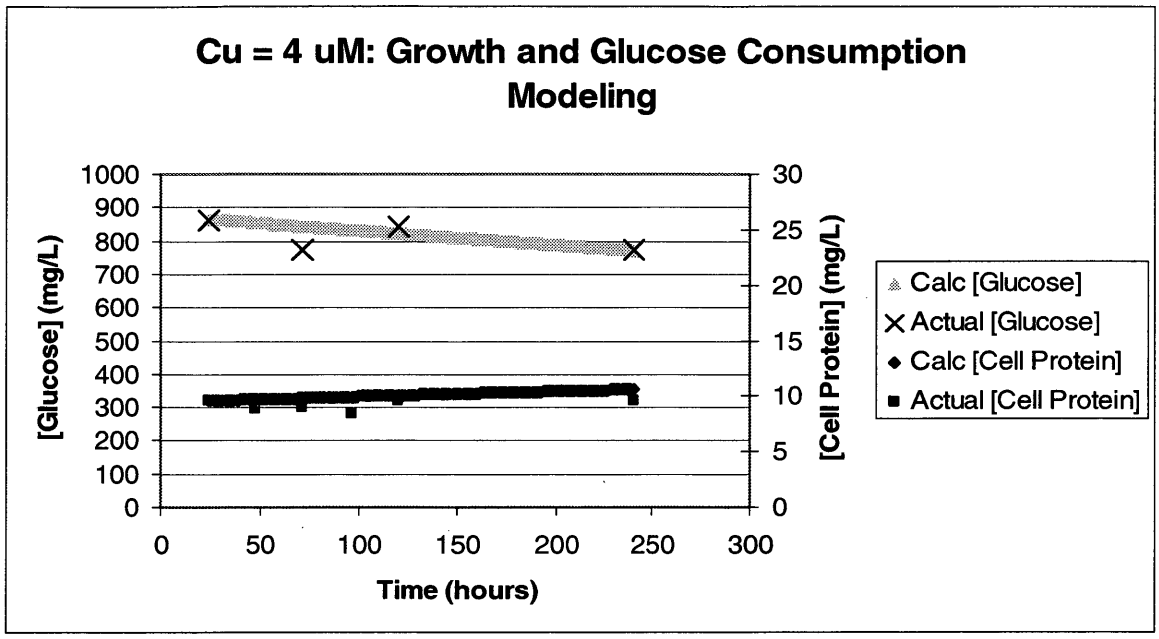

Figure 3.21 Monod data modeling of bottles containing Cu = 4 μM

Although, upon observing figure 3.20, there appears to be a strong correlation between the model and the sample data, the R^2 and P values say otherwise, with a R^2 value of 0.157, and a P value of 0.0134.

Table 3.7 and figure 3.22 show the modeling of bottles with 6 μM of copper.

Table 3.7 Monod constants values for bottles containing Cu = 6 μM

Cu = 6 uM	
μ_{max}, 1/hr	0.09
Y, mg Protein/mg glu	0.025
K_{eff}, mg glucose/L	100000
b, 1/hr	0.0006

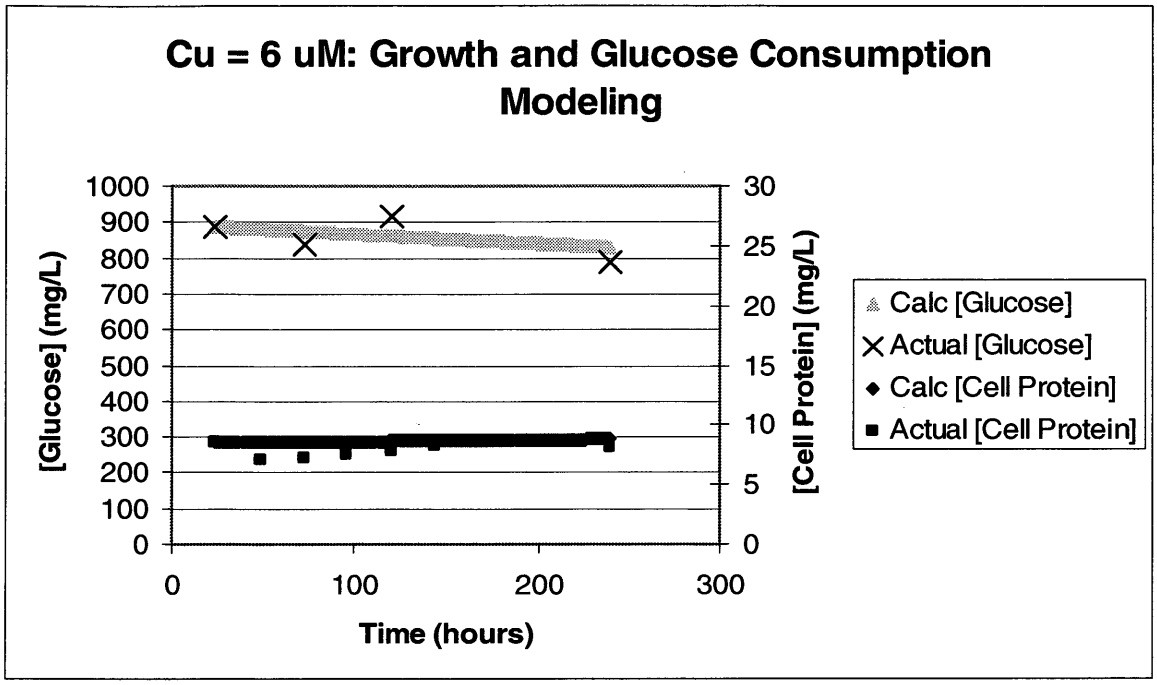

Figure 3.22 Monod data modeling of bottles containing Cu = 6 μM

As was seen with the modeling of bottles containing 4 μM of copper, the graph appears to show a correlation between the model and the cell protein concentration, but no statistical correlation can be made based on the R^2 value of 0.0769, and a P value of 0.006.

Table 3.8 and figure 3.23 shows the modeling of growth and glucose consumption of bottles containing 8 μM of copper.

Table 3.8 Monod constants values for bottles containing Cu = 8 μM

Cu = 8 uM	
μ_{max}, 1/hr	0.09
Y, mg Protein/mg glu	0.025
K_{eff}, mg glucose/L	50000
b, 1/hr	0.0006

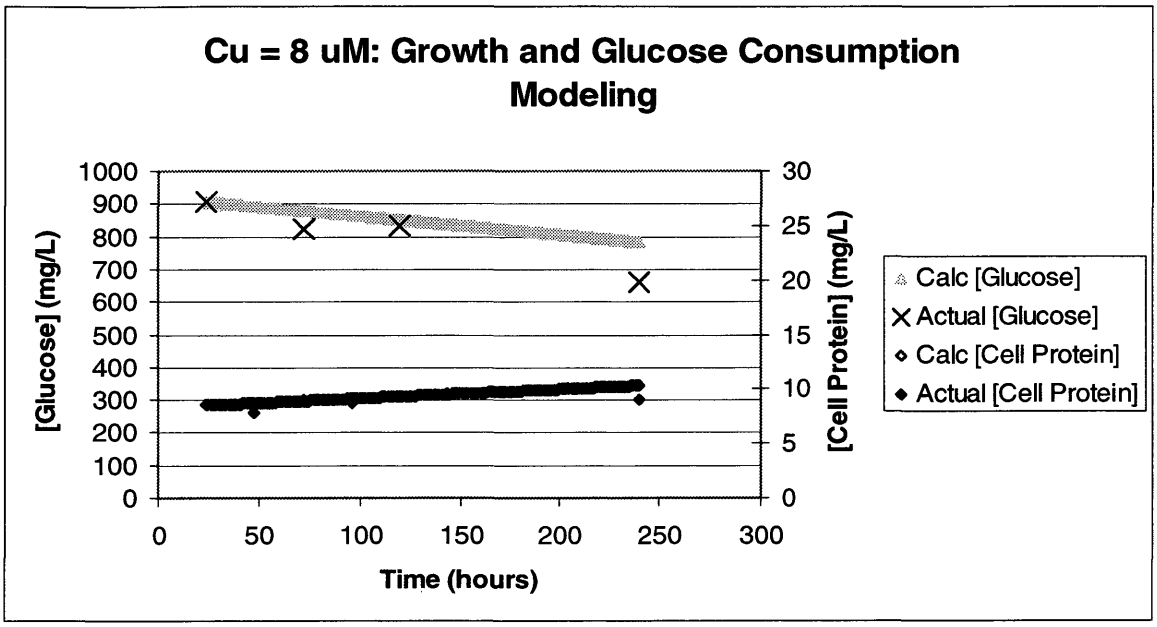

Figure 3.23 Monod data modeling of bottles containing Cu = 8 μM

The model fits the data better than it did for bottles at copper concentrations of 4 and 6 μM. A R^2 value of 0.64, and a P value of 0.237, were obtained.

Table 3.9 and figure 3.24 shows the modeling of growth and glucose consumption of bottles containing 9 μM of copper.

Table 3.9 Monod constants values for bottles containing Cu = 9 μM

Cu = 9 uM	
μ_{max}, 1/hr	0.09
Y, mg Protein/mg glu	0.025
K_{eff}, mg glucose/L	125000
b, 1/hr	0.0006

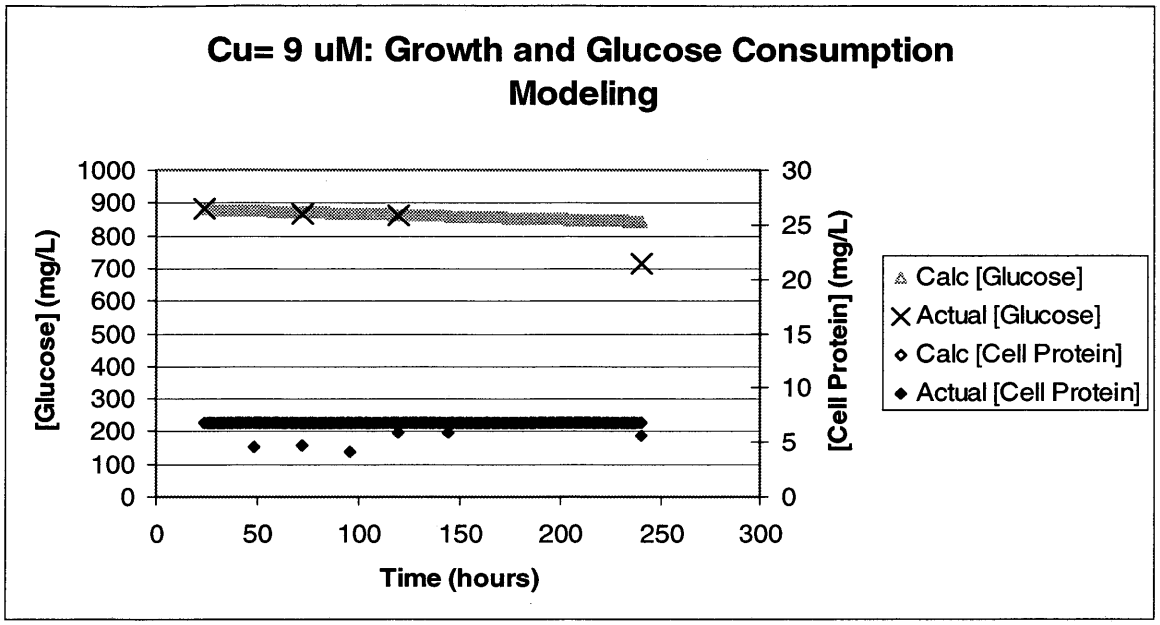

Figure 3.24 Monod data modeling of bottles containing Cu = 9 μM

As was seen with bottles containing 4 and 6 μM of copper, there was no statistical correlation found between the data and the model. A R^2 value of 0.0706, and a P value of 0.0069, were obtained.

The Monod model appeared to do a good job of modeling the growth and glucose patterns for the control bottles and the bottles containing 3.2 μM of copper or less. Little to no statistical correlation between the models values and the sample values could be obtained for copper containing bottles at or above 4 μM. This could be a result of the

toxicity threshold that is occurring at these copper concentrations, or perhaps a simple competitive inhibition model doesn't accurately represent the effects of copper on cell growth. Table 3.10 below shows the variability in K_{eff} applied for modeling at the various copper concentrations.

Table 3.10 Summary of changes in K_{eff} with copper concentration

[Copper]	K_{eff}
Control = 0 uM	700
2 uM	7000
2.5 uM	5000
3.2 uM	12000
4 uM	68000
6 uM	100000
8 uM	50000
9 uM	125000

K_{eff} can be also be calculated using a competitive inhibition equation, which relates the changes in K to the changes in concentration of the inhibitor. In this case the inhibitor is copper, and Equation (3.1) represents the equation used to relate K to the concentration of copper.

$$K_{eff} = K\left(1+\frac{I}{K_I}\right)$$

Equation (3.1)

where

I = concentration of the inhibitor (mg/L)

K_I = an inhibition concentration of the competitive inhibitor (mg/L)

K_I was calculated in Microsoft Excel using the solver function to try and minimize the difference between the K_{eff} values used in the Monod model to fit the data, and the K_{eff} calculated using Equation (3.1). K_I was found to be about 0.062 mg/L, which is very small and indicates a strong inhibitor. Figure 3.25 shows the relationship between K_{eff} and copper concentration, as well as the predicted K_{eff} calculated from the competitive inhibition equation.

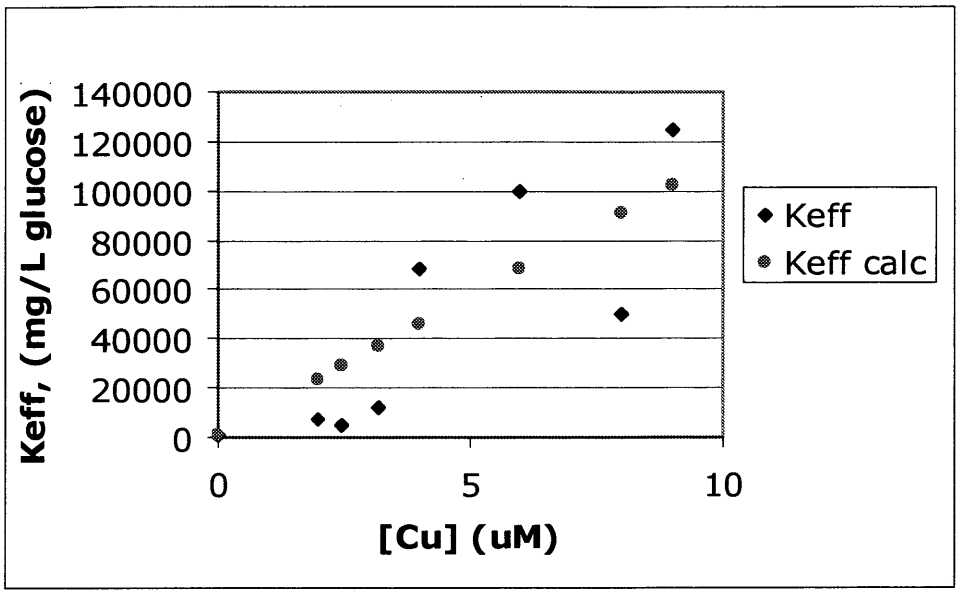

Figure 3.25 Relationship between K_{eff} and copper concentration

The predicted K_{eff} and the K_{eff} used to create the best fit of the Monod model to the data only had an R^2 value of 0.698, and this suggest that competitive inhibition may not be the best way to describe the inhibitory effects that copper has on *C. flavigena*'s enzymes. The next possibility is that copper has a non-competitive inhibitory effect on *C. flavigena*'s enzymes, and this can be tested by keeping K constant and varying μ_{max}. The following figures show the Monod model cell protein and glucose consumption values compared with the collected data when μ_{max} is adjusted. Table 3.11 through table

3.17 shows the change in μ_{max} values for the Monod model as copper concentrations increase from 2 μM to 9 μM, holding all other variables constant. Figure 3.26 through Figure 3.32 shows the fit of the Monod model to the data.

Table 3.11 Monod constants values for bottles containing Cu = 2 μM (μ_{max})

Cu = 2 uM	
μ_{max}, 1/hr	0.018
Y, mg Protein/mg glu	0.025
K_{eff}, mg glucose/L	700
b, 1/hr	0.0008

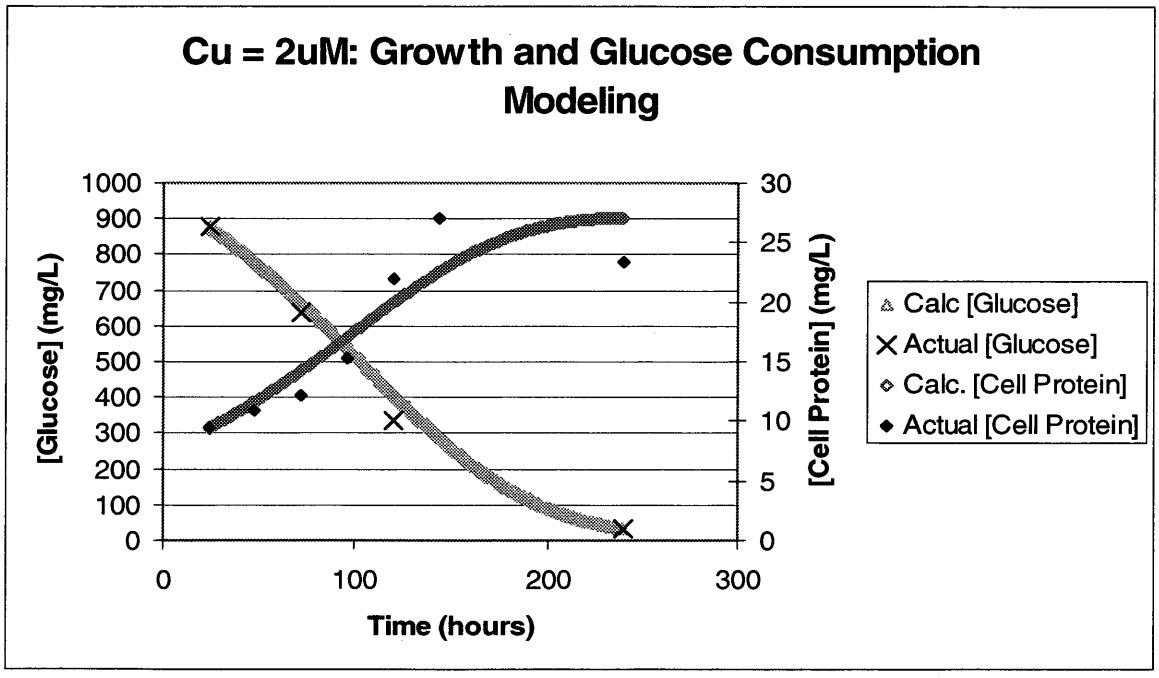

Figure 3.26 Monod data modeling of bottles containing Cu = 2 μM (μ_{max})

Table 3.12 Monod constants values for bottles containing Cu = 2.5 μM (μ_{max})

Cu = 2.5 uM	
μ_{max}, 1/hr	0.02
Y, mg Protein/mg glu	0.025
K_{eff}, mg glucose/L	700
b, 1/hr	0.0008

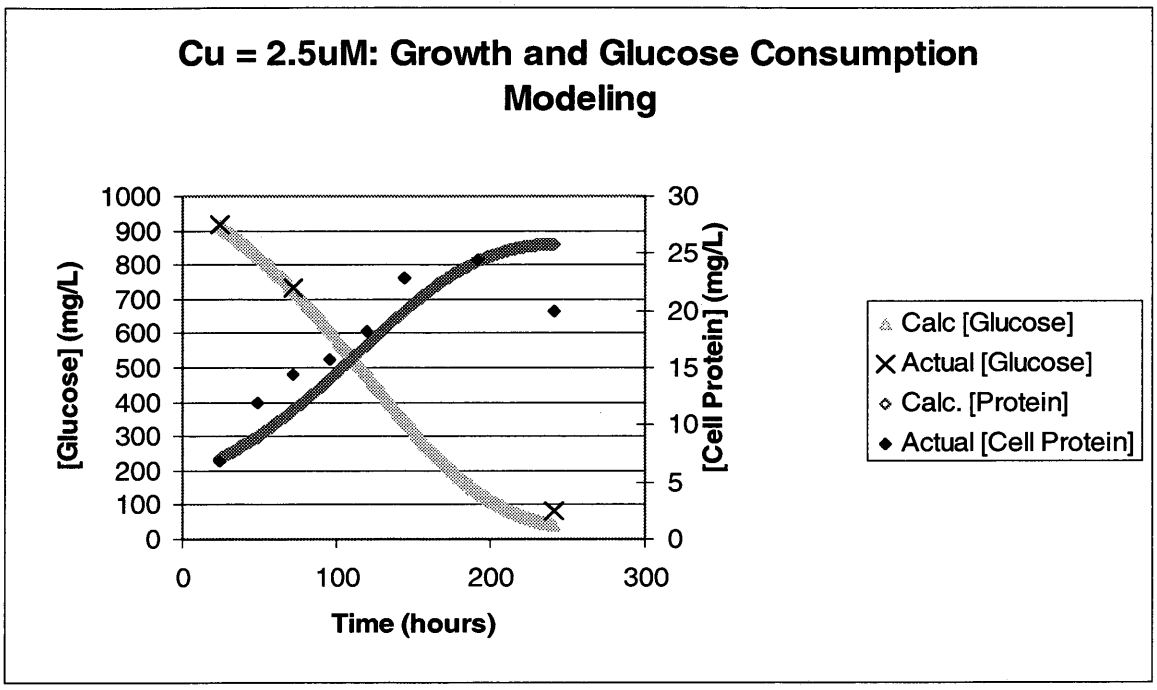

Figure 3.27 Monod data modeling of bottles containing Cu = 2.5 μM (μ_{max})

Table 3.13 Monod constants values for bottles containing Cu = 3.2 μM (μ_{max})

Cu = 3.2 uM	
μ_{max}, 1/hr	0.011
Y, mg Protein/mg glu	0.025
K_{eff}, mg glucose/L	700
b, 1/hr	0.0008

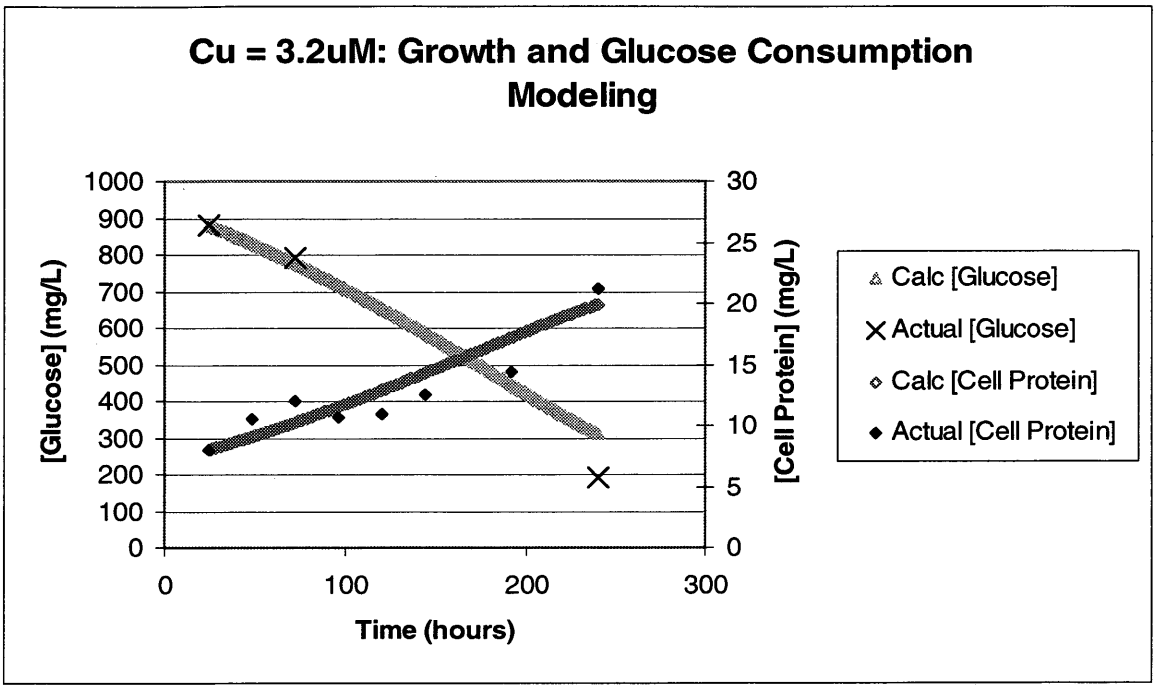

Figure 3.28 Monod data modeling of bottles containing Cu = 3.2 μM (μ_{max})

Table 3.14 Monod constants values for bottles containing Cu = 4 μM (μ_{max})

Cu = 4 uM	
μ_{max}, 1/hr	0.0012
Y, mg Protein/mg glu	0.025
K_{eff}, mg glucose/L	700
b, 1/hr	0.0008

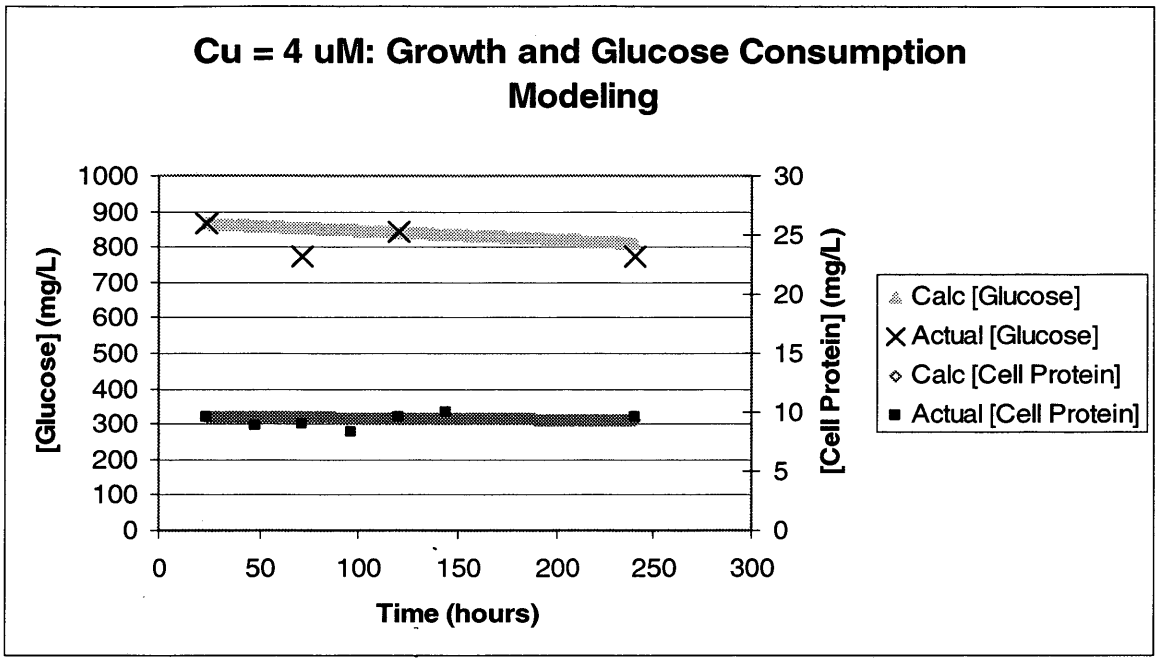

Figure 3.29 Monod data modeling of bottles containing Cu = 4 μM (μ_{max})

Table 3.15 Monod constants values for bottles containing Cu = 6 μM (μ_{max})

Cu = 6 uM	
μ_{max}, 1/hr	0.0004
Y, mg Protein/mg glu	0.025
K_{eff}, mg glucose/L	700
b, 1/hr	0.0008

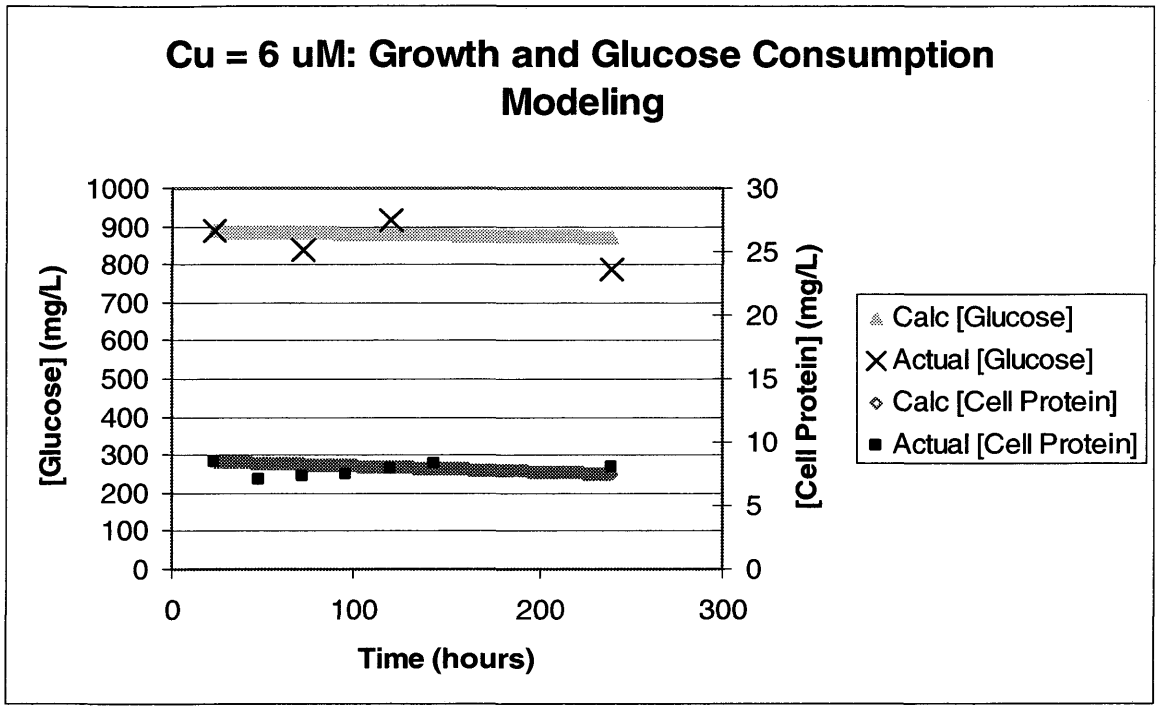

Figure 3.30 Monod data modeling of bottles containing Cu = 6 μM (μ_{max})

Table 3.16 Monod constants values for bottles containing Cu = 8 μM (μ_{max})

Cu = 8 uM	
μ_{max}, 1/hr	0.0022
Y, mg Protein/mg glu	0.025
K_{eff}, mg glucose/L	700
b, 1/hr	0.0008

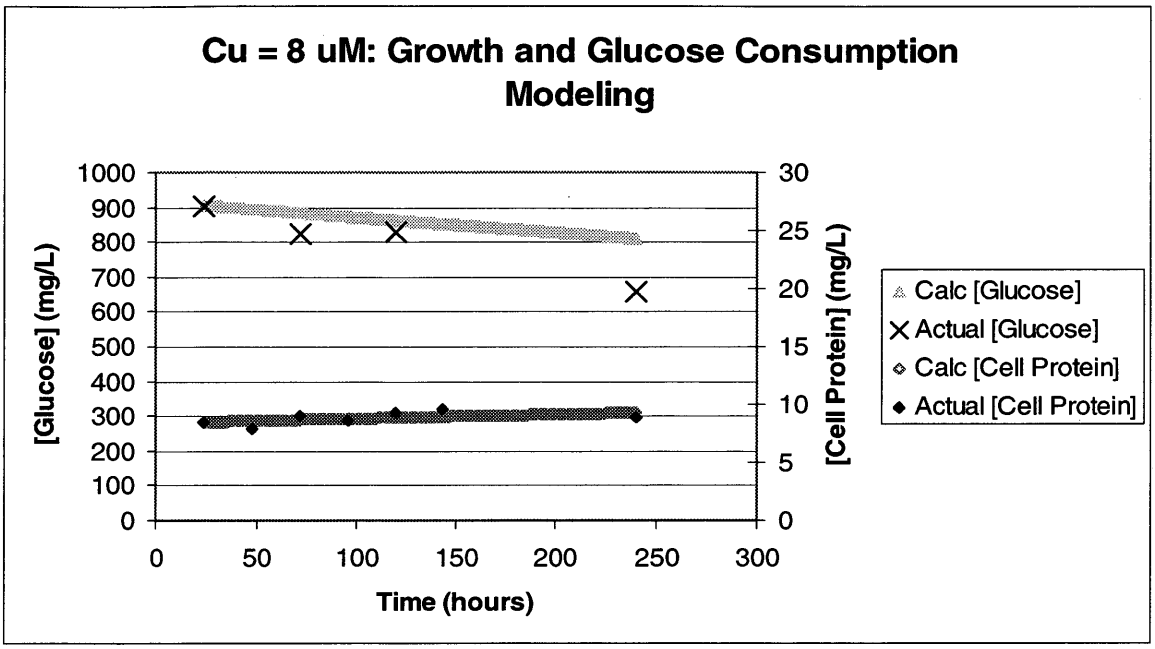

Figure 3.31 Monod data modeling of bottles containing Cu = 8 μM (μ_{max})

Table 3.17 Monod constants values for bottles containing Cu = 9 μM (μ_{max})

Cu = 9 uM	
μ_{max}, 1/hr	0
Y, mg Protein/mg glu	0.025
K_{eff}, mg glucose/L	700
b, 1/hr	0.0008

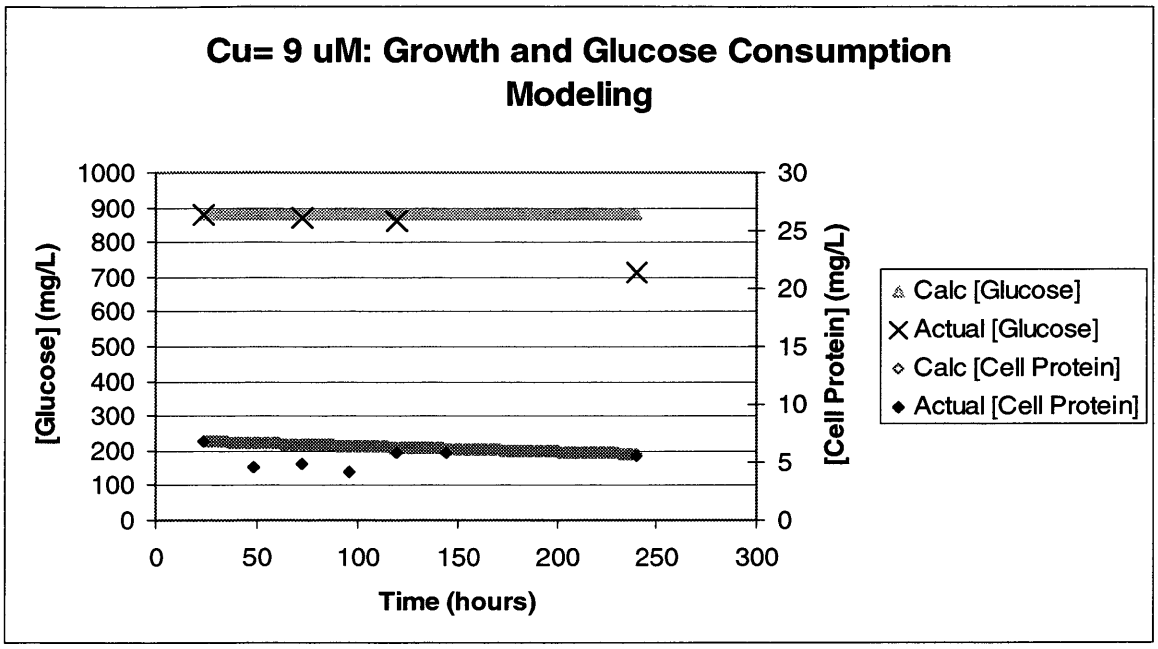

Figure 3.32 Monod data modeling of bottles containing Cu = 9 μM (μ_{max})

The model appears to fit the data well. μ_{max} (μ_{eff}) was then put into Table 3.18 below, which shows the variability in μ_{eff} (μ_{max}) applied for modeling at the various copper concentrations.

Table 3.18 Summary of changes in μ_{max} with copper concentration

[Copper]	μ_{eff}
Control = 0 uM	0.1
2 uM	0.018
2.5 uM	0.02
3.2 uM	0.011
4 uM	0.0012
6 uM	0.0004
8 uM	0.0022
9 uM	0

μ_{eff} can also be calculated using a non-competitive inhibition equation, which relates the changes in μ_{max} to the changes in concentration of the inhibitor. In this case the inhibitor is copper, and Equation (3.2) represents the equation used to relate μ_{max} to the concentration of copper.

$$\mu_{eff} = \frac{\mu_{max}}{\left(1 + \frac{I}{K_I}\right)}$$

Equation (3.2)

K_I was calculated in Microsoft Excel using the solver function to try and minimize the difference between the μ_{eff} values used in the Monod model to fit the data, and the μ_{eff} calculated using Equation (3.1). K_I was found to be about 0.37 mg/L. Figure 3.33 shows the relationship between μ_{eff} and copper concentration, as well as the predicted μ_{eff} calculated from the competitive inhibition equation.

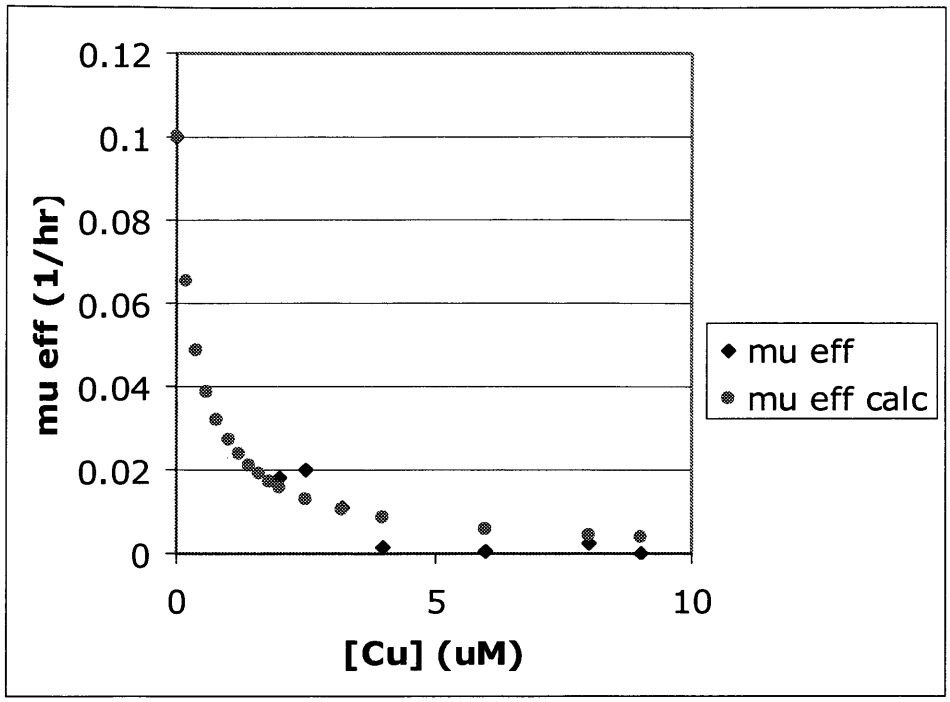

Figure 3.33 Relationship between μ_{max} and copper concentration

The predicted μ_{eff} and the μ_{eff} used to create the best fit of the Monod model to the data had an R^2 value of 0.98, and this suggest that non-competitive inhibition does a better job of describing the inhibitory effects of copper on *C. flavigena*'s enzymes than competitive inhibition modeling.

3.4 Zinc Results

Concentrations of zinc ranging from 4.3 μM (0.28 mg/L) to 23 μM (1.5 mg/L) were used during experiments. The determination of a threshold concentration at which cell growth would not occur, and/or the establishment of an LC_{50}, was the goal of these experiments. Since experiments were conducted in batch, using serum bottles, the

experiments were run until cell decay began to occur in the control bottles, which happened to be 10 days (240 hours) for *C. flavigena*. As noted in the materials and method section, samples were taken either daily or periodically throughout experiments to determine changes in cell, glucose, and solution phase metal concentrations, organic acid production, and pH. Every bottle was performed in quadruplicate to insure accuracy of sample measurements and all data values used for interpretation were the average of the 4 replicates.

3.4.1 Growth Curves

It seemed logical to start conducting experiments with zinc concentrations double that of the copper concentrations used since many previous toxicity studies have found copper to be more toxic than zinc. Figure 3.34 shows the growth curves observed as zinc concentrations were increased.

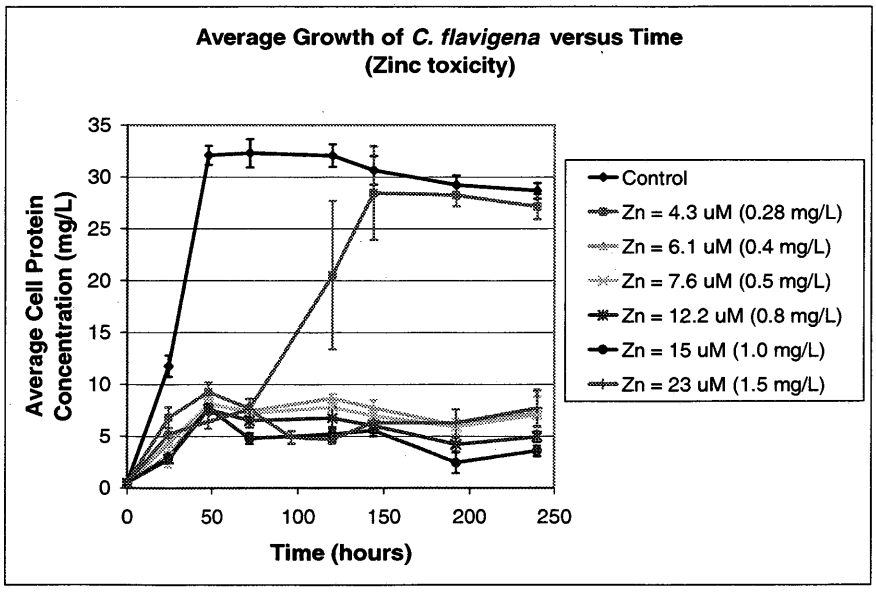

Figure 3.34 Growth curves at zinc concentrations of 4.3 μM to 23 μM

There are three things that stand out in Figure 3.34. Within the first 24 hours there appears to be a slight decrease in growth for zinc containing bottles relative to the control, which is unlike what was seen with copper. Secondly, there is a definite toxicity threshold observed for zinc concentrations at or above 6.1 μM (0.4 mg/L). This resembles what was observed with the copper experiments. The third thing to notice is the large standard deviation for cell protein at 120 hours (day 5) for a zinc concentration of 4.3 μM (0.28 mg/L). The standard deviation represents the 4 replicate values, and the large variability in cell growth between bottles suggests that a critical toxicity threshold may be occurring at that zinc concentration. Overall, growth inhibition is occurring in the bottles containing 4.3 M (0.28 mg/L) of zinc, while a toxic threshold effect is occurring at concentrations equal to or greater than 6.1 (0.4 mg/L) of zinc.

3.4.2 Glucose Consumption Curves

As with the copper experiments, each serum bottle initially contained 1000 mg/L of glucose. Samples taken from experimental bottles were centrifuged, to remove liquid from cell mass, and the decant was then frozen and analyzed within 24 hours of when sample was taken to insure no further consumption of glucose would occur beyond sampling time. All absorbance readings were performed at a wavelength of 490 nm. Figure 3.35 represents glucose consumption at zinc concentrations ranging from 2.2 μM (control bottles) to 23 μM.

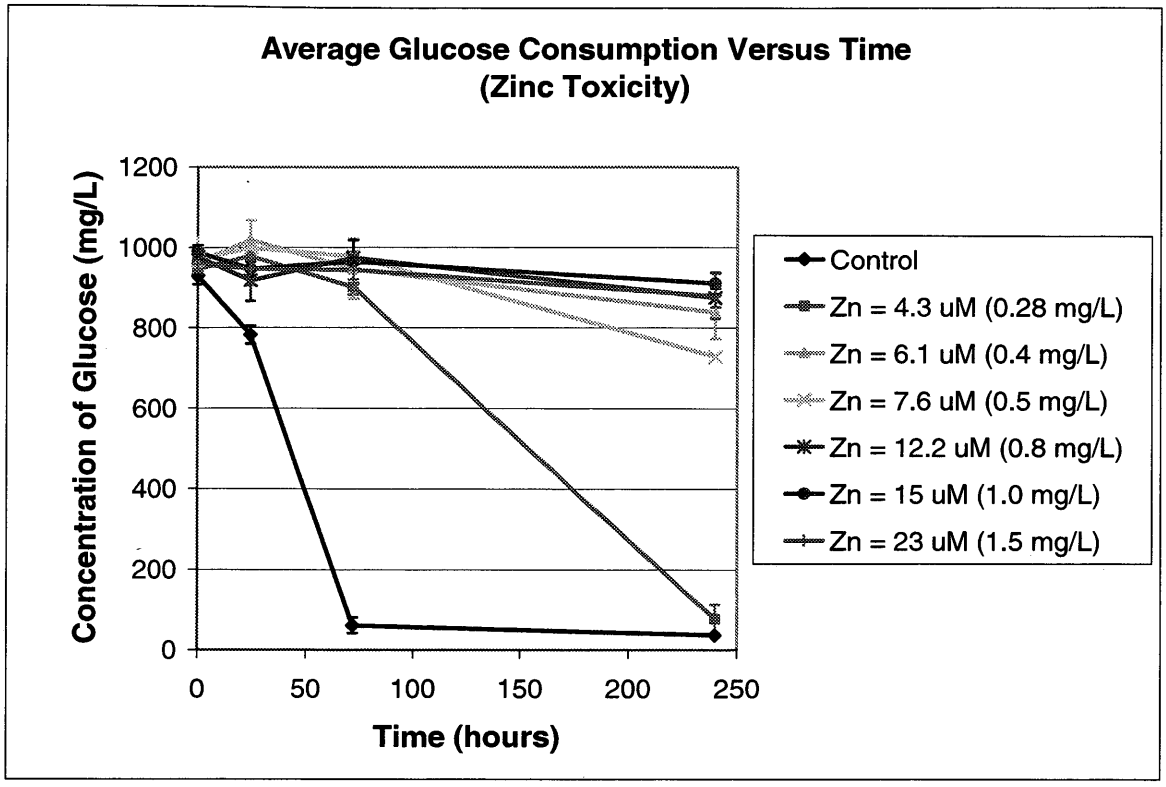

Figure 3.35 Glucose consumption for zinc concentrations of 2.2 μM to 23 μM

There are three patterns that stand out on Figure 3.35. First, there appears to be a lag in glucose consumption for the first 72 hours in bottles containing 0.28 mg/L (4.3 μM) of zinc. Secondly, a reduced glucose consumption rate is seen at a zinc concentration of 0.28 mg/L (4.3 μM), which supports the data from Figure 3.25, where reduced growth rates were observed in those bottles. Thirdly, a large reduction in glucose consumption rate is observed in bottles containing zinc concentrations at or greater than 0.4 mg/L (6.1 μM), and this supports the observation of low biomass concentration found in those bottles (Figure 3.34).

3.4.3 Solution Phase Metals Analysis

Zinc concentration for the beginning and the end of the 10 day experiments was verified through ICP (AES) analysis. This was done to insure that the proper concentration of zinc was added and maintained throughout the experiment. The results from ICP analysis are summarized in Figure 3.36 below.

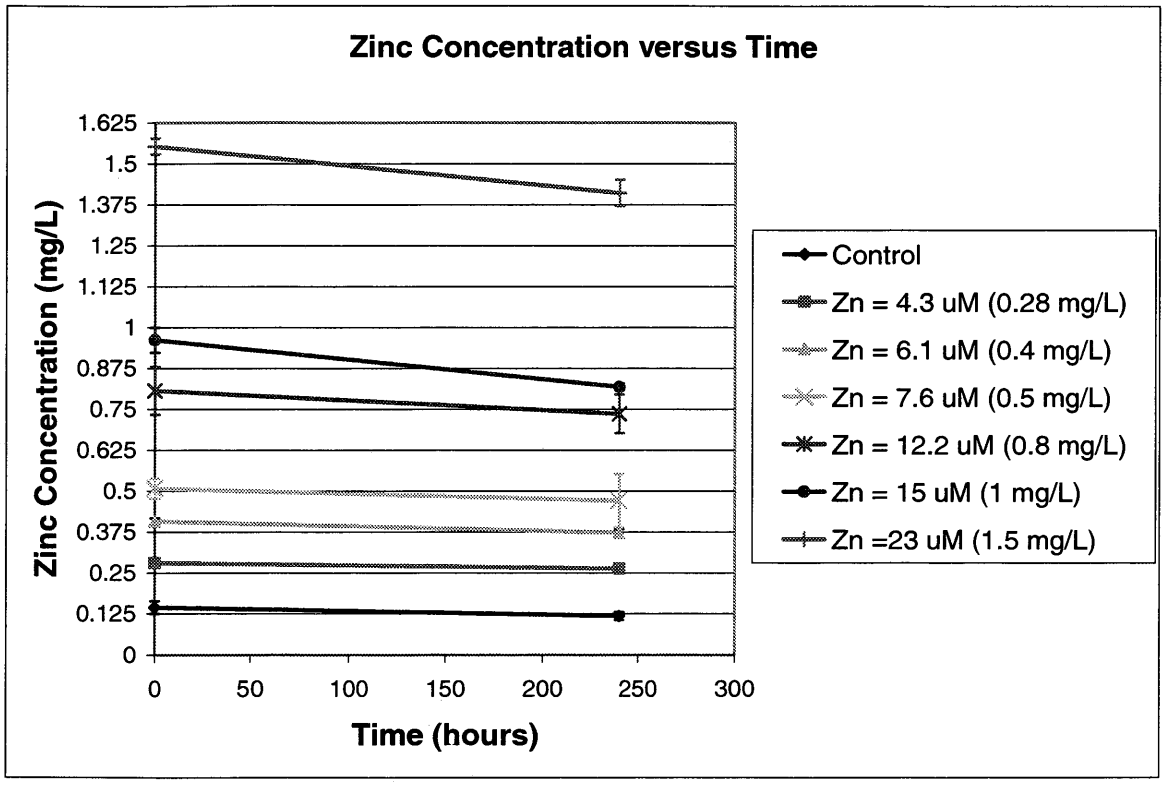

Figure 3.36 Solution Phase Metals Analysis

Figure 3.36 shows little change in solution phase zinc concentration during the experiment. As was seen with the copper analysis, a slight decrease in metal concentration seems to be happening uniformly throughout the experimental bottles. The average percent difference from beginning to end for a given zinc concentration was

about 10%. Since none dropped below that of the next lower zinc concentration the changes were not noted when determining toxicity.

3.4.4 Organic Acid Analysis

The organic acids succinate, lactate, formate, and acetate were produced during the zinc toxicity experiments, and Figure's 3.37, 3.38, 3.39, and 3.40 show the quantities produced.

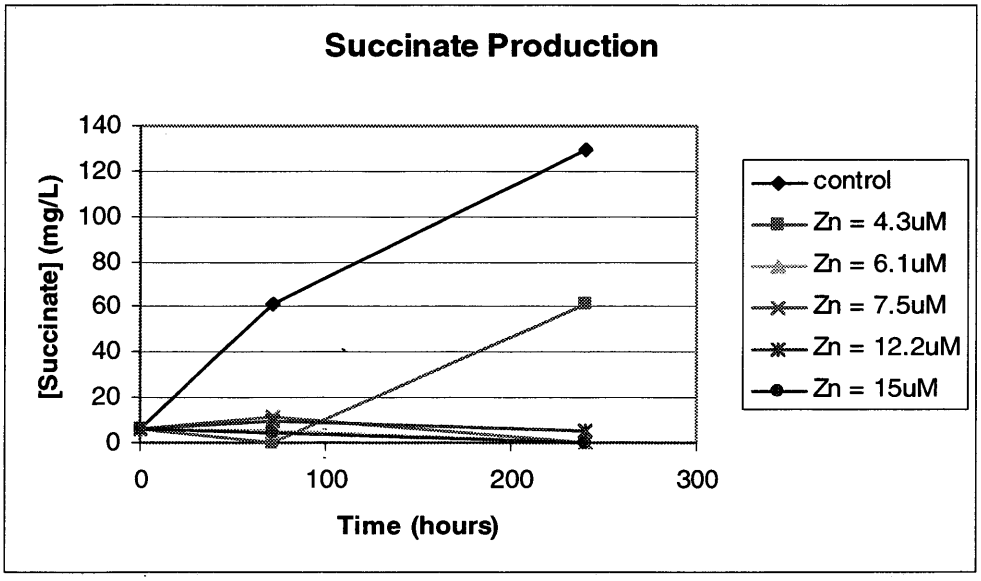

Figure 3.37 Succinate production in zinc containing bottles

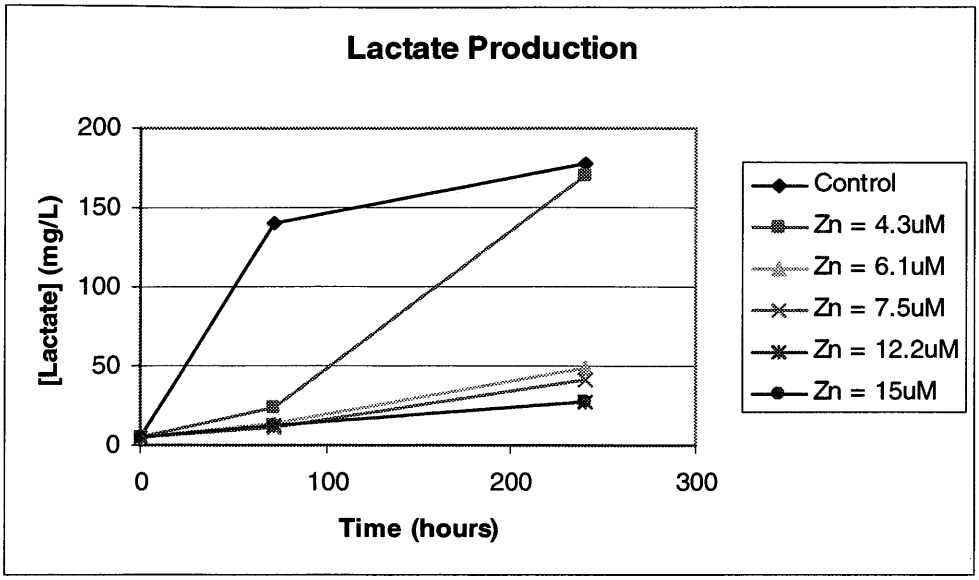

Figure 3.38 Lactate production in zinc containing bottles

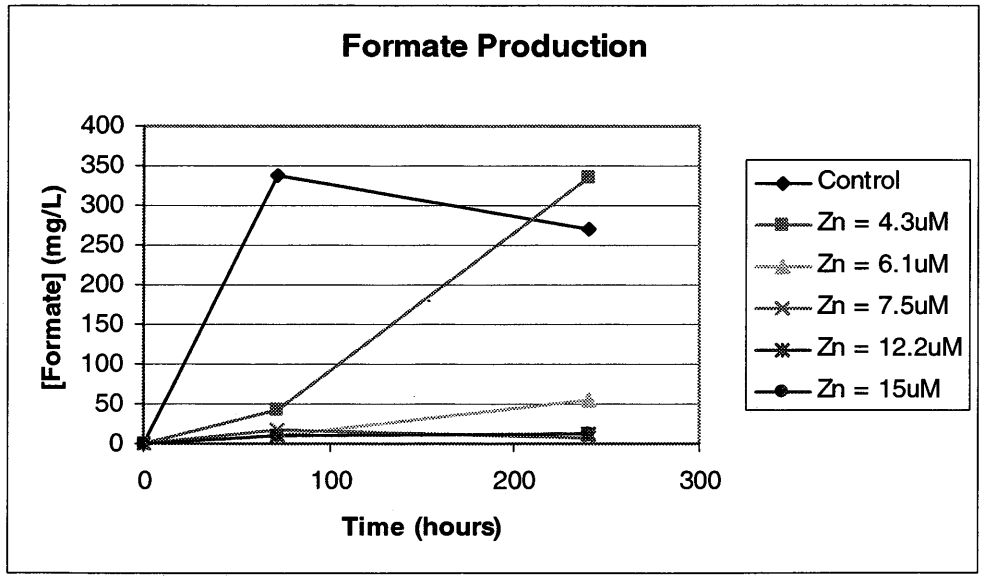

Figure 3.39 Formate production in zinc containing bottles

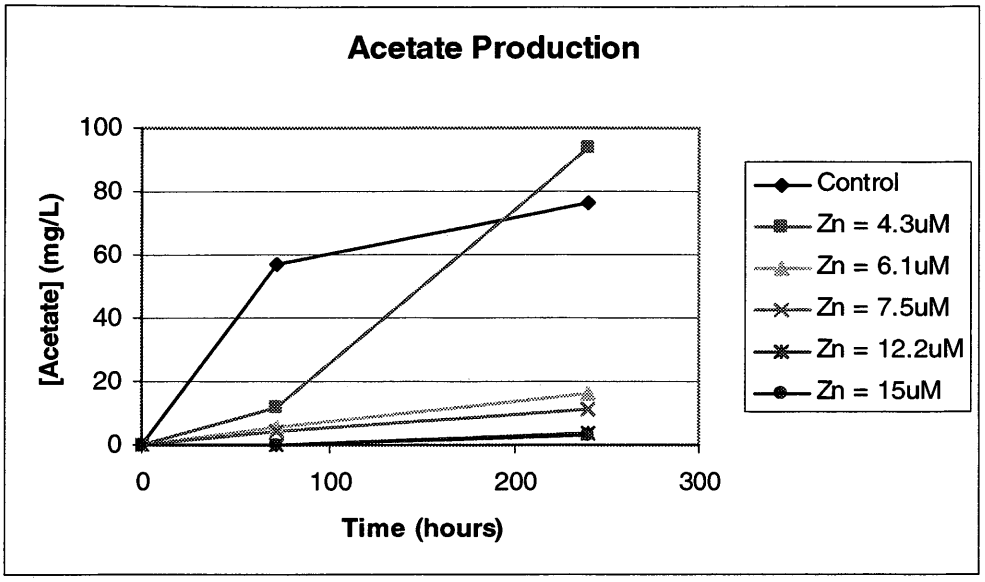

Figure 3.40 Acetate production in zinc containing bottles

A clear threshold in production of succinate can be seen in Figure 3.37 at zinc concentrations of 6.1 μM and greater, where as lactate, formate, and acetate production at those zinc concentrations appear to have a highly suppressed rate of production, rather than a threshold. By the end of the experiments we see a complete recovery in production of lactate for bottles containing zinc at a concentration of 4.3 μM, relative to the control. However, with respect to formate and acetate production, the amount produced in bottles containing 4.3 μM of zinc exceeds the concentrations produced in the control bottles. This suggests that substrate utilization pathways within the cell could be affected by the presence of zinc, as was also seen with copper, and cause a shift in the type of organic acid produced.

3.4.5 Complexation of Zinc with Organic Acids – MINTEQ Modeling

As with the copper experiments, the extent of zinc speciation and binding with organic acids was determined using MINTEQ. Figure 3.41 shows the graphical interpretation of the concentration of free zinc ion available at a particular time within the bottles containing an initial zinc ion concentration ranging between 0.28 mg/L (4.3 μM) to 0.8 mg/L (12 μM).

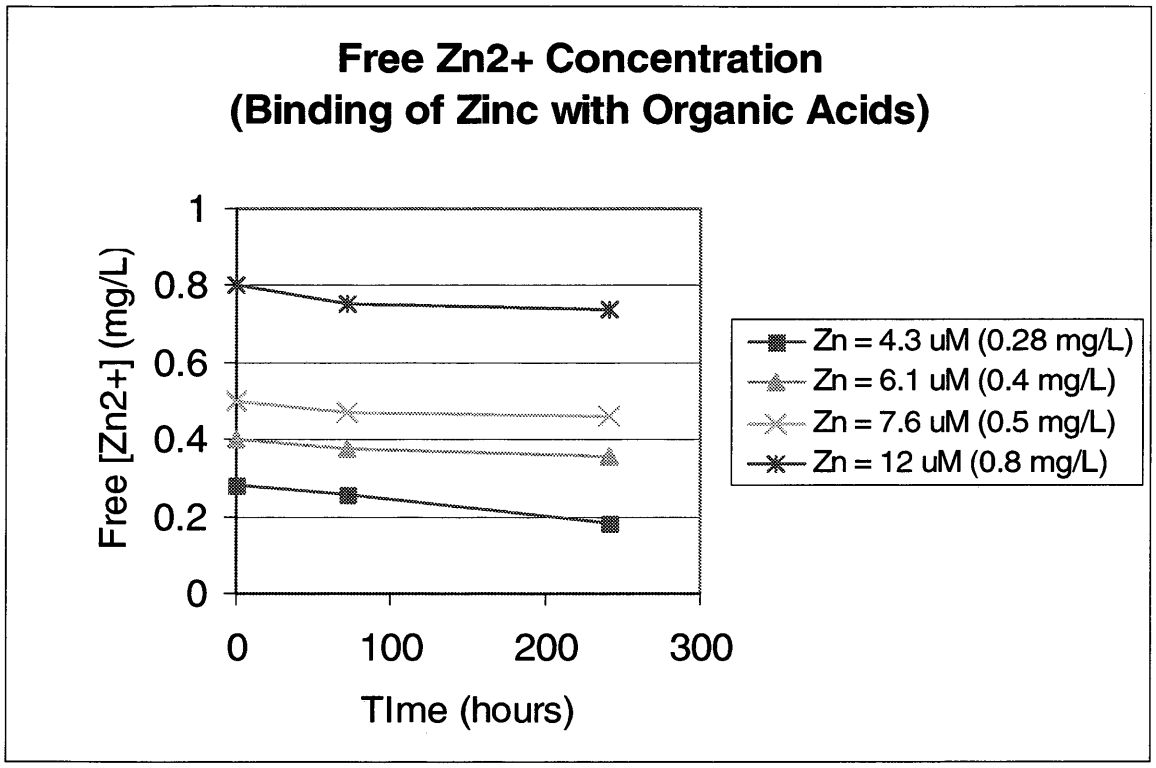

Figure 3.41 Free Zn^{2+} solution concentration: binding with organic acids

Unlike what was seen with the copper ion, zinc has very little binding occurring at low organic acid concentrations, with about 92-94% remaining as a free Zn^{2+}. As the organic acid concentration increased, the percentage of free Zn^{2+} decreased, although this

is hard to defer from the graph. When looking at the raw output from MINTEQ in Appendix G, in the bottles containing 4.3 μM of initial zinc, one can see that the percentage of free zinc decreased from 93 to 66, which corresponded to the large increase in organic acid production during those two points in time.

3.4.6 Monitoring of pH

Solution pH was monitored throughout the experiments to insure that optimal growth conditions were maintained. Figure 3.42 below shows that the pH in any given bottle did not drop below pH 6.2.

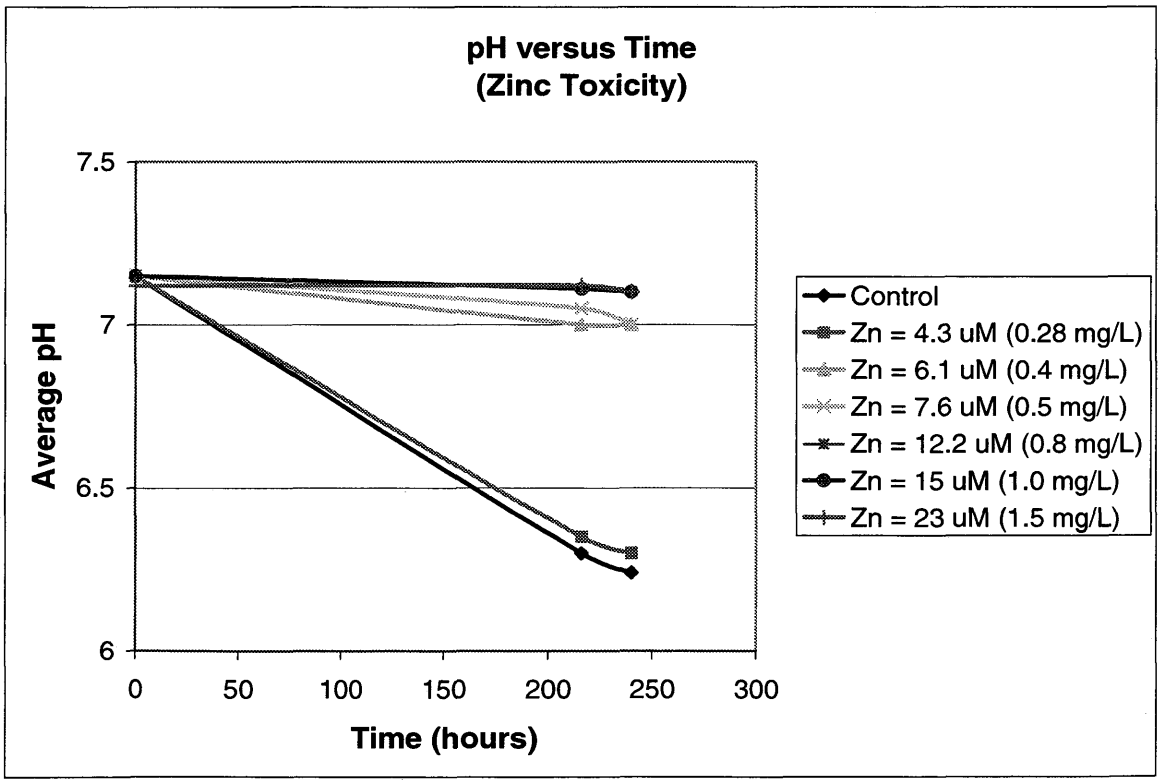

Figure 3.42 pH in zinc containing bottles

3.4.7 Monod Modeling of Growth – Inhibition Determination

Table 3.19 shows the best fit values for Monod constants that were used for modeling the control bottle data during zinc experiments. Figure 3.43 is a graphical representation of the Monod model compared with the control bottles growth and glucose consumption data.

Table 3.19 Monod constants values for control bottles (zinc experiments)

	Control
μ_{max}, 1/hr	0.15
Y, mg Protein/mg	0.029
K_s, mg glucose/L	700
b, 1/hr	0.0011

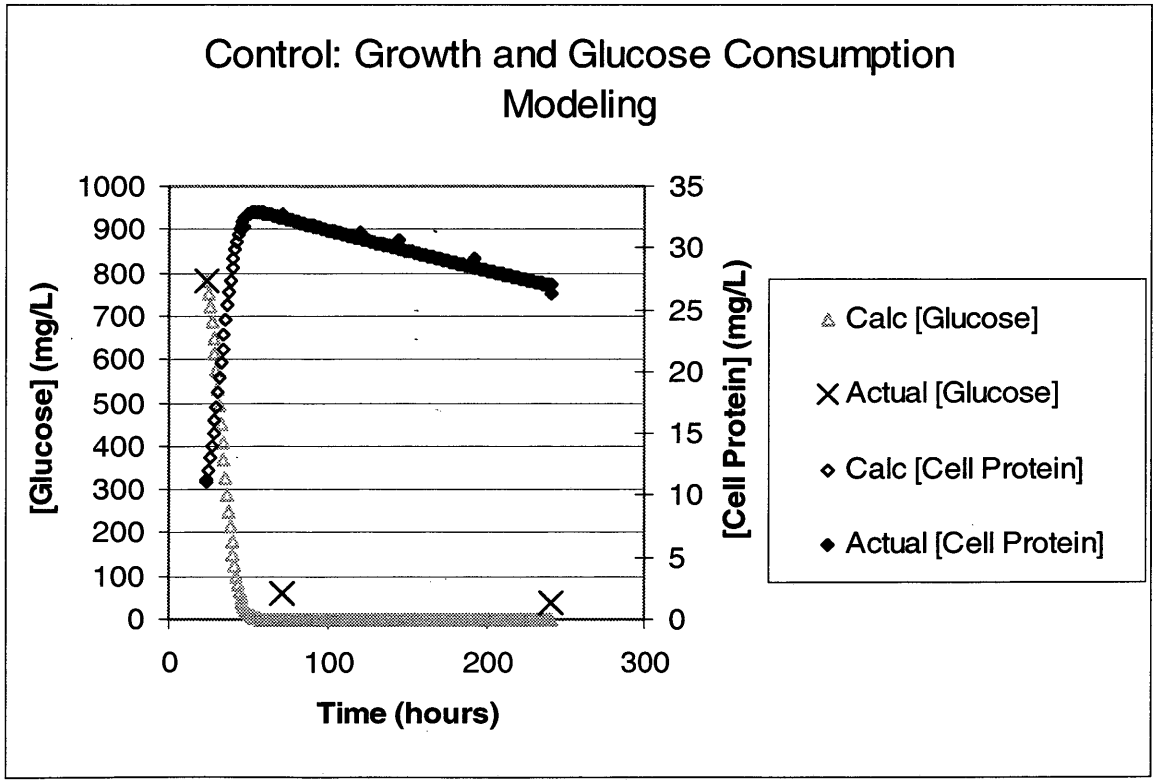

Figure 3.43 Monod modeling of control bottles data (zinc experiments)

A R^2 value of 0.994 and a P value of 0.632 were obtained for the correlation of the Monod model with the sample data. These values suggest a very strong statistical correlation between the models values and the sample values for cell protein concentrations.

Table 3.20 below shows the Monod values, and the changes made to the Monod equation to effectively model the growth in bottles containing zinc at a concentration of 4.3 μM. Only the K constant had to be altered, and this would suggest that competitive inhibition between the substrate and the copper is occurring. Figure 3.44 gives a graphical representation of the Monod model values compared with the experimental values obtained for growth and glucose consumption at a zinc concentration of 4.3 μM.

Table 3.20 Monod constants values for bottles containing Zn = 4.3 μM

Zn = 4.3 uM (.28 mg/L)	
μ_{max}, 1/hr	0.15
Y, mg Protein/mg glu	0.029
K_{eff}, mg glucose/L	5500
b, 1/hr	0.0011

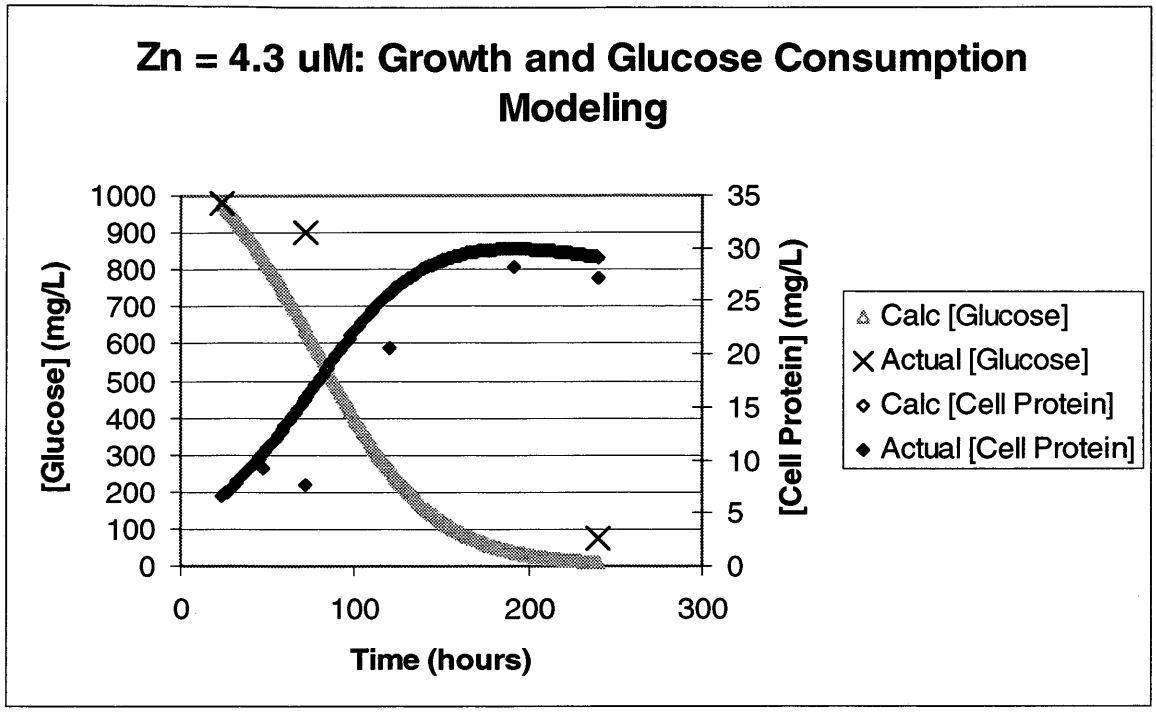

Figure 3.44 Monod data modeling of bottles containing Zn = 4.3 μM

A statistical correlation between the model and the sample data was found based on a R^2 value of 0.912. As for the P value, it is right above the value that would determine the model and the sample data to be statistically different (0.0594). Based on these findings, the model appears to be a relatively good fit to the data.

Since competitive inhibition could explain the changes in growth and glucose consumption patterns thus far, it seemed appropriate to continue to change only the K constant within the model for the remaining modeling of zinc containing bottles. Table 3.21 and Figure 3.45 show the modeling changes and graphical results for bottles containing 6.1 μM of zinc.

Table 3.21 Monod constants values for bottles containing Zn = 6.1 μM

Zn = 6.1 uM (0.4 mg/L)	
μ_{max}, 1/hr	0.15
Y, mg Protein/mg glu	0.029
K_{eff}, mg glucose/L	31500
b, 1/hr	0.0011

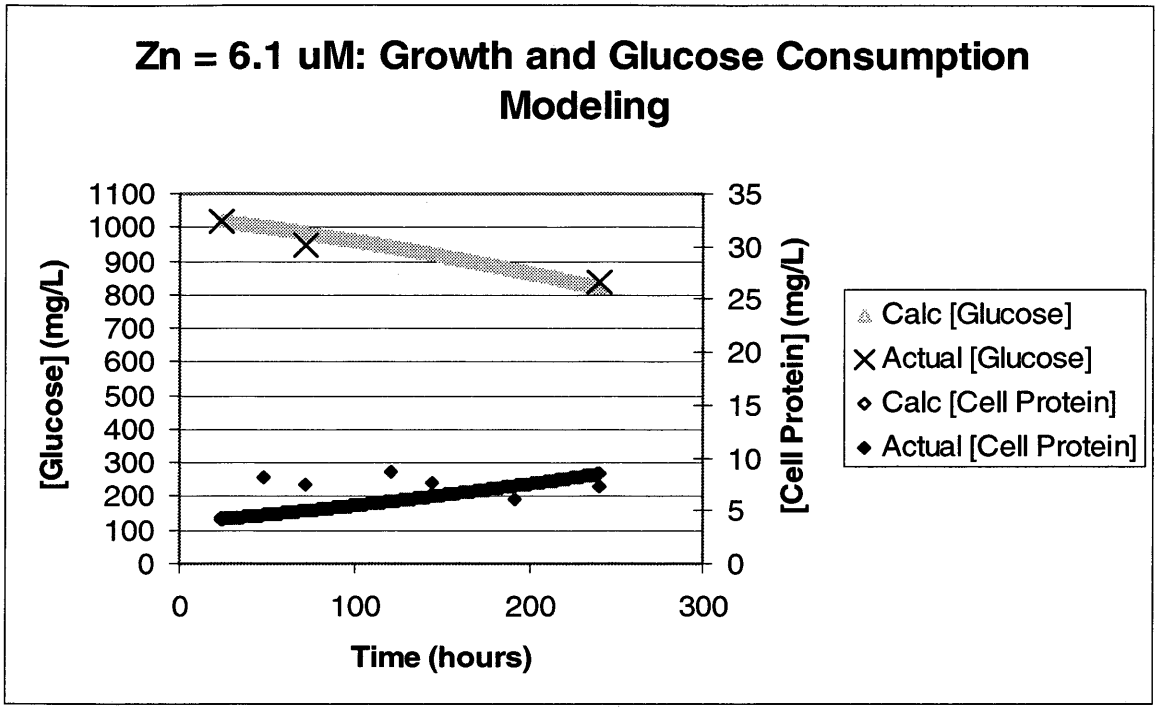

Figure 3.45 Monod data modeling of bottles containing Zn = 6.1 μM

The P value of 0.197 suggests that the model and the sample data values are not statistically significantly different, even though the R^2 value of 0.0305 shows no correlation.

Table 3.22 and Figure 3.46 below show the modeling results for bottles with a zinc concentration of 7.6 μM.

Table 3.22 Monod constants values for bottles containing Zn = 7.6 μM

Zn = 7.6 uM (0.5 mg/L)	
μ_{max}, 1/hr	0.15
Y, mg Protein/mg glu	0.029
K_{eff}, mg glucose/L	21500
b, 1/hr	0.0011

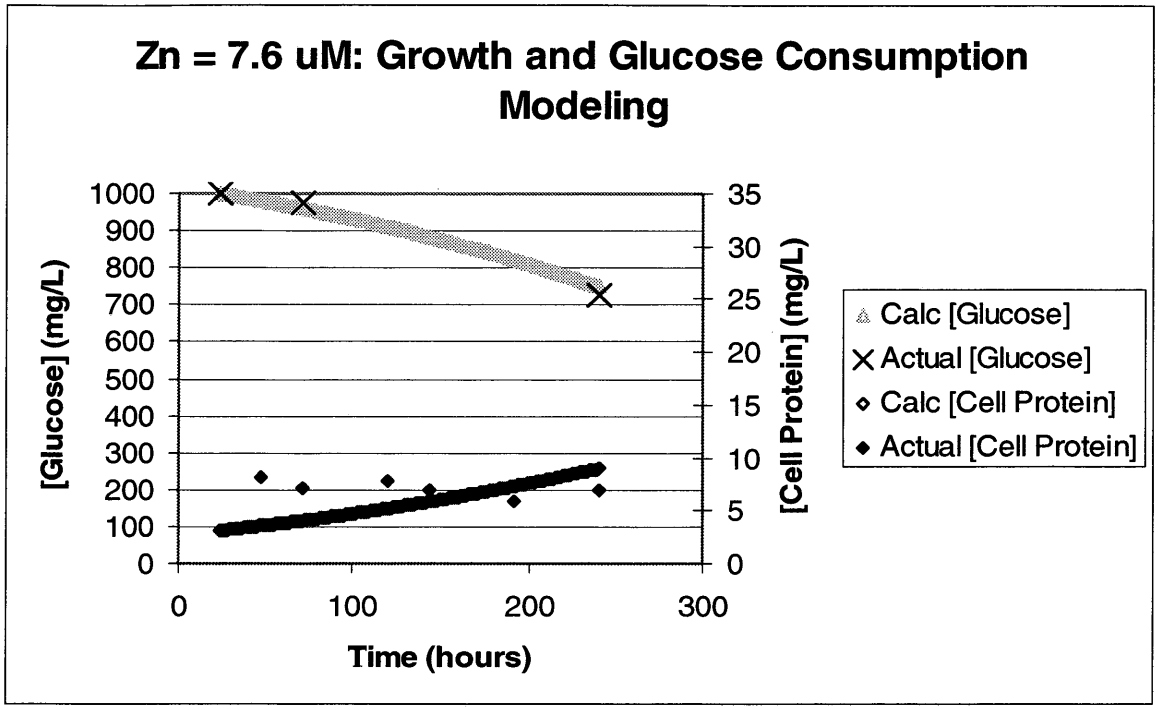

Figure 3.46 Monod data modeling of bottles containing Zn = 7.6 μM

Similar to the statistical findings of bottles at a zinc concentration of 6.1 μM, the P value of 0.2654 suggests that the model and the sample data values are not statistically significantly different, where as the R^2 value of 0.0382 suggests no correlation.

Table 3.23 and Figure 3.47 show the modeling changes and graphical results for bottles containing 12 μM of zinc.

Table 3.23 Monod constants values for bottles containing Zn = 12 μM

Zn = 12 uM (0.8 mg/L)	
μ_{max}, 1/hr	0.15
Y, mg Protein/mg glu	0.029
K_{eff}, mg glucose/L	28000
b, 1/hr	0.0011

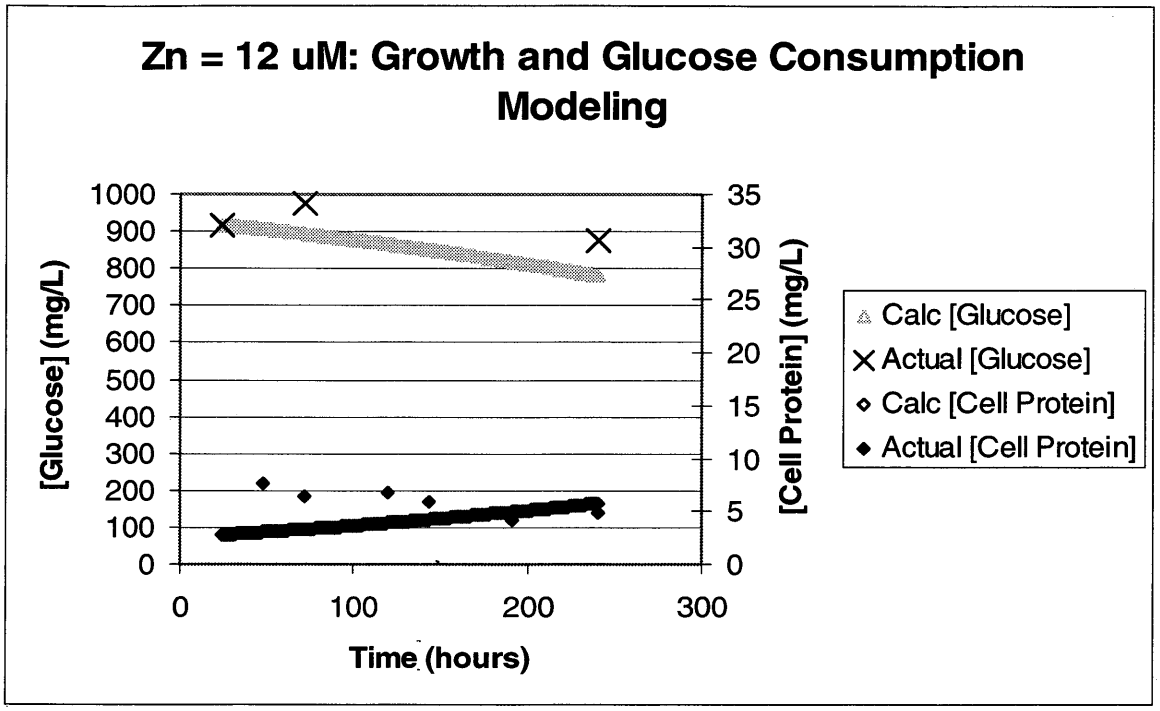

Figure 3.47 Monod data modeling of bottles containing Zn = 12 μM

Again, as with the statistical findings for bottles at zinc concentrations of 6.1 μM and 7.6 μM, the P value of 0.1029 suggests that the model and the sample data values are not statistically significantly different, yet the R^2 value of 0.023 suggests no correlation.

Table 3.24 and Figure 3.48 show the modeling changes and graphical results for bottles containing 15 μM of zinc.

Table 3.24 Monod constants values for bottles containing Zn = 15 μM

Zn = 15 uM (1 mg/L)	
μ_{max}, 1/hr	0.15
Y, mg Protein/mg glu	0.029
K_{eff}, mg glucose/L	41000
b, 1/hr	0.0011

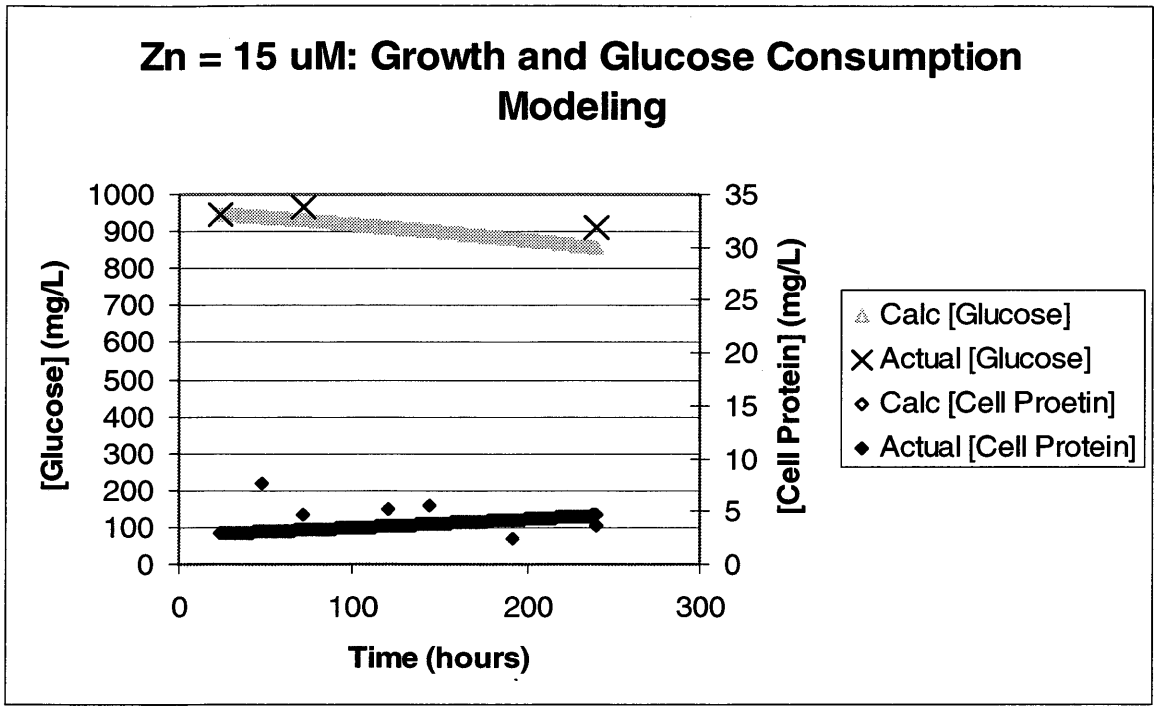

Figure 3.48 Monod data modeling of bottles containing Zn = 15 μM

Again, as with the statistical findings for bottles at zinc concentrations of 6.1 μM, 7.6 μM, and 12 μM, the P value of 0.2905 suggests that the model and the sample data values are not statistically significantly different, yet the R^2 value of 0.1634 suggests no correlation.

Table 3.25 and Figure 3.49 show the modeling changes and graphical results for bottles containing 23 μM of zinc.

Table 3.25 Monod constants values for bottles containing Zn = 23 μM

Zn = 23 uM (1.5 mg/L)	
μ_{max}, 1/hr	0.15
Y, mg Protein/mg glu	0.029
K_{eff}, mg glucose/L	52000
b, 1/hr	0.0011

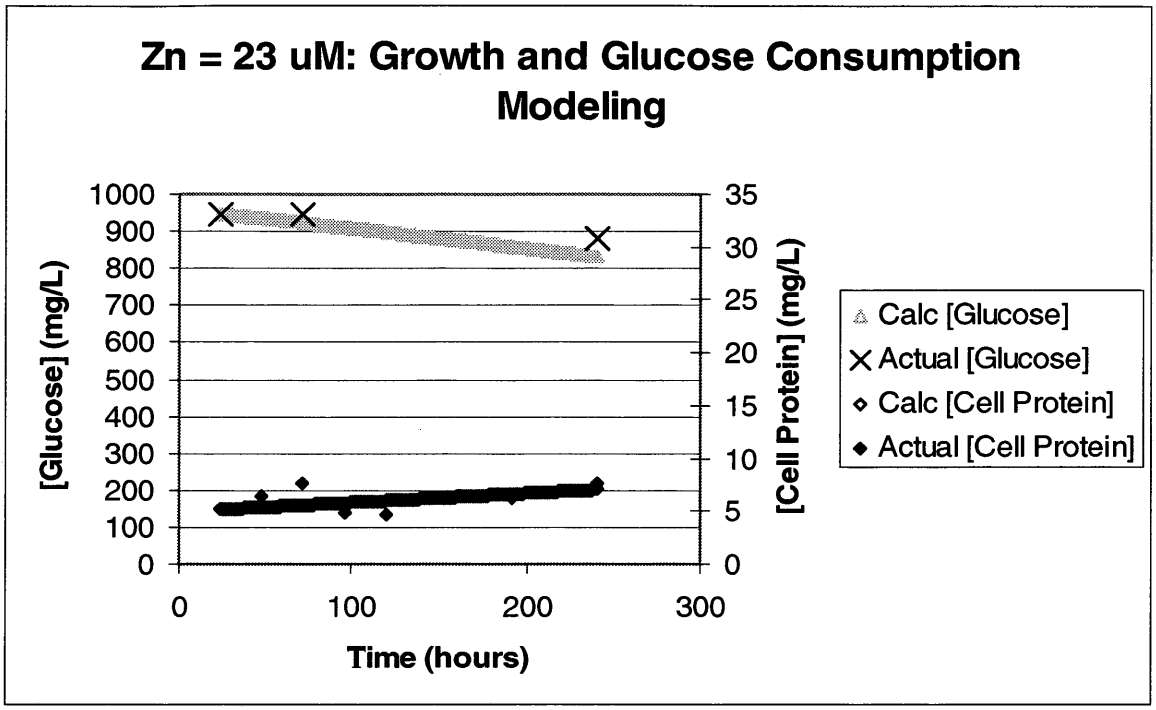

Figure 3.49 Monod data modeling of bottles containing Zn = 23 μM

Just as was observed with the statistical findings for bottles at zinc concentrations of 6.1 μM, 7.6 μM, 12 μM, and 15 μM, the P value of 0.7396 suggests that the model and the sample data values are not statistically significantly different, yet the R^2 value of 0.1647 suggests no correlation.

The Monod equation did a good job of modeling the growth and glucose patterns for the control bottles and the bottles containing 4.3 μM of zinc. Although the two-tailed

paired t-test showed no statistical significant difference between the model values and the actual data values (which means there is a correlation between the values produced by the model and the actual collected data values) at zinc concentrations of 6.1 μM and higher, the R^2 values at these zinc concentrations showed no correlation.. Yet, looking at Table 3.26 below, which summarizes the variability in values for K_{eff}, clearly shows that the K_{eff} values increase regularly as the zinc concentration increases. Figure 3.50 shows the relationship between K_{eff} and copper concentration, as well as the predicted K_{eff} calculated from the competitive inhibition equation.

Table 3.26 Summary of changes in K_{eff} with zinc concentration

[Zinc]	K_{eff}
Control = 0 mg/L	700
Zn = 4.3 uM	5500
Zn = 6.1 uM	31500
Zn = 7.6 uM	21500
Zn = 12 uM	28000
Zn = 15 uM	41000
Zn = 23 uM	52000

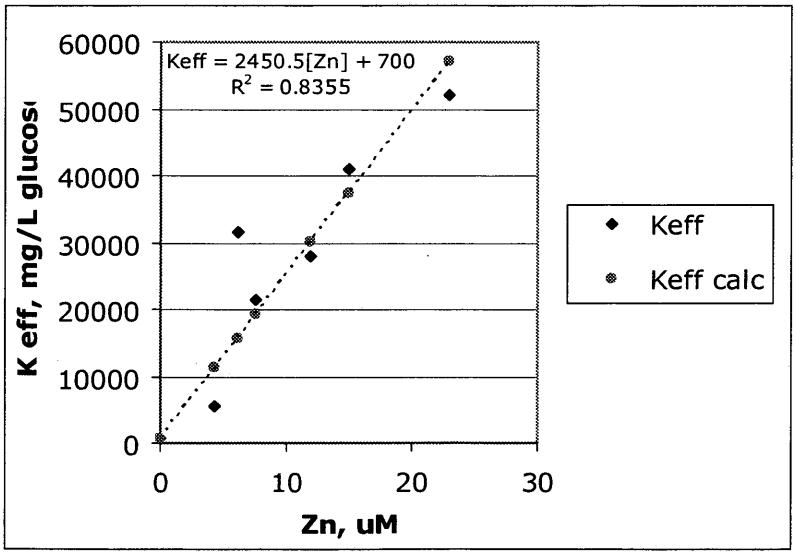

Figure 3.50 Relationship between K_{eff} and copper concentration

The predicted K_{eff} and the K_{eff} used to create the best fit of the Monod model to the data had an R^2 value of 0.836, and this suggest that competitive inhibition may be the best way to describe the inhibitory effects that zinc has on *C. flavigena*'s enzymes. This supports the positive statistical correlation found between the model and the actual data when conducting the two-tailed paired t-test.

3.5 Discussion

A copper toxicity threshold appears to be achieved between 3.2 μM (0.2 mg/L) and 4 μM (0.26 mg/L), and *C. flavigena* was able to recover from the toxic effects of copper concentrations at or below 0.2 mg/L, based on the observations made during the 10 day experiment. There is a possibility that *C. flavigena*'s growth would have recovered at higher copper concentrations had the experiments been run longer, ultimately giving the bacteria more time to acclimate, and produce more organic acids that can complex copper. Even though total cell biomass was comparable to the control bottles for copper concentrations less than or equal to 0.2 mg/L by the end of the experiment, the rate of growth was still inhibited at these copper concentrations. Had the experiment been stopped at day 6, it would have been concluded that *C. flavigena* experienced 50% inhibition (LC_{50}) in total cell protein at a copper concentration of 0.2 mg/L (3.2 μM). This is 5 times lower than that observed for *Desulfovibrio desulfuricans* (SRB), which experienced 50% inhibition (LC_{50}) in total cell protein at a copper concentration of 1.0 mg/L (16 μM) (Sani et al. 2001). Utgikar et al. (2001) found toxic effects (defined as the point when sulfate reduction no longer occurs) of copper ions on a mixed-culture of SRB to occur at 12 mg/L. As for similar toxicity studies, sulfate reduction was found to cease for copper concentrations ranging form 3 to 50 mg/L (Booth and Mercer, 1963; Saleh et al., 1964; Temple and Le Roux, 1964; Loka Bharathi et al., 1990; Hao et al., 1994). Although toxicity was determined based on growth, the

toxicity threshold, where growth ceased to occur for *C. flavigena*, could be related to the idea of complete inhibition of sulfate reduction for SRB, and the threshold observed for *C. flavigena* at 0.26 mg/L (0.4 μM) of copper, is much lower than that observed for SRB.

As for the mechanism of copper inhibition, the Monod equation suggested that non-competitive inhibition is a strong possibility. Keeping in mind that the Monod model is only a tool for understanding mechanisms, it is clear that this model is too simplistic to provide definitive answers regarding inhibition mechanisms for *C. flavigena*.

With respect to zinc toxicity experiments, *C. flavigena* exhibited a toxicity threshold between concentrations of 4.3 μM (0.28 mg/L) and 6.1 μM (0.4 mg/L). This suggests that *C. flavigena* is much more sensitive to zinc than *Desulfovibrio desulfuricans*, which exhibited little inhibition in growth rate based on the slight increase in lag phase, and no toxic effects based on complete recovery in total cell at 16 μM of Zn(II) (Sani et al. 2001). Utgikar et al. (2001) found toxic effects (defined as the point when sulfate reduction no longer occurs) of zinc to be 20 mg/L for mixed-culture of SRB. As for similar toxicity studies, sulfate reduction was found to cease for zinc concentrations ranging form 13 to 40 mg/L (Hao et al., 1994; Poulson et al., 1997). The large standard deviations observed in biomass concentration between replicate bottles at day 5 (120 hours) for Zn = 0.28 mg/L suggests that a critical threshold had been achieved. As with the copper experiments, perhaps *C. flavigena* would recover from the inhibition at higher zinc concentrations had the experiments been run for a longer period of time. Modeling of the growth data with the Monod equation suggested that competitive inhibition was likely the toxicity mechanism. It did a good job of modeling the growth in all the bottles.

Heavy metals have been reported to reach toxic concentrations for SRB over a wide range, spanning from a few mg/L to as much as 100 mg/L (Booth and Mercer, 1963; Hao et al., 1994; Loka Bharathi et al., 1990; Poulsen et al., 1997; Saleh et al., 1964; Sani et al., 2001; Temple and Le Roux, 1964; Utgikar et al., 2001 and 2002). Table 3.27

summarizes some of the findings of toxicity research conducted on SRB (Utgikar et al. 2002).

Table 3.27 Metal concentrations found to stop sulfate reduction activity in SRB.

Table I. Heavy metal toxicity to SRB.

Metal	SRB strain	Toxic concentration, mg/L	Reference
Cu	*Desulfovibrio* strains	20–50	Booth and Mercer (1963)
	Desulfovibrio strains	3	Temple and Le Roux (1964)
	Desulfovibrio strains	2–20	Saleh et al. (1964)
	Mixed culture	4–20	Hao et al. (1994)
	Mixed culture	12	Utgikar et al. (2001)
Zn	Mixed culture	25–40	Hao et al. (1994)
	Mixed culture	20	Utgikar et al. (2001)
	Desulfovibrio desulfuricans	13	Poulson et al. (1997)
Pb	Mixed culture	75–80	Hao et al. (1994)
	Strain L-60[a]	125	Loka Bharathi et al. (1990)
Cd	Mixed culture	>4–20	Hao et al. (1994)
	Strain L-60[a]	54	Loka Bharathi et al. (1990)
Ni	Mixed culture	10–20	Hao et al. (1994)
	Desulfovibrio desulfuricans	10	Poulson et al. (1997)
Cr	Mixed culture	60	Hao et al. (1994)
Hg	Strain L-60[a]	74	Loka Bharathi et al. (1990)
Mixture (Cr, Ni, Cu, Cd, Zn, Pb)	Mixed culture	20	Hao et al. (1994)

[a]Resembles *Desulfosarcina*.

As one can see when comparing the toxicity findings from this experiment with other toxicity studies conducted on SRB, *C. flavigena* proved to be much more sensitive to copper and zinc than SRB. In addition, both SRB and *C. flavigena* appear to tolerate higher concentrations of zinc compared to copper. The greater sensitivity of the cellulolytic fermenters should be considered in the selection of APTS for a specific site.

3.5.1 Comparison of Results to Hypothesis

The first hypothesis that *C. flavigena* would experience greater inhibition by copper and zinc then that found for SRB was supported by comparing previous research finding with the toxicity data collected in this study. It was also found that *C. flavigena* could be exposed to 6.1 μM of zinc compared to 4.1μM of copper and achieve similar toxicity threshold results. This supports the second hypothesis that copper would be more toxic than zinc.

3.5.2 Complexing of Metals with Organic Acids

Naturally occurring organic matter can influence the mobility of a metal (Beveridge T.J. and Doyle R.J. (eds), 1989). The succinate, acetate, lactate, and formate produced by *C. flavigena* can complex metals and reduce toxicity. Because all experiments were conducted with a pure culture, in a closed system, the organic acid byproducts were able to unnaturally build-up during the experiments. Normally SRB would consume the organic acids, and what wasn't consumed would be washed through the APTS due to hydraulic flow of the AMD. The presence of these organic acids during the experiments complicates the toxicity measurements. When modeling was done in MINTEQ, it was apparent that as the concentration of total organic acids increased, the percentage of complexed copper or zinc ions also increased. Although both metals were affected by the presence of organic acids, copper ions complex more readily, with about 50% complexed at very low organic acid concentrations, while zinc remained above 90% as free ion when the organic acid concentration was low. All and all, this suggests that inhibitions caused by metal ions may be over come, given enough time to produce an adequate amount of organic acids.

The question still unanswered, is at what metal concentration will there be no recovery? Long-term toxicity studies would need to be conducted to properly answer this question, and this should be conducted on a mixed-culture which complicates the results. Also, in a natural system the organic acids would be consumed by other microorganisms, and this leads one to wonder if the protection exhibited from organic acids can only be established in laboratory, pure culture-conditions. A review of metal toxicity on microorganisms, written by Giller et al. (1998), eludes to the problem of defining and quantifying bioavailability of metals in natural soil conditions due to the many factors affecting metal speciation and mobility. Wolt (1994) stated that in reality, bioavailability cannot be measured, because it is assessed based on microbial growth and evaluation of the toxicity and uptake of a given metal after the fact. As with many experiments, we simplify the system of interest in order to understand it, and the more realistic the scenario becomes the less certain we can be of the outcome.

CHAPTER 4 CONCLUSIONS

4.1 Major Results and Conclusions

The research conducted in this study was done to improve our understanding of metal toxicity and possible thresholds on a cellulolytic - fermenting bacteria, specifically *Cellulomonas flavigena*. Because cellulolyitc bacteria play an essential role in APTS by providing useable substrate for SRB, it was important to examine the effects of metals on their cellular activity. *C. flavigena* appeared to be more sensitive to metal toxicity than SRB, and this should be considered when deciding if passive treatment will work at a particular site. Although there are many factors contributing to the failure of AMD passive treatment systems, the knowledge of metal toxicity thresholds for cellulose degraders can help, at least in small part, to establish limitations of these systems. By recognizing realistic limitations of APTS we can begin to focus on ways to supplement or compliment APTS and improve AMD passive treatment technologies.

4.2 Future Work Opportunities

As with any research study, there are many questions left unanswered. While conducting this experiment and writing this paper, I came up with some suggestions on how to improve this work. In addition, there are several studies that should be done in order to expand our knowledge of the microbial ecology and the workings of an APTS.

With respect to this study, I would first recommend conducting these experiments in a chemostat type setting, where fresh nutrient broth would be fed in, byproducts would be washed away, and growth alone could be observed. Chemostat studies are very time

consuming for initial start-up and maintenance compared to batch experiments. However, the toxicity results from this research provide a good starting point for future experiments using cellulolytic-fermenting bacteria. Another modification would be to conduct these experiments with actual mine drainage. Doing this would complicate the system, because many metals would be present as well as hardness, but it would be a more realist scenario. In addition to these changes I would recommend looking more closely at sorption and internalization of metals. Internalization could be the actual cause of inhibition, rather than sorption, and this could help us understand the system better. With all that said, simply looking at a wider variety of metals would be useful too.

As for expanding beyond our knowledge of toxicity for *C. flavigena*, the next step should look at a mixed culture. Again, I think a chemostat study would prove the most useful. Long-term toxicity studies, however, would need to be conducted to properly answer the question regarding at what concentration of metal will the bacteria no longer be able to recover, and I think the current toxicity methods will need to be re-worked to achieve this. And finally, it would be interesting to determine if binding of metals with organic acids is kinetically faster than binding metals with sulfide produced by SRB, because if this is the case than perhaps SRB activity could be reduced over time in heavy metal laden waters due to the substrate being in an unavailable form for microbial uptake.

There are so many research opportunities with respect to microbial toxicity, the real question is what approach will prove the most realistic, while still remaining simple enough to provide useful information. Unfortunately, this is the dilemma many researchers find themselves in, and toxicity research is no different. If there is one thing this research project has taught me, it is that the goal of research is not just about finding the answer, but about perfecting upon the next question.

REFERENCES CITED

Babich H., and Stotszky G. (1983) "Temperature, pH, salinity, hardness, and particulates mediate nickel toxicity to eubacteria, an actinomycete, and yeasts in lake, simulated estuaries, and sea waters". *Aquat. Toxicol. 3*: 195-208.

Barton, L.L., and Tomie F.A. (1995) "Characteristics and activities of sulfate-reducing bacteria". In L.L. Barton (Ed.), *Sulphate Reducing Bacteria,* pp. 1-22. Plenum Press: New York, NY.

Bagnara C., Gaudin C., and Bélaïch J. P. (1987) "Physiological properties of *Cellulomoma fermentans*, a mesophilic cellulolytic bacterium". *Appl. Microbiol. Biotechnol. 26*: 170–176.

Benner S.G., Blowes D.W., and Ptacek C.J. (1997) "A Full-Scale Porous Reactive Wall for Prevention of Acid Mine Drainage". *Groundwater Monitoring and Remediation 17*: 99-107.

Berg J.M., Tymoczko J.L., and Stryer L. (2002) *Biochemistry*. W. H. Freeman and Company: New York, NY.

Beveridge T.J., and Murray R.G.E. (1976) "Uptake and retention of metals by cell walls of *Bacillus subtilis*". *J. Bacteriol. 127*: 1502-1518.

Beveridge T.J (1978) "The response of cell walls of *Bacillus subtilis* to metals and to electron microscope stains". *Can J. Microbiol. 24*: 89-104.

Beveridge T.J., and R. Murray G.E. (1980) "Sites of metal deposition in the cell walls of *Bacillus subtilis*". *J. Bacteriol. 141*: 876-887.

Beveridge T.J., and Doyle R.J. (Eds) (1989) *Metal Ions and Bacteria*. John Wiley and Sons, Inc. New York, NY.

Booth G.H., and Mercer S.J. (1963) "Resistance of copper to some oxidizing and reducing bacteria". *Nature. 199*:622.

Díaz-Raviña M., and Bååth E. (1996) "Development of Metal Tolerance in Soil Bacterial Communities Exposed to Experimentally Increased Metal Levels". *Applied and Environ. Microbiol. 62*(8): 2970-2977.

Dubois M., Gilles K.A., Hamilton J.K., Rebers P.A., and Smith F. (1956) "Colorimetric method for determination of sugars and related substances". *Anal. Chem. 28*:350.

Duxbury T., and Bicknell B. (1983) "Metal-tolerant bacterial populations from natural and metal-polluted soils". *Soil Biol. Biochem. 15*: 243–250.

Farmer G.H., Updegraff D.M., Lazorchak J.M., and Bates E.R. (1995) "Evaluation of metal removal and toxicity reduction in a low sulfate mine drainage by constructed wetlands". In: Proceedings of 12th Annual Meeting of American Society for Surface Mining and Reclamation, pp.78-89.

Giller K.E., Witter E., and McGrath S.P. (1998) "Toxicity of heavy metals to microorganisms and microbial processes in agricultural soils: a review". *Soil Biol. Biochem. 30* (10). 1389-1414.

Hao O.J., Huang L., Chen J.M., and Buglass R.L. (1994) "Effects of metal additions on sulfate reduction activity in wastewaters". *Toxicol. Environ. Chem. 46*:197-212.

Hemsi P.S., Shackelford C.D., and Figueroa L.A. (2005) "Modeling the influence of decomposing organic solids on sulfate reduction rates for iron prescipitation". *Environ. Sci. Technol. 39* (9). 3215 -3225.

Hopkin S.P. (1989) *Ecophysiology of metals in terrestrial invertebrates.* Elsevier Applied Science. New York, NY.

Hoyle B.D., and Beveridge T.J. (1983) Binding of metallic ions to the outer membrane of Escherichia coli". *Appli. Environ. Microbiol. 46*: 749-756.

Hu Z., Chandran K., Grasso D., and Smets B. (2003) "Impact of metal sorption and internalization on nitrification inhibition". *Environ. Sci. Technol. 37*: 728-734.

Huisman J., Ten Hoopen H.J.G., and Fuchs A. (1980) "The effect of temperature upon the toxicity of mercuric chloride in *Scenedesmus acutus*". *Environ. Pollut. 22A*: 33-44.

KTH Department of Land and Water Resources Engineering. http://www.lwr.kth.se/English/OurSoftware/vminteq/

Lakzian A., Murphy P., Tumer A., Beynon J., and Giller K. (2002) "*Rhizobium leguminosarum* bv. *viciae* populations in soils with increasing heavy metal contamination: abundance, plasmid profiles, diversity and metal tolerance". *Soil Biol. And Biochem. 34*: 519-529.

Logan M.V. (2003) "Microbial activity and the rate-limiting step in degradation of cellulose-based organic material to support sulfate reduction in anaerobic columns treating synthetic mine drainage". M.S. Thesis, T5797, Colorado School of Mines, Golden, CO.

Loka Bharathi P.A., Sathe V., and Chandramohan D. (1990) "Effect of lead, mercury, cadmium on a sulphate-reducing bacterium". *Environ. Pollut. 67*:361-374.

Lynd L.R., Weimer P.J., Zyl W.H., and Pretorius I.S. (2002) "Microbial cellulose utilization: fundamentals and biotechnology". *Microbiol. and Molecular Biol. Rev. 66*(3): 506–577.

Marquis R.E., Mayzel K., and Cartensen E.L. (1976). "Cation exchange in cell walls of gram-positive bacteria". *Ca. J. Microbiol. 22*: 975-982.

Mazidji C. N., Koopman B., Bitton G., and Neita D. (1992) "Distinction between heavy metal and organic toxicity using EDTA chelation and microbial assays". *Environ. Toxicol. Water Quality: An Int. J.* 7:339-353.

Mosey F.E., and Hughes D.A. (1975) "The toxicity of heavy metal ions to anaerobic digestions". *Water Pollut. Cont. 74*:18-39.

Poulson S.R., Colberg P.J.S., and Drever J.I. (1997) "Toxicity of heavy metals (Ni, Zn) to *Desulfovibrio desulfuricans*". *Geomicrobiol. J. 14:*41-49.

Rittman B.E., and McCarty P.L (2001) *Environmental Biotechnology: Principles and Applications*. McGraw-Hill Companies, Inc. New York, NY.

Saleh A.M., Macpherson R., and Miller J.D.A. (1964). "Effects of inhibitors on sulphate-reducing bacteria: a compilation". *J. Appl. Bact. 27*(2):281-293.

Sani R.K., Peyton B.M., and Brown L.T. (2001) "Copper-indused inhibition of growth of *Desulfovibrio desulfuricans* G20: Assessment of its toxicity and correlation with those of zinc and lead". *Appl. And Environ. Microbiol. 67*(10): 4765-4772.

Sani R.K., Peyton B., Smith W., Apel W., and Petersen J. (2002) "Dissimilatory reduction of Cr(VI), Fe(III), and U(VI) by *Cellulomonas* isolates". *Appl. Microbiol. Biotechnol. 60*:192-199.

Starr M., Stolp H., Truper H., Balows A., and Schlegel H. (1981) "The Prokaryotes: A Handbook on Habitats, Isolation, and Identification of Bacteria". Vol. 2. Springer-Verlag Berlin Heidelberg: New York, NY.

Szeto C., and Nyberg D. (1979) "The effect of temperature on copper tolerance of *Paramecium*, Bull". *Environ. Contam. Toxicol. 21*: 131-135.

Temple K.L., and Le Roux N.W. (1964) "Syngenesis of sulfide ores: sulfate-reducing bacteria and copper toxicity". *Econ. Geol. 59*:271-278.

United States Environmental Protection Agency (USEPA) (1995) "Historic hardrock mining: the west's toxic legacy". EPA 908-F-95-002.

Utigikar V.P., Chen B.Y., Tabak H.H., Bishop D.F., and Govind R. (2000) "Treatment of acid mine drainage: I. Equilibrium biosorption of zinc and copper on non-viable activated sludge". *Int. Biodeterior. Biodegrad. 46*:19-28.

Utigikar V.P., Chen B.Y., Chaudhary N., Tabak H.H., Haines J.R., and Govind R. (2001) "Acute toxicity of acid mine water heavy metals to acetate-utilizing sulfate-reducing bacteria". Paper accepted for publication by *Environ. Toxicol. Chem.*

Utigikar V.P., Tabak H.H., Haines J.R., and Govind R. (2002) "Quantification of toxic and inhibitory impact of copper and zinc on mixed cultures of sulfate-reducing bacteria". *Biotechnol. Bio-eng. 82*(3):306-312.

Western Governor's Association. http://www.westgov.org/wga/publicat/miningre.pdf

Wolt, J. (1994) *Soil Solution Chemistry.* John Wiley. New York, NY.

APPENDIX

APPENDIX A

Agar Plating Procedure to Insure Purity

1. add 4g of beef broth and 6 g of Agar and mix together in a flask containing1000mL DI water. Place a magnetic stir rod into flask and cover flask with plastic cap or aluminum foil.
2. Autoclave flask for 45 minutes. Remove from autoclave while flask is still very warm, and place flask on stir table until cool enough to touch.
3. Under a sterile hood pour mixture into sterile petri dishes, cover with petri lids, and allow mixture to solidify.
4. After Petri dishes have solidified cells can be transferred from 2 mL freezer vials using a sterile inoculation loop.
5. Once cells have been inoculated onto the Petri dish, cover, turn upside down, and place in sterile bag (same bag Petri dishes came in), and allow colonies to grow for 24 -48 hours.
6. Plating this microorganism allowed for purity observations to be made based on growing colonies. Plating was done throughout experiments.

APPENDIX B

Monitoring Growth: Coomassie Protein Assay SOP

Necessary Equipment:

1. 5 screw cap *plastic* vials (~15 ml) – used for dilutions and mixing of reagents
2. *plastic* disposable 3 ml cuvettes – used in spectrophotometer
3. Kim Wipes
4. 100 – 1000 microliter pipet
5. 10-20 microliter pipet
6. appropriate pipet tips
7. Vortex machine
8. 100 C oven
9. Spectrophotometer – *(at 595 nm wavelength)*

Necessary Reagents:

1. DI water
2. 1 M NaOH
3. 6 M HCl
4. Coomassie (Bradford) Protein Assay Reagent – *G250 dye, methanol, etc.*
5. Albumin Standard – *2mg/ml*

Creating Standard Curve:

(This procedure is based on simulating the addition of reagents used to lyse a living cell in order to measure it's protein content, even though albumin is already in a measurable state. All conditions for the standard must be the same as those used on the actual samples for comparison purposes, therefore we used a method established by Sani et al. 2001, "Assessment of lead toxicity to Desulfovibrio desulfuricans G20: influence of components of lactate C medium".)

1. Turn on Spectrophotometer to 595 nm. Needs to warm up for about 30 min.
2. In a sterile, disposable, plastic, 15 mL vial with cap, dilute albumin vial from 2 mg/mL to 0.2 mg/mL. (0.8 ml Albumin in 7.2 ml DI water).
3. All albumin standards must be put into sterile, plastic, disposable vials because the dye used in the procedure will stain glass.
4. Final total volume will equal 2.1 ml once reagents are added, but samples taken from experiment bottles will initially be 0.5 mL, so the known concentration for

the albumin will be created for a volume of 0.5 mL. The 0.2 mg/mL stock solution of albumin needs to be diluted with DI water to achieve concentrations ranging from 5 to 40 μg/mL (at 5 – 10 μg/mL intervals), final volume = 0.5 mL.

5. Remember to also have a "Blank" containing no albumin, but subject to all the following procedures.
6. Add 0.5 ml of 1 M NaOH to each sample.
7. Place samples in 100 °C oven for 10 min.
8. Remove from oven and allow to cool for 15 min.
9. Add 0.1 ml of 6 M HCl.
10. Vortex.
11. Add 1.0 ml Coomassie Reagent Dye.
12. Vortex
13. Let sit for 20 min.
14. Pipet out 2 ml of each prepared sample into 3 ml *plastic* cuvettes (dye will stain, so no glassware used). This should be done for the blank, and every standard concentration of sample. (*Always use a new pipet tip in between each sample to prevent contamination.*).
15. Record absorbance reading from spectrophotometer, be sure to re-blank between each reading for accuracy assurance in readings.
16. When finished, dispose of samples and other liquid waste into labeled container. Label should read what will be in it, such as < 1 M NaOH, < 6 M HCl, Coomassie Reagent Dye, Albumin. Also put your name and Date on the pink labeling tag and attach it to the waste container.
17. Turn off spectrophotometer, and properly clean-up work area.
18. Plot data and create a calibration curve. Should get an R^2 value around 0.95 or better, otherwise repeat above steps.

Unknown Sample analysis and Comparison to Standard Curve:

(method described by Sani et al. 2001, "Assessment of lead toxicity to Desulfovibrio desulfuricans G20: influence of components of lactate C medium".)

1. Remove 0.5 ml sample aseptically from serum bottles and put in plastic culture tubes/vial with screw caps. (*3 ml minimum volume*).
2. add 0.5 ml of 1 M NaOH.
3. Cap tubes and place in 100 °C oven fro 10 min.
4. Remove from oven and let cool for 15 min.
5. Then add 0.1 ml of 6 M HCl.
6. Vortex.
7. Add 1 ml of Coomassie reagent dye to each tube.
8. Vortex.
9. Let sit for about 20 min.

10. Measure absorbance for each sample at 595 nm wavelength on the same spectrophotometer as used for the standard curve (must use throughout experiment for comparison purposes). Make sure to run a known standard sample to insure accuracy of calibration curve and appropriate comparison.
11. Compare absorbance readings with the standard calibration curve or standard equation to determine protein concentrations.
12. Repeat above steps at for samples taken throughout the experiment.
13. When finished, dispose of samples and other liquid waste into labeled container. Label should read what will be in it. Also put your name and date on the pink labeling tag and attach it to the waste container.

APPENDIX C

Sampling Data Collected for Growth Determination

Copper Experiments:

$Abs_{595nm} = -4e^{-6}([Protein])^3 + 0.0003([Protein])^2 + 0.0023([Protein]) - 0.0047$

	24 hours			48 hours			72 hours			96 hours		
	Abs	Abs w/ Eq	[Protein]$_g$ uess (µg/mL)	Abs	Abs w/ Eq	[Protein]$_g$ uess (µg/mL)	Abs	Abs w/ Eq	[Protein]$_g$ uess (µg/mL)	Abs	Abs w/ Eq	[Protein]$_g$ uess (µg/mL)
Control 1	0.0349	0.0347	**8.6**	0.1097	0.1097	**17.9**	0.1941	0.1944	**26.7**	0.1917	0.1915	**26.4**
Control 2	0.0259	0.0259	**7.2**	0.0862	0.0864	**15.3**	0.1698	0.1700	**24.2**	0.1906	0.1905	**26.3**
Control 3	0.0306	0.0309	**8**	0.0953	0.0952	**16.3**	0.1884	0.1886	**26.1**	0.1985	0.1983	**27.1**
Control 4	0.036	0.0360	**8.8**	0.0848	0.0847	**15.1**	0.1947	0.1944	**26.7**	0.1996	0.1993	**27.2**
1 Cu = 0.002 mM	0.0353	0.0354	**8.7**	0.0427	0.0429	**9.8**	0.0878	0.0873	**15.4**	0.185	0.1847	**25.7**
2 Cu = 0.002 mM	0.046	0.0457	**10.2**	0.0604	0.0600	**12.1**	0.0696	0.0695	**13.3**	0.1086	0.1087	**17.8**
3 Cu = 0.002 mM	0.0394	0.0394	**9.3**	0.0516	0.0516	**11**	0.0627	0.0623	**12.4**	0.0873	0.0873	**15.4**
4 Cu = 0.002 mM	0.0362	0.0360	**8.8**	0.041	0.0408	**9.5**	0.0498	0.0494	**10.7**	0.0642	0.0647	**12.7**
1 Cu = 0.0025 mM	0.0247	0.0247	**7**	0.0599	0.0592	**12**	0.0836	0.0838	**15**	0.0875	0.0873	**15.4**
2 Cu = 0.0025 mM	0.0288	0.0290	**7.7**	0.0586	0.0584	**11.9**	0.0793	0.0795	**14.5**	0.1015	0.1014	**17**
3 Cu = 0.0025 mM	0.028	0.0277	**7.5**	0.0585	0.0584	**11.9**	0.0731	0.0737	**13.8**	0.0834	0.0838	**15**
4 Cu = 0.0025 mM	0.0157	0.0158	**5.4**	0.0383	-0.0047		0.0545	-0.0047		0.0446	-0.0047	
1 Cu = 0.0032 mM	0.0332	0.0334	**8.4**	0.0487	0.0486	**10.6**	0.0573	0.0569	**11.7**	0.0669	0.0671	**13**
2 Cu = 0.0032 mM	0.0333	0.0334	**8.4**	0.0519	0.0516	**11**	0.0597	0.0592	**12**	0.042	0.0422	**9.7**
3 Cu = 0.0032 mM	0.0305	0.0309	**8**	0.0473	0.0472	**10.4**	0.0601	0.0600	**12.1**	0.0498	0.0494	**10.7**
4 Cu = 0.0032 mM	0.0278	0.0277	**7.5**	0.0471	0.0472	**10.4**	0.0608	0.0607	**12.2**	0.0402	0.0408	**9.5**
1 Cu = 0.004 mM	0.0361	0.0360	**8.8**	0.0343	0.0341	**8.5**	0.0343	0.0341	**8.5**	0.0305	0.0309	**8**
2 Cu = 0.004 mM	0.0407	0.0408	**9.5**	0.0366	0.0367	**8.9**	0.036	0.0360	**8.8**	0.0338	0.0334	**8.4**
3 Cu = 0.004 mM	0.0423	0.0429	**9.8**	0.0401	0.0401	**9.4**	0.0365	0.0367	**8.9**	0.0357	0.0354	**8.7**
4 Cu = 0.004 mM	0.0471	0.0472	**10.4**	0.0367	0.0367	**8.9**	0.0421	0.0429	**9.8**	0.034	0.0341	**8.5**
1 Cu = 0.006 mM	0.036	0.0360	**8.8**	0.0193	0.0190	**6**	0.0277	0.0277	**7.5**	0.0263	0.0265	**7.3**
2 Cu = 0.006 mM	0.0383	0.0387	**9.2**	0.0265	0.0265	**7.3**	0.0316	0.0315	**8.1**	0.0304	0.0309	**8**
3 Cu = 0.006 mM	0.0337	0.0334	**8.4**	0.0262	0.0265	**7.3**	0.0229	0.0230	**6.7**	0.0277	0.0277	**7.5**
4 Cu = 0.006 mM	0.0286	0.0284	**7.6**	0.0283	0.0284	**7.6**	0.0239	0.0236	**6.8**	0.0272	0.0271	**7.4**
1 Cu = 0.008 mM	0.0338	0.0341	**8.5**	0.0272	0.0271	**7.4**	0.0366	0.0367	**8.9**	0.0303	0.0309	**8**
2 Cu = 0.008 mM	0.0324	0.0321	**8.2**	0.0303	0.0302	**7.9**	0.0345	0.0347	**8.6**	0.0368	0.0367	**8.9**
3 Cu = 0.008 mM	0.0364	0.0360	**8.8**	0.0337	0.0334	**8.4**	0.038	0.0381	**9.1**	0.0359	0.0360	**8.8**
4 Cu = 0.008 mM	0.0334	0.0334	**8.4**	0.0288	0.0290	**7.7**	0.0401	0.0401	**9.4**	0.0365	0.0367	**8.9**
1 Cu = 0.009 mM	0.0233	0.0236	**6.8**	0.01	0.0104	**4.3**	0.0145	0.0143	**5.1**	0.0088	0.0086	**3.9**
2 Cu = 0.009 mM	0.0222	0.0230	**6.7**	0.0133	0.0133	**4.9**	0.0087	0.0086	**3.9**	0.011	0.0118	**4.6**
3 Cu = 0.009 mM	0.024	0.0241	**6.9**	0.0163	0.0164	**5.5**	0.0187	0.0185	**5.9**	0.0087	0.0086	**3.9**
4 Cu = 0.009 mM	0.0221	0.0224	**6.6**	0.0081	0.0082	**3.8**	0.0102	0.0100	**4.2**	0.01	0.0104	**4.3**

	120 hours			144 hours			192 hours			240 hours		
	Abs	Abs w/ Eq	$[Protein]_g$ uoss (µg/mL)	Abs	Abs w/ Eq	$[Protein]_g$ uoss (µg/mL)	Abs	Abs w/ Eq	$[Protein]_g$ uoss (µg/mL)	Abs	Abs w/ Eq	$[Protein]_g$ uoss (µg/mL)
Control 1	0.1974	0.1974	**27**	0.1918	0.1915	**26.4**				0.1656	0.1660	**23.8**
Control 2		-0.0047		0.2008	0.2003	**27.3**				0.176	0.1758	**24.8**
Control 3	0.1981	0.1983	**27.1**	0.2064	0.2061	**27.9**				0.1899	0.1896	**26.2**
Control 4	0.2	0.2003	**27.3**	0.2117	0.2119	**28.5**				0.1922	0.1925	**26.5**
1 Cu = 0.002 mM	0.2	0.2003	**27.3**	0.2093	0.2090	**28.2**				0.1685	0.1680	**24**
2 Cu = 0.002 mM	0.1713	0.1709	**24.3**	0.218	0.2158	**28.9**				0.1581	0.1582	**23**
3 Cu = 0.002 mM	0.1524	0.1524	**22.4**	0.1899	0.1896	**26.2**				0.1581	0.1582	**23**
4 Cu = 0.002 mM	0.1206	0.1208	**19.1**	0.1885	0.1886	**26.1**				0.1671	0.1670	**23.9**
1 Cu = 0.0025 mM	0.1174	0.1171	**18.7**	0.169	0.1690	**24.1**	0.1649	0.1651	**23.7**	0.1283	0.137896	**20.9**
2 Cu = 0.0025 mM	0.094	0.0943	**16.2**	0.1243	0.1246	**19.5**	0.1763	0.1768	**24.9**	0.1326	0.132155	**20.3**
3 Cu = 0.0025 mM	0.1257	0.1255	**19.6**	0.1793	0.1798	**25.2**	0.1761	0.1758	**24.8**	0.1173	0.11706	**18.7**
4 Cu = 0.0025 mM	0.0481	-0.0047		0.0579	-0.0047		0.0892	-0.0047		0.1285	0.128351	**19.9**
1 Cu = 0.0032 mM	0.0474	0.0472	**10.4**	0.0664	0.0663	**12.9**	0.0743	0.0745	**13.9**	0.1556	0.155309	**22.7**
2 Cu = 0.0032 mM	0.0505	0.0501	**10.8**	0.0664	0.0663	**12.9**	0.0725	0.0728	**13.7**	0.0596	0.059188	**12**
3 Cu = 0.0032 mM	0.0548	0.0546	**11.4**	0.0644	0.0647	**12.7**	0.09	0.0899	**15.7**	0.127	0.127402	**19.8**
4 Cu = 0.0032 mM	0.0571	0.0569	**11.7**	0.0589	0.0584	**11.9**	0.0772	0.0770	**14.2**	0.1353	0.138856	**21**
1 Cu = 0.004 mM	0.0356	0.0354	**8.7**	0.0435	0.0436	**9.9**				0.0347	0.0347	**8.6**
2 Cu = 0.004 mM	0.0363	0.0360	**8.8**	0.0419	0.0415	**9.6**				0.0351	0.0354	**8.7**
3 Cu = 0.004 mM	0.0409	0.0408	**9.5**	0.044	0.0443	**10**				0.0455	0.0457	**10.2**
4 Cu = 0.004 mM	0.0566	0.0561	**11.6**	0.0483	0.0486	**10.6**				0.0522	0.0523	**11.1**
1 Cu = 0.006 mM	0.0267	0.0265	**7.3**	0.0323	0.0321	**8.2**				0.0293	0.0290	**7.7**
2 Cu = 0.006 mM	0.0298	0.0296	**7.8**	0.0367	0.0367	**8.9**				0.0338	0.0334	**8.4**
3 Cu = 0.006 mM	0.0274	0.0277	**7.5**	0.0286	0.0284	**7.6**				0.0279	0.0277	**7.5**
4 Cu = 0.006 mM	0.0366	0.0367	**8.9**	0.0347	0.0347	**8.6**				0.0356	0.0354	**8.7**
1 Cu = 0.008 mM	0.0333	0.0334	**8.4**	0.041	0.0415	**9.6**				0.0354	0.0354	**8.7**
2 Cu = 0.008 mM	0.0393	0.0394	**9.3**	0.0377	0.0374	**9**				0.0379	0.0374	**9**
3 Cu = 0.008 mM	0.041	0.0408	**9.5**	0.0412	0.0415	**9.6**				0.0391	0.0394	**9.3**
4 Cu = 0.008 mM	0.0434	0.0436	**9.9**	0.044	0.0443	**10**				0.0359	0.0360	**8.8**
1 Cu = 0.009 mM	0.0201	0.0201	**6.2**	0.0202	0.0201	**6.2**				0.0223	0.0224	**6.6**
2 Cu = 0.009 mM	0.0164	0.0164	**5.5**	0.0198	0.0201	**6.2**				0.0185	0.0180	**5.8**
3 Cu = 0.009 mM	0.0213	0.0213	**6.4**	0.0199	0.0201	**6.2**				0.0167	0.0164	**5.5**
4 Cu = 0.009 mM	0.0159	0.0158	**5.4**	0.0145	0.0143	**5.1**				0.0119	0.0118	**4.6**

Average Cell Protein Concentrations (mg/L): Copper Experiments

	Controls		Cu = 0.002 mM		Cu = 0.0025 mM		Cu = 0.0032 mM	
Time (hour	Protein	SD	Protein	SD	Protein	SD	Protein	SD
0	0.5	0	0.5	0	0.5	0	0.5	0
24	8.15	0.718795	9.433333	0.70946	6.9	1.042433	8.075	0.4272
48	16.15	1.279323	10.86667	1.305118	11.93333	0.057735	10.6	0.282843
72	25.925	1.184272	12.13333	1.320353	14.43333	0.602771	12	0.216025
96	26.75	0.465475	15.3	2.55147	15.8	1.058301	10.725	1.60494
120	27.13333	0.152753	21.93333	2.631223	18.16667	1.761628	11.075	0.585235
144	27.525	0.895824	27.06667	1.5885	22.93333	3.023795	12.6	0.476095
192					24.46667	0.665833	14.375	0.906918
240	25.325	1.257975	23.3	0.519615	19.95	1.137248	21.16667	1.457166

	Cu = 0.004 mM		Cu = 0.006 mM		Cu = 0.008 mM		Cu = 0.009 mM	
Time (hour	Protein	SD	Protein	SD	Protein	SD	Protein	SD
0	0.5	0	0.5	0	0.5	0	0.5	0
24	9.625	0.665207	8.5	0.68313	8.475	0.25	6.75	0.129099
48	8.925	0.368556	7.05	0.714143	7.85	0.420317	4.625	0.736546
72	9	0.559762	7.275	0.655108	9	0.33665	4.775	0.906918
96	8.4	0.294392	7.55	0.310913	8.65	0.43589	4.175	0.340343
120	9.65	1.347838	7.875	0.713559	9.275	0.634429	5.875	0.499166
144	10.025	0.419325	8.325	0.561991	9.55	0.412311	5.925	0.55
192								
240	9.65	1.212436	8.075	0.567891	8.95	0.264575	5.625	0.826136

Zinc Experiments:

Bottle # (mg/L)	24 hours			48 hours			72 hours			96 hours		
	Abs	Abs w/ Eq	[Protein]$_g$ uess (µg/mL)	Abs	Abs w/ Eq	[Protein]$_g$ uess (µg/mL)	Abs	Abs w/ Eq	[Protein]$_g$ uess (µg/mL)	Abs	Abs w/ Eq	[Protein]$_g$ uess (µg/mL)
Control 1		-0.0047		0.2463	0.245948	**32.1**	0.2551	0.255054	**33.1**	0.2137	0.213857	**28.7**
Control 2		-0.0047		0.2371	0.237607	**31.2**	0.2565	0.256853	**33.3**	0.2147	0.214821	**28.8**
Control 3	0.0529	0.053072	**11.2**	0.2465	0.246867	**32.2**	0.2613	0.261314	**33.8**	0.2282	0.228198	**30.2**
Control 4	0.0442	0.0443	**10**	0.2308	0.231035	**30.5**	0.2474	0.247784	**32.3**	0.2081	0.208061	**28.1**
Control 1	0.0686	0.068732	**13.2**	0.2565	0.256853	**33.3**	0.2575	0.257749	**33.4**			
Control 2	0.0566	0.056871	**11.7**	0.246	0.245948	**32.1**	0.2585	0.258644	**33.5**			
Control 3	0.05	0.050093	**10.8**	0.2435	0.243182	**31.8**	0.239	0.23854	**31.3**			
Control 4	0.0541	0.053825	**11.3**	0.2364	0.236672	**31.1**	0.2348	0.234798	**30.9**			
1 Zn = 0.28 mg/L	0.0245	0.024728	**7**	0.0429	0.042887	**9.8**	0.0313	0.031487	**8.1**			
2 Zn = 0.28 mg/L	0.0031	0.030852	**8**	0.0451	0.045012	**10.1**	0.0331	0.033417	**8.4**			
3 Zn = 0.28 mg/L	0.0022	0.021827	**6.5**	0.0382	0.038059	**9.1**	0.0299	0.029594	**7.8**			
4 Zn = 0.28 mg/L	0.0169	0.016886	**5.6**	0.0301	0.030852	**8**	0.0209	0.020697	**6.3**			
1 Zn = 0.4 mg/L	0.0136	0.0138	**5**	0.0288	0.028352	**7.6**	0.0269	0.026521	**7.3**			
2 Zn = 0.4 mg/L	0.0114	0.011361	**4.5**	0.0347	0.034724	**8.6**	0.0316	0.031487	**8.1**			
3 Zn = 0.4 mg/L	0.0123	0.012322	**4.7**	0.0324	0.032127	**8.2**	0.0267	0.026521	**7.3**			
4 Zn = 0.4 mg/L	0.0042	0.004395	**2.9**	0.0303	0.030221	**7.9**	0.0245	0.024728	**7**			
1 Zn = 0.5 mg/L	0.0013	0.001416	**2.1**	0.0278	0.027738	**7.5**	0.0312	0.031487	**8.1**			
2 Zn = 0.5 mg/L	0.006	0.006013	**3.3**	0.0346	0.034724	**8.6**	0.0215	0.021827	**6.5**			
3 Zn = 0.5 mg/L	0.003	0.002863	**2.5**	0.033	0.03277	**8.3**	0.0285	0.028971	**7.7**			
4 Zn = 0.5 mg/L	0.0125	0.012322	**4.7**	0.0335	0.033417	**8.4**	0.0219	0.021827	**6.5**			
1 Zn = 0.8 mg/L	0.0028	0.002863	**2.5**	0.0254	0.025321	**7.1**	0.0213	0.021259	**6.4**			
2 Zn = 0.8 mg/L	0.006	0.006013	**3.3**	0.0308	0.030852	**8**	0.021	0.021259	**6.4**			
3 Zn = 0.8 mg/L	0.0045	0.004395	**2.9**	0.0268	0.026521	**7.3**	0.0272	0.027127	**7.4**			
4 Zn = 0.8 mg/L	0.0031	0.002863	**2.5**	0.0307	0.030852	**8**	0.0182	0.017952	**5.8**			
1 Zn = 1.0 mg/L	0.006	0.006013	**3.3**	0.0285	0.028352	**7.6**	0.016	0.015838	**5.4**			
2 Zn = 1.0 mg/L	0.0023	0.002493	**2.4**	0.0323	0.032127	**8.2**	0.0103	0.010419	**4.3**			
3 Zn = 1.0 mg/L	0.0033	0.003238	**2.6**	0.0302	0.030221	**7.9**	0.0107	0.010887	**4.4**			
4 Zn = 1.0 mg/L	0.0062	0.006431	**3.4**	0.0258	0.025919	**7.2**	0.0152	0.0138	**5**			
1 Zn = 1.5 mg/L	0.0127	0.01281	**4.8**	0.0167	0.01636	**5.5**	0.0253	0.025321	**7.1**	0.0114	0.011361	**4.5**
2 Zn = 1.5 mg/L	0.0158	0.015838	**5.4**	0.0209	0.020697	**6.3**	0.0362	0.036713	**8.9**	0.0176	0.017416	**5.7**
3 Zn = 1.5 mg/L	0.0156	0.015838	**5.4**	0.0254	0.025321	**7.1**	0.0294	0.029594	**7.8**	0.0133	0.013302	**4.9**
4 Zn = 1.5 mg/L	0.0145	0.014302	**5.1**	0.0228	0.022974	**6.7**	0.0219	0.021827	**6.5**	0.0108	0.010887	**4.4**

Bottle # (mg/L)	120 hours			144 hours			192 hours			240 hours		
	Abs	Abs w/ Eq	[Protein]$_g$ uess (µg/mL)	Abs	Abs w/ Eq	[Protein]$_g$ uess (µg/mL)	Abs	Abs w/ Eq	[Protein]$_g$ uess (µg/mL)	Abs	Abs w/ Eq	[Protein]$_g$ uess (µg/mL)
Control 1	0.2299	0.229144	**30.3**	0.2347	0.234798	**30.9**	0.2242	0.224398	**29.8**	0.1705	0.169962	**24.2**
Control 2	0.2233	0.219622	**29.3**	0.2394	0.239471	**31.4**	0.2119	0.211929	**28.5**	0.1582	0.158232	**23**
Control 3	0.2417	0.24133	**31.6**	0.2563	0.236672	**31.1**	0.211	0.210963	**28.4**	0.1799	0.17976	**25.2**
Control 4	0.2257	0.225349	**29.9**	0.2156	0.215783	**28.9**	0.2175	0.217704	**29.1**	0.1607	0.160183	**23.2**
Control 1	0.2539	0.253248	**32.9**	0.2435	0.243182	**31.8**	0.2191	0.219622	**29.3**	0.2229	0.222491	**29.6**
Control 2	0.2517	0.251434	**32.7**	0.2356	0.235736	**31**	0.2247	0.224398	**29.8**	0.2153	0.215783	**28.9**
Control 3	0.246	0.245948	**32.1**		-0.0047		0.2253	0.225349	**29.9**	0.207	0.207092	**28**
Control 4	0.2306	0.231035	**30.5**	0.2171	0.217704	**29.1**	0.2059	0.206122	**27.9**	0.2082	0.208061	**28.1**
1 Zn = 0.28 mg/L	0.1882	0.188575	**26.1**	0.234	0.23386	**30.8**	0.1976	0.197368	**27**	0.1845	0.184659	**25.7**
2 Zn = 0.28 mg/L	0.1981	0.199317	**27.2**	0.2469	0.246867	**32.2**	0.2043	0.204181	**27.7**	0.2007	0.200291	**27.3**
3 Zn = 0.28 mg/L	0.0887	0.08813	**15.5**	0.2152	0.214821	**28.8**	0.2149	0.214821	**28.8**	0.196	0.196393	**26.9**
4 Zn = 0.28 mg/L	0.0692	0.069546	**13.3**	0.1444	0.148508	**22**	0.2202	0.220579	**29.4**	0.2123	0.212893	**28.6**
1 Zn = 0.4 mg/L	0.0363	0.036046	**8.8**	0.0336	0.033417	**8.4**	0.0207	0.020697	**6.3**	0.0398	0.03942	**9.3**
2 Zn = 0.4 mg/L	0.0375	0.037384	**9**	0.0327	0.03277	**8.3**	0.0193	0.019036	**6**	0.0287	0.028352	**7.6**
3 Zn = 0.4 mg/L	0.0352	0.035383	**8.7**	0.026	0.025919	**7.2**	0.0201	0.020139	**6.2**	0.021	0.021259	**6.4**
4 Zn = 0.4 mg/L	0.0303	0.030852	**8**	0.0247	0.024728	**7**	0.0169	0.016886	**5.6**	0.0188	0.018491	**5.9**
1 Zn = 0.5 mg/L	0.0229	0.022974	**6.7**	0.0224	0.022398	**6.6**	0.0177	0.017416	**5.7**	0.0153	0.015321	**5.3**
2 Zn = 0.5 mg/L	0.0339	0.034069	**8.5**	0.0214	0.021827	**6.5**	0.0201	0.020139	**6.2**	0.1536	-0.0047	
3 Zn = 0.5 mg/L	0.0337	0.034069	**8.5**	0.0301	0.030221	**7.9**	0.0232	0.022974	**6.7**	0.0419	0.041489	**9.6**
4 Zn = 0.5 mg/L	0.0272	0.027738	**7.5**	0.0235	0.023554	**6.8**	0.0133	0.013302	**4.9**	0.0201	0.020139	**6.2**
1 Zn = 0.8 mg/L	0.0148	0.01481	**5.2**	0.0189	0.019036	**6**	0.0142	0.014302	**5.1**	0.0118	0.011839	**4.6**
2 Zn = 0.8 mg/L	0.0272	0.027738	**7.5**	0.0215	0.021259	**6.4**	0.0067	0.006854	**3.5**	0.0125	0.012322	**4.7**
3 Zn = 0.8 mg/L	0.0259	0.025321	**7.1**	0.021	0.020697	**6.3**	0.01	0.009956	**4.2**	0.0141	0.01281	**4.8**
4 Zn = 0.8 mg/L	0.0252	0.025321	**7.1**	0.0157	0.015321	**5.3**	0.0084	0.009044	**4**	0.017	0.017416	**5.7**
1 Zn = 1.0 mg/L	0.0192	0.019036	**6**	0.0129	0.01281	**4.8**	0.004	0.004004	**2.8**	0.007	0.006854	**3.5**
2 Zn = 1.0 mg/L	0.0116	0.011361	**4.5**	0.016	0.01636	**5.5**	0.002	-0.0021	**1**	0.0051	0.005194	**3.1**
3 Zn = 1.0 mg/L	0.0164	0.01636	**5.5**	0.0187	0.019036	**6**	0.006	0.006013	**3.3**	0.0104	0.010419	**4.3**
4 Zn = 1.0 mg/L	0.0123	0.012322	**4.7**	0.0185	0.018491	**5.9**	0.0033	0.003238	**2.6**	0.0064	0.006431	**3.4**
1 Zn = 1.5 mg/L	0.0108	0.010887	**4.4**	0.0214	0.021259	**6.4**	0.0203	0.020139	**6.2**	0.0451	0.045012	**10.1**
2 Zn = 1.5 mg/L	0.0105	0.010419	**4.3**	0.0219	0.021827	**6.5**	0.0238	0.023554	**6.8**	0.03	0.030221	**7.9**
3 Zn = 1.5 mg/L	0.0149	0.01481	**5.2**	0.0212	0.021259	**6.4**	0.0286	0.028352	**7.6**	0.0227	0.022398	**6.6**
4 Zn = 1.5 mg/L	0.0134	0.013302	**4.9**	0.0185	0.018491	**5.9**	0.015	0.011361	**4.5**	0.02	0.020139	**6.2**

Average Cell Protein Concentration (mg/L): Zinc Experiments

	Control 2		Controls 1		Zn = 0.28 mg/L		Zn = 0.4 mg/L	
Time (hours)	Protein	SD	Protein	SD	Protein	SD	Protein	SD
0	0.5	0	0.5	0	0.5	0	0.5	0
24	11.75	1.034408	10.6	0.848528	6.775	1.001249	4.275	0.939415
48	32.075	0.917878	31.5	0.804156	9.25	0.932738	8.075	0.4272
72	32.275	1.367175	33.125	0.623832	7.65	0.932738	7.425	0.471699
96			28.95	0.888819				
120	32.05	1.087811	30.275	0.974252	20.525	7.14347	8.625	0.434933
144	30.63333	1.386843	30.575	1.135415	28.45	4.520693	7.725	0.727438
192	29.225	0.921502	28.95	0.645497	28.225	1.078193	6.025	0.30957
240	28.65	0.750555	23.9	1.013246	27.125	1.195478	7.3	1.512173

	Zn = 0.5 mg/L		Zn = 0.8 mg/L		Zn = 1 mg/L		Zn = 1.5 mg/L	
Time (hours)	Protein	SD	Protein	SD	Protein	SD	Protein	SD
0	0.5	0	0.5	0	0.5	0	0.5	0
24	3.15	1.147461	2.8	0.382971	2.925	0.499166	5.175	0.287228
48	8.2	0.483046	7.6	0.469042	7.725	0.4272	6.4	0.68313
72	7.2	0.824621	6.5	0.663325	4.775	0.518813	7.575	1.030776
96							4.875	0.590903
120	7.8	0.87178	6.725	1.034005	5.175	0.699405	4.7	0.424264
144	6.95	0.645497	6	0.496655	5.55	0.544671	6.3	0.270801
192	5.875	0.767572	4.2	0.668331	2.425	0.994569	6.275	1.314978
240	7.033333	2.267892	4.95	0.506623	3.575	0.512348	7.7	1.756891

APPENDIX D

Glucose Analysis SOP

Necessary Equipment:

1. 6 of the 100 ml volumetric Flasks (only used for diluting/creating the standards)
2. Screw cap *glass* test tubes (~15 ml) – used for mixing reagents. (As many as there are samples)
3. Sterile disposable plastic vials (15 mL) for prepping experimental samples. (As many as there are samples)
4. *Quartz or glass* 1 ml cuvettes – used in spectrophotometer
5. Kim Wipes
6. 100 – 1000 microliter pipet
7. Repipetter (for concentrated Acid)
8. appropriate pipet tips
9. Vortex machine
10. 80 °C oven (for drying out glucose to be weighed and added to solution)
11. Hot bath for soaking samples (30 °C)
12. Spectrophotometer – *(at 490 nm wavelength)*

Necessary Reagents:

1. DI water
2. Glucose
3. 5 % phenol solution
4. Concentrated Sulfuric Acid (H_2SO_4)
5. 80% EtOH

Standard Curve for Known Glucose Concentrations:

(This procedure was created by Dubois, M., K.A. Gilles, J.K. Hamilton, P.A. Rebers, and F. Smith. 1956. Colorimetric method for determination of sugars and related substances. Anal. Chem. 28:350.)

1. Turn on hot bath to low, with a thermometer to obtain a 30 °C temp.
2. Turn of spectrophotometer (needs 30 + min. to warm up).
3. The stock glucose solution will be prepared by weighing out dry glucose (oven dried fro 48 hours at 80 °C) to a weight of 1.0000 grams. Place the weighed glucose into a 100 ml Volumetric Flask. Add DI water to bring to volume, and mix well.

4. To the remaining 5 volumetric flasks (100 ml) add 10 ml of 80% EtOH solution.
5. We then will perform serial dilutions adding varying amounts of the stock solution with DI to the 5 volumetric flasks containing EtOH. Examples of desired concentrations are given in the table below:

Stock Dilutions:

Desired Conc. (mg/mL)	Stock soln (mL)	EtOH (mL)	DI water (mL)	Final Volume (mL)
0	0	10	90	100
0.025	0.25	10	89.75	100
0.05	0.5	10	89.5	100
0.075	0.75	10	89.25	100
0.1	1	10	89	100

6. Take 0.5 ml aliquots of each dilution and place in labeled glass test tubes.
7. Add 0.5 mL of 5% phenol solution.
8. Add 2.5 mL of Concentrated H_2SO_4 using the repipetter (*do not allow acid to run down outside of test tube, the addition of acid is very important to the reproducibility of this test.*)
9. Be careful, test tubes will become hot upon the addition of acid.
10. Vortex after each addition of acid to the sample.
11. Vortex all samples again after all samples are pipetted.
12. Place test tubes on rack in the 30 °C hot bath for 20 min.
13. Romove samples form bath, vortex, and let sit at room temperature for 30 minutes.
14. Make sure bubbles are not present during absorbance readings.
15. Using acid resistant quartz cuvettes, take readings at 490 nm wavelength, making sure to blank in between each reading.
16. Can air dry cuvettes between sample readings using air blower in hood area.
17. When finished, dispose of samples and other liquid waste into labeled container. Label should read what will be in it. Also put your name and date on the pink labeling tag and attach it to the waste container.
18. Turn off spectrophotometer and water bath, and properly clean-up work area.
19. Plot data and create a calibration curve. Should get a R^2 value around 0.96 or better, otherwise repeat above steps.

Note: KEEP SAMPLES OUT OF SUNLIGHT

Unknown Sample analysis and Comparison to Standard Curve:

1. Remove 1.5 ml sample aseptically from serum bottles and put in plastic culture tubes (*2 ml minimum volume*).
2. Centrifuge for 5 min at 12,000g and then filter liquid sample through Whatman 541 filter paper to remove any fine particles.
3. Pipette 1 mL of the filtered extract into a 15 mL sterile plastic, disposable, caped vial.
4. Add 1 mL of 80% EtOH.
5. Bring to 10 mL volume with DI water (add 8 mL).
6. mix well.
7. Take 0.5 ml aliquot of diluted sample and place in labeled glass test tubes.
8. Add 0.5 mL of 5% phenol solution.
9. Add 2.5 mL of Concentrated H_2SO_4 using the repipetter (*do <u>not</u> allow acid to run down outside of test tube, the addition of acid is very important to the reproducibility of this test.*)
10. Be careful, test tubes will become hot upon the addition of acid.
11. Vortex after each addition of acid to the sample.
12. Vortex all samples again after all samples are pipetted.
13. Place test tubes on rack in the 30 °C hot bath for 20 min.
14. Romove samples form bath, vortex, and let sit at room temperature for 30 minutes.
15. Make sure bubbles are not present during absorbance readings.
16. Using acid resistant quartz cuvettes, take readings at 490 nm wavelength, making sure to blank in between each reading. Also, always do a reading a the a known standard sample every 10-15 samples to insure instrument accuracy.
17. Can air dry cuvettes between sample readings using air blower in hood area.
18. When finished, dispose of samples and other liquid waste into labeled container. Label should read what will be in it. Also put your name and date on the pink labeling tag and attach it to the waste container.
19. Turn off spectrophotometer and water bath, and properly clean-up work area.
20. Compare data to calibration curve.

APPENDIX E

Sampling Data Collected for Glucose Consumption Analysis

Glucose Absorbance Readings: Copper Experiments

ABSORBANCE	Controls				Cu = 0.002 mM				Cu = 0.0025 mM				Cu = 0.0032 mM			
Time (hours)	Control #1	Control #2	Control #3	Control #4	1	2	3	4	1	2	3	4	1	2	3	4
0	0.7598	0.747	0.792	0.7972	0.835	0.8598	0.8516	0.8609	0.816	0.818	0.8258	0.8126	0.8126	0.8236	0.8535	0.8268
24	0.7057	0.7661	0.785	0.7843	0.8051	0.7803	0.7733	0.8101	0.8286	0.7941	0.8574	0.8268	0.7829	0.7693	0.8828	0.7324
72	0.1674	0.3345	0.2151	0.1765	0.5262	0.5324	0.6468	0.6675	0.6331	0.6485	0.7233	0.6425	0.728	0.7128	0.715	0.697
120	0.0876	0.0959	0.1644	0.1054	0.0557	0.3303	0.4559	0.5272								
240	0.0136	0.0024	0.0401	0.0043	0.0266	0.0296	0.0339	0.0349	0.0986	0.0647	0.0664	0.0732	0.2129	0.4454	0.1657	0.152

ABSORBANCE	Cu = 0.004 mM				Cu = 0.006 mM				Cu = 0.008 mM				Cu 0.009 mM			
Time (hours)	1	2	3	4	1	2	3	4	1	2	3	4	1	2	3	4
0	0.9431	0.8591	0.8962	0.8733	0.9426	0.9154	0.8594	0.8462	0.8514	0.8393	0.8516	0.8491	0.7917	0.8563	0.8364	0.8404
24	0.7095	0.732	0.8239	0.7859	0.8267	0.8047	0.8584	0.7733	0.8142	0.7891	0.8298	0.8338	0.8177	0.7307	0.8514	0.7811
72	0.6025	0.7434	0.7427	0.7054	0.7709	0.7888	0.7527	0.7151	0.7342	0.7677	0.7468	0.7234	0.7425	0.7967	0.7738	0.8281
120	0.7575	0.7562	0.7537	0.7832	0.8111	0.838	0.8696	0.7915	0.7606	0.7467	0.7749	0.7191	0.7802	0.7598	0.7485	0.8229
240	0.7205	0.7167	0.6738	0.6839	0.7301	0.7187	0.7322	0.6622	0.7153	0.6417	0.6054	0.4248	0.5265	0.5691	0.7068	0.7829

Average Glucose Concentration: Copper Experiments

CONC mg/L	Controls		Cu = 0.002 mM		Cu = 0.0025 mM		Cu = 0.0032 mM	
	[Glucose]	SD	[Glucose]	SD	[Glucose]	SD	[Glucose]	SD
Time (hours)								
0	856.5556	23.71823	943.0278	9.843867	905.5556	2.773808	917.8056	15.83419
24	841.3056	38.13392	876.7778	16.6954	915.1389	25.30785	879.7037	83.64855
72	244.75	82.01656	635.8519	79.15501	731.9444	42.61559	789	10.68139
120	122.4722	35.24216	334.7778	107.3223				
240	13.33333	15.85587	31.27778	0.844022	80.69444	13.98439	193.0741	32.05418

CONC mg/L	Cu = 0.004 mM		Cu = 0.006 mM		Cu = 0.008 mM		Cu = 0.009 mM	
	[Glucose]	SD	[Glucose]	SD	[Glucose]	SD	[Glucose]	SD
Time (hours)								
0	988.6944	37.41831	986.4444	47.32527	938.6111	3.013077	920.1111	27.3338
24	863.8889	47.86519	887.1852	26.37504	904.0278	19.07238	880.1389	54.01818
72	772.6667	70.35112	837.5278	31.56577	822.1389	17.69713	869.0833	36.74998
120	843.9444	11.87828	916.0556	34.22211	830.25	22.98698	860.8333	32.97023
240	772.9167	22.52077	786.3333	33.15381	659.6667	133.717	714.6944	129.009

Glucose Absorbance Readings : Zinc Experiments

ABSORBANCE	Controls				Zn = 0.0043 mM				Zn = 0.0061 mM				Zn = 0.0076 mM			
Time (hours)	Control #1	Control #2	Control #3	Control #4	1	2	3	4	1	2	3	4	1	2	3	4
0	0.8611	0.81	0.8369	0.8524	0.8796	0.8599	0.8299	0.8509	0.8263	0.8922	0.8579	0.8996	0.9128	0.8781	0.9134	0.8006
24	0.7259	0.6943	0.7274	0.6805	0.9011	0.9087	0.8551	0.8685	0.8811	0.9742	0.8946	0.8914	0.8695	0.903	0.9488	0.8855
72	0.0508	0.0487	0.0442	0.0884	0.7847	0.8226	0.8169	0.8297	0.8723	0.9105	0.7507	0.8827	0.8949	0.8884	0.867	0.881
240	0.0365	0.033	0.0393	0.0365	0.1254	0.0516	0.0547	0.0568	0.7005	0.7091	0.8215	0.7992	0.7867	0.3954	0.6801	0.773

ABSORBANCE	Zn = 0.0122 mM				Zn = 0.015 mM				Zn = 0.023 mM			
Time (hours)	1	2	3	4	1	2	3	4	1	2	3	4
0	0.88	0.8805	0.9029	0.8644	0.8908	0.9178	0.8725	0.8877	0.8592	0.8455	0.8396	0.8141
24	0.8881	0.7768	0.8023	0.848	0.8366	0.8516	0.8815	0.85	0.7996	0.8884	0.9009	0.8468
72	0.902	0.8752	0.8736	0.8645	0.9367	0.8612	0.8733	0.8121	0.8365	0.8871	0.8415	0.8214
240	0.8208	0.7975	0.7742	0.7673	0.8502	0.8161	0.8354	0.7867	0.7216	0.8317	0.9086	0.7335

Average Glucose Concentration: Zinc Experiments

CONC mg/L	Controls		Zn = 0.0043mM		Zn=0.0061mM		Zn = 0.0076mM	
	[Glucose]	SD	[Glucose]	SD	[Glucose]	SD	[Glucose]	SD
Time (hours)								
0	930	21.47138	946.6389	19.47039	962.1111	34.07702	970.1389	55.49811
24	782.1389	22.50983	978.0556	25.07362	1018.852	48.67571	998.4444	34.61215
72	61.02778	19.26256	900.4167	18.65007	945.5	75.17981	977.4722	9.868001
240	36.91667	-0.5779	76.69444	36.08982	838.3056	65.12839	728.5556	198.6366

CONC mg/L	Zn = 0.0122mM		Zn = 0.015mM		Zn = 0.023mM	
	[Glucose]	SD	[Glucose]	SD	[Glucose]	SD
Time (hours)						
0	976.5	14.15665	987.8889	17.49698	959.0278	16.63182
24	917.4444	51.333	946.4722	17.6115	946.4167	41.51511
72	973.0278	14.50298	964.1389	53.52608	943.5	34.60312
240	874.2778	23.5429	910	27.02284	878.6111	55.45566

APPENDIX F

Organic Acid Sampling Data

Control 1 & 2 (0 hrs)

Time	Acid	Peak Area	Peak Area	Avg Peak	Avg Conc.
0	succ	22.63	0	11.315	5.818677
0	lact	0	42.88	21.44	4.813651
0	form	0	0	0	0
0	acet	0	0	0	0

Control 1 & 2 (72 hrs)

Time	Acid	Peak Area	Peak Area	Avg Peak	Avg Conc.
72	succ	112.32	126.9	119.61	61.50879
72	lact	654.1	590.86	622.48	139.7575
72	form	938.2	1316.3	1127.25	337.3889
72	acet	255.04	230.6	242.82	56.66877

Control 1 & 2 (240 hrs)

Time	Acid	Peak Area	Peak Area	Avg Peak	Avg Conc.
240	succ	239.9	264	251.95	129.5639
240	lact	803.28	774.9	789.09	177.1643
240	form	920.9	878.5	899.7	269.2826
240	acet	332.9	317.9	325.4	75.9411

Zn 4.3µM 1 & 2 (72 hrs)

Time	Acid	Peak Area	Peak Area	Avg Peak	Avg Conc.
72	succ	0	0	0	0
72	lact	107.9	99.6	103.75	23.29367
72	form	153.4	131.2	142.3	42.59076
72	acet	54	46.8	50.4	11.76223

Zn 4.3µM 1 & 2 (240 hrs)

Time	Acid	Peak Area	Peak Area	Avg Peak	Avg Conc.
240	succ	118.1	120.5	119.3	61.34938
240	lact	753.3	758.4	755.85	169.7014
240	form	1114.4	1118.7	1116.55	334.1863
240	acet	400.1	403.6	401.85	93.78282

Zn 6.1µM 1 & 2 (72 hrs)

Time	Acid	Peak Area	Peak Area	Avg Peak	Avg Conc.
72	succ	0	21.8	10.9	5.605266
72	lact	72.9	50.3	61.6	13.83026
72	form	0	69.8	34.9	10.44566
72	acet	26.2	23.1	24.65	5.75276

Zn 6.1µM 1 & 2 (240 hrs)

Time	Acid	Peak Area	Peak Area	Avg Peak	Avg Conc.
240	succ	0	0	0	0
240	lact	187.9	247.4	217.65	48.86619
240	form	145.7	228.9	187.3	56.05938
240	acet	54.9	85.5	70.2	16.38311

Zn 7.5µM 1 & 2 (72 hrs)

Time	Acid	Peak Area	Peak Area	Avg Peak	Avg Conc.
72	succ	21.6	21.4	21.5	11.05626
72	lact	54.7	50.1	52.4	11.76471
72	form	53.7	58.1	55.9	16.73102
72	acet	18.3	19.9	19.1	4.457514

Zn 7.5µM 1 & 2 (240 hrs)

Time	Acid	Peak Area	Peak Area	Avg Peak	Avg Conc.
240	succ	0	0	0	0
240	lact	228.7	133.6	181.15	40.67131
240	form	0	47	23.5	7.033612
240	acet	79.7	17.8	48.75	11.37716

Zn 12.2µM 1 & 2 (72 hrs)

Time	Acid	Peak Area	Peak Area	Avg Peak	Avg Conc.
72	succ	19.4	19.5	19.45	10.00206
72	lact	53.8	53.4	53.6	12.03413
72	form	36.3	34.8	35.55	10.64021
72	acet	0	0	0	0

Zn 12.2µM 1 & 2 (240 hrs)

Time	Acid	Peak Area	Peak Area	Avg Peak	Avg Conc.
240	succ	0	21.9	10.95	5.630978
240	lact	130.6	118.7	124.65	27.98608
240	form	44.2	47	45.6	13.6482
240	acet	16.3	17.5	16.9	3.944083

Zn 15µM 1 & 2 (72 hrs)

Time	Acid	Peak Area	Peak Area	Avg Peak	Avg Conc.
72	succ	0	18.3	9.15	4.705338
72	lact	66	45.4	55.7	12.50561
72	form	32.2	31.7	31.95	9.562719
72	acet	0	0	0	0

Zn 15µM 1 & 2 (240 hrs)

Time	Acid	Peak Area	Peak Area	Avg Peak	Avg Conc.
240	succ	0	0	0	0
240	lact	118.1	124.3	121.2	27.2115
240	form	37.7	41.2	39.45	11.80749
240	acet	14.1	14.8	14.45	3.372307

Control 1 & 2 (0 hrs)

Time	Acid	Peak Area	Peak Area	Avg Peak	Avg Conc.
0	succ	22.63	0	11.315	5.818677
0	lact	0	42.88	21.44	4.813651
0	form	0	0	0	0
0	acet	0	0	0	0

Control 1 & 2 (72 hrs)

Time	Acid	Peak Area	Peak Area	Avg Peak	Avg Conc.
72	succ	112.32	126.9	119.61	61.50879
72	lact	654.1	590.86	622.48	139.7575
72	form	938.2	1316.3	1127.25	337.3889
72	acet	255.04	230.6	242.82	56.66877

Control 1 & 2 (240 hrs)

Time	Acid	Peak Area	Peak Area	Avg Peak	Avg Conc.
240	succ	239.9	264	251.95	129.5639
240	lact	803.28	774.9	789.09	177.1643
240	form	920.9	878.5	899.7	269.2826
240	acet	332.9	317.9	325.4	75.9411

Cu 2µM 1 & 2 (72 hrs)

Time	Acid	Peak Area	Peak Area	Avg Peak	Avg Conc.
72	succ	43	43	43	22.11252
72	lact	119	99	109	24.47238
72	form	371	280	325.5	97.423
72	acet	113	93.3	103.15	24.07291

Cu 2µM 1 & 2 (240 hrs)

Time	Acid	Peak Area	Peak Area	Avg Peak	Avg Conc.
240	succ	170	181	175.5	90.24992
240	lact	701	623.9	662.45	148.7315
240	form	1028.3	1064.2	1046.25	313.1454
240	acet	372.2	395	383.6	89.52368

Cu 2.5µM 1 & 2 (144 hrs)

Time	Acid	Peak Area	Peak Area	Avg Peak	Avg Conc.
144	succ	74.3	74.51	74.405	38.26237
144	lact	297.8	298	297.9	66.8837
144	form	675.8	676	675.9	202.2986
144	acet	212.7	212.7	212.7	49.63943

Cu 2.5µM 1 & 2 (240 hrs)

Time	Acid	Peak Area	Peak Area	Avg Peak	Avg Conc.
240	succ	169.6	166.4	168	86.39309
240	lact	714.8	708.3	711.55	159.7553
240	form	1070.3	1079.6	1074.95	321.7354
240	acet	369	371	370	86.34974

Cu 3.2µM 1 & 2 (144 hrs)

Time	Acid	Peak Area	Peak Area	Avg Peak	Avg Conc.
144	succ	46.5		46.5	23.91237
144	lact	149.6		149.6	33.58779
144	form	330.4		330.4	98.88959
144	acet	105.9		105.9	24.7147

Cu 3.2µM 1 & 2 (240 hrs)

Time	Acid	Peak Area	Peak Area	Avg Peak	Avg Conc.
240	succ	106.6	73.3	89.95	46.2563
240	lact	434.7	287.1	360.9	81.02829
240	form	1127	772	949.5	284.1878
240	acet	310	204.5	257.25	60.03641

Cu 4µM 1 & 2 (72 hrs)

Time	Acid	Peak Area	Peak Area	Avg Peak	Avg Conc.
72	succ	25.9	0	12.95	6.659467
72	lact	73.9	117.9	95.9	21.53121
72	form	154.8	176.6	165.7	49.59444
72	acet	50	55.3	52.65	12.28733

Cu 4µM 1 & 2 (240 hrs)

Time	Acid	Peak Area	Peak Area	Avg Peak	Avg Conc.
240	succ	43.9	106.4	75.15	38.64548
240	lact	96.8	114.1	105.45	23.67535
240	form	210.8	267	238.9	71.5034
240	acet	72.3	87.1	79.7	18.6002

Cu 6µM 1 & 2 (72 hrs)

Time	Acid	Peak Area	Peak Area	Avg Peak	Avg Conc.
72	succ	31.3	33.7	32.5	16.71295
72	lact	105.8	100.8	103.3	23.19264
72	form	125.7	109.8	117.75	35.24288
72	acet	38.5	33.5	36	8.401596

Cu 6µM 1 & 2 (240 hrs)

Time	Acid	Peak Area	Peak Area	Avg Peak	Avg Conc.
240	succ	66.99	60.3	63.645	32.7291
240	lact	86.91	82.2	84.555	18.98406
240	form	123.4	117.2	120.3	36.00611
240	acet	40.5	40	40.25	9.393451

Cu 8µM 1 & 2 (72 hrs)

Time	Acid	Peak Area	Peak Area	Avg Peak	Avg Conc.
72	succ	0	0	0	0
72	lact	192.8	209.5	201.15	45.16165
72	form	144.5	108	126.25	37.78696
72	acet	43.9	58.5	51.2	11.94894

Cu 8µM 1 & 2 (240 hrs)

Time	Acid	Peak Area	Peak Area	Avg Peak	Avg Conc.
240	succ	0	35	17.5	8.99928
240	lact	274.5	147.3	210.9	47.3507
240	form	232.2	90.3	161.25	48.26255
240	acet	69.3	17.7	43.5	10.15193

Cu 9µM 1 & 2 (72 hrs)

Time	Acid	Peak Area	Peak Area	Avg Peak	Avg Conc.
72	succ	240	296.6	268.3	137.9718
72	lact	108	123.4	115.7	25.97665
72	form	22.4	26.1	24.25	7.258089
72	acet	30.2	26.8	28.5	6.651264

Cu 9µM 1 & 2 (240 hrs)

Time	Acid	Peak Area	Peak Area	Avg Peak	Avg Conc.
240	succ	0	50	25	12.85611
240	lact	248.5	0	124.25	27.89627
240	form	105.9	66.5	86.2	25.79989
240	acet	24	0	12	2.800532

APPENDIX G

Raw values from MINTEQ Modeling

Cu = 2.5 uM (144 hrs)		
Component	**% of total component concentration**	**Species name**
Cu+2	**35.266**	**Cu+2**
	0.061	Cu-(Acetate)2 (aq)
	9.193	CuOH+
	0.159	Cu(OH)2 (aq)
	0.154	Cu2(OH)2+2
	0.052	CuH-Succinate+
	16.405	**Cu-Succinate (aq)**
	12.113	**Cu-Formate+**
	0.922	Cu-(Lactate)2 (aq)
	21.245	**Cu-Lactate+**
	4.428	**Cu-Acetate+**
Acetate-1	99.457	Acetate-1
	0.531	H-Acetate (aq)
	0.011	Cu-Acetate+
Formate-1	99.941	Formate-1
	0.052	H-Formate (aq)
Lactate-1	99.855	Lactate-1
	0.071	Cu-Lactate+
	0.068	H-Lactate (aq)
Succinate-2	96.453	Succinate-2
	0.126	Cu-Succinate (aq)
	3.416	H-Succinate-

Cu = 2.5 uM (240 hrs)		
Component	**% of total component concentration**	**Species name**
Cu+2	**23.278**	**Cu+2**
	0.073	Cu-(Acetate)2 (aq)
	5.72	CuOH+
	0.097	Cu(OH)2 (aq)
	0.062	Cu2(OH)2+2
	0.068	CuH-Succinate+
	20.98	**Cu-Succinate (aq)**
	11.783	**Cu-Formate+**
	0.016	Cu-(Lactate)3-
	3.084	**Cu-(Lactate)2 (aq)**
	30.966	**Cu-Lactate+**
	3.873	**Cu-Acetate+**
Acetate-1	99.472	Acetate-1
	0.521	H-Acetate (aq)
Formate-1	99.945	Formate-1
	0.051	H-Formate (aq)
Lactate-1	99.882	Lactate-1
	0.043	Cu-Lactate+
	0.066	H-Lactate (aq)
Succinate-2	96.696	Succinate-2
	0.071	Cu-Succinate (aq)
	3.228	H-Succinate-

Cu = 3.2 uM Component	% of total component concentration	(144 hrs) Species name
Succinate-2	96.164	Succinate-2
	0.234	Cu-Succinate (aq)
	3.596	H-Succinate-
Acetate-1	99.44	Acetate-1
	0.541	H-Acetate (aq)
	0.019	Cu-Acetate+
Cu+2	**45.429**	**Cu+2**
	0.015	Cu-(Acetate)2 (aq)
	12.505	**CuOH+**
	0.22	Cu(OH)2 (aq)
	0.343	Cu2(OH)2+2
	0.048	CuH-Succinate+
	15.391	**Cu-Succinate (aq)**
	8.223	**Cu-Formate+**
	0.341	Cu-(Lactate)2 (aq)
	14.926	**Cu-Lactate+**
	2.555	**Cu-Acetate+**
Formate-1	99.935	Formate-1
	0.053	H-Formate (aq)
	0.012	Cu-Formate+
Lactate-1	99.802	Lactate-1
	0.123	Cu-Lactate+
	0.069	H-Lactate (aq)

Cu = 3.2 uM Component	% of total component concentration	(240 hrs) Species name
Succinate-2	96.528	Succinate-2
	0.134	Cu-Succinate (aq)
	3.332	H-Succinate-
Acetate-1	99.461	Acetate-1
	0.527	H-Acetate (aq)
	0.012	Cu-Acetate+
Cu+2	**32.034**	**Cu+2**
	0.052	Cu-(Acetate)2 (aq)
	8.141	CuOH+
	0.139	Cu(OH)2 (aq)
	0.153	Cu2(OH)2+2
	0.054	CuH-Succinate+
	16.865	**Cu-Succinate (aq)**
	14.955	**Cu-Formate+**
	1.163	Cu-(Lactate)2 (aq)
	22.552	**Cu-Lactate+**
	3.888	**Cu-Acetate+**
Formate-1	99.941	Formate-1
	0.051	H-Formate (aq)
Lactate-1	99.847	Lactate-1
	0.078	Cu-Lactate+
	0.067	H-Lactate (aq)

Cu = 4 uM Component	% of total component concentration	(72 hrs) Species name
Succinate-2	95.826	Succinate-2
	0.424	Cu-Succinate (aq)
	3.743	H-Succinate-
Acetate-1	99.418	Acetate-1
	0.549	H-Acetate (aq)
	0.033	Cu-Acetate+
Cu+2	**56.466**	**Cu+2**
	16.238	CuOH+
	0.29	Cu(OH)2 (aq)
	0.73	Cu2(OH)2+2
	0.011	Cu3(OH)4+2
	0.019	CuH-Succinate+
	6.248	**Cu-Succinate (aq)**
	5.471	**Cu-Formate+**
	0.193	Cu-(Lactate)2 (aq)
	12.712	**Cu-Lactate+**
	1.615	**Cu-Acetate+**
Formate-1	99.926	Formate-1
	0.054	H-Formate (aq)
	0.02	Cu-Formate+
Lactate-1	99.713	Lactate-1
	0.211	Cu-Lactate+
	0.07	H-Lactate (aq)

Cu = 4 uM Component	% of total component concentration	(240 hrs) Species name
Succinate-2	96.08	Succinate-2
	0.3	Cu-Succinate (aq)
	3.613	H-Succinate-
Acetate-1	99.433	Acetate-1
	0.542	H-Acetate (aq)
	0.024	Cu-Acetate+
Cu+2	**44.149**	**Cu+2**
	12.223	CuOH+
	0.216	Cu(OH)2 (aq)
	0.424	Cu2(OH)2+2
	0.076	CuH-Succinate+
	24.659	**Cu-Succinate (aq)**
	5.856	**Cu-Formate+**
	0.167	Cu-(Lactate)2 (aq)
	10.314	**Cu-Lactate+**
	1.901	**Cu-Acetate+**
Formate-1	99.932	Formate-1
	0.053	H-Formate (aq)
	0.015	Cu-Formate+
Lactate-1	99.769	Lactate-1
	0.157	Cu-Lactate+
	0.069	H-Lactate (aq)

Cu = 6 uM Component	% of total component concentration	(72 hrs) Species name
Succinate-2	95.674	Succinate-2
	0.576	Cu-Succinate (aq)
	3.743	H-Succinate-
Acetate-1	99.406	Acetate-1
	0.549	H-Acetate (aq)
	0.044	Cu-Acetate+
Cu+2	**52.419**	**Cu+2**
	15.096	CuOH+
	0.27	Cu(OH)2 (aq)
	0.922	Cu2(OH)2+2
	0.019	Cu3(OH)4+2
	0.043	CuH-Succinate+
	14.118	**Cu-Succinate (aq)**
	3.562	**Cu-Formate+**
	0.196	Cu-(Lactate)2 (aq)
	12.352	**Cu-Lactate+**
	1.001	**Cu-Acetate+**
Formate-1	99.919	Formate-1
	0.054	H-Formate (aq)
	0.027	Cu-Formate+
Lactate-1	99.635	Lactate-1
	0.286	Cu-Lactate+
	0.07	H-Lactate (aq)

Cu = 6 uM Component	% of total component concentration	(240 hrs) Species name
Succinate-2	95.789	Succinate-2
	0.507	Cu-Succinate (aq)
	3.697	H-Succinate-
Acetate-1	99.413	Acetate-1
	0.547	H-Acetate (aq)
	0.04	Cu-Acetate+
Cu+2	**47.729**	**Cu+2**
	13.56	CuOH+
	0.241	Cu(OH)2 (aq)
	0.75	Cu2(OH)2+2
	0.014	Cu3(OH)4+2
	0.074	CuH-Succinate+
	24.098	**Cu-Succinate (aq)**
	3.276	**Cu-Formate+**
	0.119	Cu-(Lactate)2 (aq)
	9.128	**Cu-Lactate+**
	1.008	**Cu-Acetate+**
Formate-1	99.922	Formate-1
	0.053	H-Formate (aq)
	0.024	Cu-Formate+
Lactate-1	99.668	Lactate-1
	0.256	Cu-Lactate+
	0.069	H-Lactate (aq)

Cu = 8 uM Component	% of total component concentration	(72 hrs) Species name
Cu+2	**52.617**	**Cu+2**
	15.231	CuOH+
	0.273	Cu(OH)2 (aq)
	1.255	Cu2(OH)2+2
	0.036	Cu3(OH)4+2
	3.908	**Cu-Formate+**
	0.76	Cu-(Lactate)2 (aq)
	24.396	**Cu-Lactate+**
	1.518	**Cu-Acetate+**
Acetate-1	99.39	Acetate-1
	0.55	H-Acetate (aq)
	0.06	Cu-Acetate+
Formate-1	99.909	Formate-1
	0.054	H-Formate (aq)
	0.037	Cu-Formate+
Lactate-1	99.518	Lactate-1
	0.024	Cu-(Lactate)2 (aq)
	0.388	Cu-Lactate+
	0.07	H-Lactate (aq)
Succinate-2	95.453	Succinate-2
	0.785	Cu-Succinate (aq)
	3.753	H-Succinate-

Cu = 8 uM Component	% of total component concentration	(240 hrs) Species name
Cu+2	**48.563**	**Cu+2**
	13.865	CuOH+
	0.247	Cu(OH)2 (aq)
	1.049	Cu2(OH)2+2
	0.027	Cu3(OH)4+2
	0.021	CuH-Succinate+
	6.761	**Cu-Succinate (aq)**
	4.473	**Cu-Formate+**
	0.745	Cu-(Lactate)2 (aq)
	23.098	**Cu-Lactate+**
	1.146	**Cu-Acetate+**
Acetate-1	99.398	Acetate-1
	0.548	H-Acetate (aq)
	0.054	Cu-Acetate+
Formate-1	99.913	Formate-1
	0.053	H-Formate (aq)
	0.034	Cu-Formate+
Lactate-1	99.556	Lactate-1
	0.023	Cu-(Lactate)2 (aq)
	0.351	Cu-Lactate+
	0.07	H-Lactate (aq)
Succinate-2	95.586	Succinate-2
	0.699	Cu-Succinate (aq)
	3.707	H-Succinate-

Zn = 4.3 uM (72 hrs)		
Component	**% of total component concentration**	**Species name**
Zn+2	**92.724**	**Zn+2**
	0.617	Zn-Acetate+
	0.852	ZnOH+
	0.105	Zn(OH)2 (aq)
	2.159	**Zn-Formate+**
	0.029	Zn-(Lactate)2 (aq)
	3.514	**Zn-Lactate+**
Lactate-1	99.871	Lactate-1
	0.058	Zn-Lactate+
	0.07	H-Lactate (aq)
Acetate-1	99.436	Acetate-1
	0.013	Zn-Acetate+
	0.551	H-Acetate (aq)
Formate-1	99.937	Formate-1
	0.054	H-Formate (aq)
Succinate-2	96.1	Succinate-2
	0.099	Zn-Succinate (aq)
	3.794	H-Succinate-

Zn = 4.3 uM (240 hrs)		
Component	**% of total component concentration**	**Species name**
Zn+2	**65.861**	**Zn+2**
	2.754	**Zn-Acetate+**
	0.513	ZnOH+
	0.06	Zn(OH)2 (aq)
	0.026	ZnH-Succinate+
	5.593	**Zn-Succinate (aq)**
	9.56	**Zn-Formate+**
	0.805	Zn-(Lactate)2 (aq)
	14.811	**Zn-Lactate+**
Acetate-1	99.471	Acetate-1
	0.521	H-Acetate (aq)
Formate-1	99.944	Formate-1
	0.051	H-Formate (aq)
Lactate-1	99.897	Lactate-1
	0.033	Zn-Lactate+
	0.066	H-Lactate (aq)
Succinate-2	96.712	Succinate-2
	0.046	Zn-Succinate (aq)
	3.238	H-Succinate-

Zn = 6.1 uM (72 hrs)		
Component	**% of total component concentration**	**Species name**
Zn+2	**94.556**	**Zn+2**
	0.326	**Zn-Acetate+**
	0.893	ZnOH+
	0.111	Zn(OH)2 (aq)
	1.308	**Zn-Succinate (aq)**
	0.53	Zn-Formate+
	0.012	Zn-(Lactate)2 (aq)
	2.259	**Zn-Lactate+**
Acetate-1	99.424	Acetate-1
	0.02	Zn-Acetate+
	0.556	H-Acetate (aq)
Formate-1	99.931	Formate-1
	0.054	H-Formate (aq)
	0.015	Zn-Formate+
Lactate-1	99.84	Lactate-1
	0.088	Zn-Lactate+
	0.071	H-Lactate (aq)
Succinate-2	95.948	Succinate-2
	0.155	Zn-Succinate (aq)
	3.89	H-Succinate-

Zn = 6.1 uM (240 hrs)		
Component	**% of total component concentration**	**Species name**
Zn+2	**88.736**	**Zn+2**
	0.768	**Zn-Acetate+**
	0.801	ZnOH+
	0.098	Zn(OH)2 (aq)
	2.627	**Zn-Formate+**
	0.116	Zn-(Lactate)2 (aq)
	6.853	**Zn-Lactate+**
Acetate-1	99.435	Acetate-1
	0.017	Zn-Acetate+
	0.548	H-Acetate (aq)
Formate-1	99.934	Formate-1
	0.053	H-Formate (aq)
	0.013	Zn-Formate+
Lactate-1	99.85	Lactate-1
	0.078	Zn-Lactate+
	0.07	H-Lactate (aq)
Succinate-2	96.136	Succinate-2
	0.129	Zn-Succinate (aq)
	3.729	H-Succinate-

Zn = 7.6 uM Component	% of total component concentration	(72 hrs) Species name
Succinate-2	95.959	Succinate-2
	0.186	Zn-Succinate (aq)
	3.848	H-Succinate-
Zn+2	**93.743**	**Zn+2**
	0.239	Zn-Acetate+
	0.875	ZnOH+
	0.108	Zn(OH)2 (aq)
	0.01	ZnH-Succinate+
	2.308	Zn-Succinate (aq)
	0.865	Zn-Formate+
	1.844	Zn-Lactate+
Acetate-1	99.422	Acetate-1
	0.024	Zn-Acetate+
	0.554	H-Acetate (aq)
Formate-1	99.928	Formate-1
	0.054	H-Formate (aq)
	0.018	Zn-Formate+
Lactate-1	99.821	Lactate-1
	0.107	Zn-Lactate+
	0.071	H-Lactate (aq)

Zn = 7.6 uM Component	% of total component concentration	(240 hrs) Species name
Succinate-2	95.937	Succinate-2
	0.185	Zn-Succinate (aq)
	3.871	H-Succinate-
Zn+2	**91.783**	**Zn+2**
	0.576	Zn-Acetate+
	0.862	ZnOH+
	0.107	Zn(OH)2 (aq)
	0.358	Zn-Formate+
	0.09	Zn-(Lactate)2 (aq)
	6.224	Zn-Lactate+
Acetate-1	99.421	Acetate-1
	0.024	Zn-Acetate+
	0.555	H-Acetate (aq)
Formate-1	99.928	Formate-1
	0.054	H-Formate (aq)
	0.018	Zn-Formate+
Lactate-1	99.82	Lactate-1
	0.106	Zn-Lactate+
	0.071	H-Lactate (aq)

Zn = 12 uM Component	% of total component concentration	(72 hrs) Species name
Succinate-2	95.806	Succinate-2
	0.307	Zn-Succinate (aq)
	3.879	H-Succinate-
Zn+2	**94.363**	**Zn+2**
	0.889	ZnOH+
	0.11	Zn(OH)2 (aq)
	2.163	Zn-Succinate (aq)
	0.528	Zn-Formate+
	1.927	Zn-Lactate+
Acetate-1	99.405	Acetate-1
	0.039	Zn-Acetate+
	0.556	H-Acetate (aq)
Formate-1	99.917	Formate-1
	0.054	H-Formate (aq)
	0.029	Zn-Formate+
Lactate-1	99.753	Lactate-1
	0.175	Zn-Lactate+
	0.071	H-Lactate (aq)

Zn = 12 uM Component	% of total component concentration	(240 hrs) Species name
Succinate-2	95.849	Succinate-2
	0.295	Zn-Succinate (aq)
	3.849	H-Succinate-
Zn+2	**92.451**	**Zn+2**
	0.209	Zn-Acetate+
	0.864	ZnOH+
	0.107	Zn(OH)2 (aq)
	1.245	Zn-Succinate (aq)
	0.717	Zn-Formate+
	0.044	Zn-(Lactate)2 (aq)
	4.358	Zn-Lactate+
Acetate-1	99.408	Acetate-1
	0.038	Zn-Acetate+
	0.554	H-Acetate (aq)
Formate-1	99.918	Formate-1
	0.054	H-Formate (aq)
	0.028	Zn-Formate+
Lactate-1	99.756	Lactate-1
	0.17	Zn-Lactate+
	0.07	H-Lactate (aq)

Starting Copper concentration		Effective conc. Over time			
(Cu 2+)	Time:	0	72	144	240
2.5 uM (0.16 mg/L)		0.16		0.05648	0.03728
3.2 uM (0.2 mg/L)		0.2		0.0908	0.064
4 uM (0.26 mg/L)		0.26	0.1469		0.1144
6 uM (0.38 mg/L)		0.38	0.19912		0.18126
8 uM (0.51 mg/L)		0.51	0.26826		0.24786

Starting Zinc concentration		Effective conc. Over time			
(Zn 2+)	Time:	0	72	144	240
4.3 uM (0.28 mg/L)		0.28	0.25956		0.18452
6.1 uM (0.4 mg/L)		0.4	0.3784		0.3548
7.6 uM (0.5 mg/L)		0.5	0.4685		0.4585
12 uM (0.8 mg/L)		0.8	0.7544		0.7392